CENTRO INTERNACIONAL DE ESTUDOS
DE DOUTORAMENTO E AVANZADOS
DA USC (CIEDUS)

TESE DE DOUTORAMENTO

OPTICAL PROPERTIES DERIVED FROM THE REFRACTIVE INDEX DISPERSION OF ALKYL-IMIDAZOLIUM BASED IONIC LIQUIDS

Bilal Saleh Mohammad Algnamat

ESCOLA DE DOUTORAMENTO INTERNACIONAL
PROGRAMA DE DOUTORAMENTO EN LÁSER FOTÓNICA Y VISIÓN

SANTIAGO DE COMPOSTELA

2019

USC
UNIVERSIDADE
DE SANTIAGO
DE COMPOSTELA

DECLARACIÓN DO AUTOR DA TESE

Optical properties derived from the refractive index dispersion of alkyl-imidazolium based ionic liquids

D. Bilal Saleh Mohammad Algnamat

Presento a miña tese, seguindo o procedemento axeitado ao Regulamento, e declaro que:

1) *A tese abarca os resultados da elaboración do meu traballo.*
2) *De selo caso, na tese faise referencia ás colaboracións que tivo este traballo.*
3) *A tese é a versión definitiva presentada para a súa defensa e coincide coa versión enviada en formato electrónico.*
4) *Confirmo que a tese non incorre en ningún tipo de plaxio doutros autores nin de traballos presentados por min para a obtención doutros títulos.*

En Santiago de Compostela, … de ….. de 2019

Asdo: Bilal Saleh Mohammad Algnamat

USC
UNIVERSIDADE
DE SANTIAGO
DE COMPOSTELA

AUTORIZACIÓN DOS DIRECTORES

Optical properties derived from the refractive index dispersion of alkyl-imidazolium based ionic liquids

Dª. María Elena López Lago e D. Raúl de la Fuente Carballo

INFORMAN:

*Que a presente tese, correspondese co traballo realizado por **D. Bilal Saleh Mohammad Algnamat**, baixo a nosa dirección, e autorizamos a súa presentación, considerando que cumpre cos requisitos exixidos no Regulamento de Estudos de Doutoramento da USC, e que como directores desta non incorre nas causas de abstención establecidas na Lei 40/2015.*

En Santiago de Compostela, … de ….. de 2019

Asdo: María Elena López Lago **Asdo: Raúl de la Fuente Carballo**

USC
UNIVERSIDADE
DE SANTIAGO
DE COMPOSTELA

Resumen

El término líquido iónico (IL) hace referencia a un tipo de materiales constituidos íntegramente por iones que se encuentran en estado líquido a temperaturas inferiores a 100^{o}C. Aunque el primer líquido iónico estable se sintetizó a principios del siglo XX, el interés por estas sales ha crecido exponencialmente en los últimos 30 años debido a sus propiedades singulares. Durante este tiempo, parte de los esfuerzos de los investigadores se orientaron a reducir la toxicidad e incrementar la estabilidad de los mismos, al tiempo que se trabajaba en la síntesis y estudio de los líquidos más adecuados para las aplicaciones propuestas (baterías, lubricantes, catálisis, etc.)

Las propiedades físicas de los líquidos iónicos están muy ligadas a su composición química siendo posible diseñar un líquido iónico que presente una propiedad determinada sin más que combinar los iones adecuados, de ahí que también sean conocidos como disolventes de diseño. Las características termofísicas más valoradas son su gran estabilidad térmica, su alta conductividad iónica, su gran ventana electroquímica, su capacidad de permanecer en estado líquido en un amplio rango de temperaturas y su baja presión de vapor; que supone que los líquidos no se evaporen, contrariamente a los que sucede con otros disolventes orgánicos, lo que supone que no sean tóxicos por inhalación. Debido a estas y otras características han sido propuestos para diversas aplicaciones en diversos campos como la química, la biotecnología, mineralogía, ingeniería, energía y en el ámbito farmacéutico.

Los líquidos iónicos son también potenciales candidatos para formar parte de dispositivos ópticos gracias a su condición de

disolventes de diseño. Su uso en este tipo de dispositivos requiere tener un conocimiento preciso de sus propiedades ópticas para asegurar un comportamiento eficiente. Por ejemplo, conocer como varía el índice de refracción con la longitud de onda es fundamental para muchas aplicaciones en campos como imagen óptica, óptica ultrarrápida, comunicaciones ópticas, óptica integrada, tecnología láser, sensorización, etc.

Tradicionalmente, los investigadores se centraron únicamente en la caracterización del índice de refracción a una única longitud de onda, la línea D de Frauhoffer que se corresponde con una longitud de onda de 589.3 nm, ignorando que el índice de refracción es una propiedad dispersiva. El objetivo principal de este trabajo es justamente determinar la dispersión cromática, y otras propiedades relacionadas con ésta, de 20 líquidos iónicos en un intervalo de longitudes de onda que abarca desde los 400 a los 1000 nm.

Los líquidos iónicos seleccionados para este estudio están constituidos por un catión orgánico combinado con un anión que puede ser inorgánico u orgánico. Se nombran usando el nombre del catión seguido del nombre del anión. Los cationes contienen anillos como el imidazolio (presente en la mayor parte de ellos), el pirrolidinio o el piperidinio. Estos anillos incorporan una o más cadenas alquílicas cuya longitud es variable. Cuando se emplea notación abreviada, las abreviaturas del catión y del anión se suelen poner entre corchetes. En este caso una de las cadenas alquílicas, la más larga, se denota por C_{Nc}, donde Nc es el número de carbonos que contiene. M identifica a un grupo metil, la cadena más corta, y la notación Im, Pip, PL representa a los anillos imidazol, piperidinio y pirrolidinio, respectivamente. Los cationes que forman parte de los líquidos iónicos estudiados son los siguientes: 1-Etil-3-metilimidazolio ($[C_2MIm]^+$), 1-Propil-3-metilimidazolio ($[C_3MIm]^+$), 1-Butil-3-metilimidazolio ($[C_4MIm]^+$), 1-Hexil-3-metilimidazolio ($[C_6MIm]^+$), 1-Octil-3-metilimidazolio ($[C_8MIm]^+$), 1-Butil-1- metilpepiridinio ($[C_4MPip]^+$), 1-(2-metoxietil)-1-metilpirrolidinio ($[MOEMPl]^+$) y 1-Butil-dimetilimidazolio ($[C_4MMIm]^+$). En cuanto a los aniones, los empleados fueron: Bis(trifluorometilsulfonil)imida ($[NTf_2]^-$), Tetrafluoroborato ($[BF_4]^-$),

Trifluorometanosulfonato (Triflato) ($[OTf]^-$), Metilsulfato ($[C_1SO_4]^-$), Etilsulfato ($[C_2SO_4]^-$), Hexilsulfato ($[C_6SO_4]^-$), Bisulfato ($[H_ySO_4]^-$) y Tiocianato ($[SCN]^-$).

Los líquidos iónicos estudiados se han clasificado en cinco grupos atendiendo a su composición:

(a) Grupo 1: a este grupo pertenecen los líquidos iónicos constituidos por cationes 1-alquil-3-metilimidazolio ($[C_{Nc}MIm]^+$, *Nc*=2, 3, 4, 6, 8) combinados con aniones $[BF_4]^-$;

(b) Grupo 2: este grupo está integrado por líquidos iónicos constituidos por cationes 1-alquil-3-metilimidazolio ($[C_{Nc}MIm]^+$, *Nc*=2, 3, 4, 6) combinados con aniones $[NTf_2]^-$;

(c) Grupo 3: en este grupo se encuentran líquidos iónicos compuestos por el catión 1-etil-3-metilimidazolio ($[C_2MIm]^+$) combinado con distintos aniones: $[BF_4]^-$, $[NTf_2]^-$, $[OTf]^-$, $[C_{1,2,6}SO_4]^-$ y $[H_ySO_4]^-$. Dentro de este grupo distinguimos un subconjunto que denominamos Subgrupo 3.1 que está constituido por los líquidos iónicos que contienen grupos sulfato, SO_4^{2-};

(d) Grupo 4: este grupo está formado por líquidos iónicos compuestos por el catión 1-butil-3-metilimidazolio ($[C_4MIm]^+$) combinado con distintos aniones: $[BF_4]^-$, $[NTf_2]^-$, $[OTf]^-$, $[C_1SO_4]^-$ y $[SCN]^-$;

(e) Grupo 5: este grupo está constituido por líquidos iónicos que contienen el anión $[NTf_2]^-$ combinado con diferentes cationes $[C_4MIm]^+$, $[C_4MPip]^+$, $[MOEMPL]^+$ y $[C_4MMIm]^+$;

Estos líquidos iónicos, en general, son muy higroscópicos y absorben fácilmente agua del ambiente. Por ello, antes de realizar los experimentos, se someten a un proceso de secado en vacío (presión inferior a 10^{-3} atm y temperatura ambiente) durante más de 48 h con el objetivo de eliminar el máximo contenido de agua. La cantidad de agua no eliminada se determina con un coulómetro Karl-Fisher de Mettler

Toledo; ésta fue inferior a 500 ppm en todos los casos (por ejemplo 194, 167, 216, 482 y 374 ppm en $[C_2MIm][BF_4]$, $[C_4MIm][NTf_2]$, $[C_2MIm][OTf]$, $[C_2MIm][C_1SO_4]$ y $[C_4MIm][SCN]$ respectivamente). Las cantidades detectadas no son suficientes para tener una influencia apreciable en la medida del índice de refracción y sus propiedades derivadas.

Tras el proceso de preparación de cada una de las muestras, se midieron la densidad y la dispersión cromática a diferentes temperaturas.

La densidad se determinó con un densímetro digital modelo Anton Paar DSA 5000; el procedimiento que utiliza se fundamenta en la densimetría de tubo vibrante (VTD) que es uno de los métodos más consolidados por su rapidez y precisión, menor que $\pm 2 \cdot 10^{-6}$ g·cm^{-3} en este trabajo. Los datos se adquirieron a cinco temperaturas: 298, 303, 308, 313, 318 and 323 K. Los resultados obtenidos fueron los esperados: disminución de la densidad conforme aumenta la temperatura o el número de átomos de carbono, *Nc*.

Los índices de refracción se midieron usando una técnica interferométrica muy precisa conocida como Interferometría de luz blanca resuelta espectralmente (SRWLI: Spectrally Resolved White Light Interferometry) adaptada a esta aplicación. Esta variante la denominamos en castellano Refractometría Espectral por Interferencia de Banda Ancha (REIBA) y en inglés, Refractive index spectroscopy by broadband interferomery (RISBI). La gran aportación de REIBA a la refractometría, frente a otras técnicas estándar y comerciales, es que nos permite obtener rápidamente el índice de refracción en un rango espectral ancho. El rango espectral accesible comprende longitudes de onda entre 400 y 1000 nm con una resolución inferior a los 2 nm. Los resultados proporcionados por REIBA se caracterizan por una incertidumbre en torno a $2 \cdot 10^{-4}$. Las medidas se tomaron en las mismas condiciones de temperatura que las de densidad.

REIBA es una técnica interferométrica que, como tal, recupera el índice de refracción a partir de una fase, que es el argumento de una función coseno. Al ser el coseno una función periódica con período 2π, la

recuperación de la fase lleva asociada una incertidumbre que se corresponde con un factor $2k\pi$ (donde k es un número entero), que en este caso, debido a los valores que puede alcanzar k, puede inducir errores en el índice de refracción que afecten a la segunda e incluso a la primera cifra decimal. Este problema se evita si se puede conocer un índice de refracción de referencia para una longitud de onda del intervalo espectral. Para ello se utiliza un refractómetro de Abbe modelo ATAGO DR-M2 que permite medir el índice de refracción a 5 longitudes de onda (486, 546, 589, 633 and 680 nm); una de ellas se emplea para medir el índice de refracción de referencia, usualmente 589 nm, y las otras 4 para verificar la validez de la técnica. Tanto el dispositivo REIBA como el refractómetro de Abbe están acoplados a un controlador de temperatura con una estabilidad de ±0.1 K

La toma de datos para cada líquido iónico se ha realizado con cierta frecuencia durante un periodo largo de tiempo para verificar la repetibilidad del método así como para comprobar el grado de conservación de la pureza de las muestras y la validez de las condiciones de almacenamiento. Es un hecho contrastado que el índice de refracción depende mucho del grado de pureza, por ello se ha tenido mucho cuidado durante el proceso de medida y de almacenamiento de que no se produzca la más mínima contaminación de las muestras que pudiera alterar los resultados. De hecho se ha detectado una gran variabilidad entre los valores del índice de refracción que se encuentran en la literatura, alcanzando diferencias mayores que 10^{-3}, diferencias que han sido atribuidas a la presencia de impurezas, contenido de agua o a errores sistemáticos inherentes a las condiciones de medida, por ejemplo.

Una vez confirmada la validez de la técnica y la adquisición de datos, se realizó un análisis de los mismos con el objetivo de identificar comportamientos y tendencias que se pudieran correlacionar con otras propiedades del material o con su composición. Se prestó especial atención a la influencia que ejercen, en el índice de refracción y propiedades derivadas, la longitud de la cadena alquílica, tanto catiónica como aniónica, el tipo de anión y la funcionalización del catión. Estas propiedades derivadas son el número de Abbe, la

velocidad e índice de grupo, la dispersión de la velocidad de grupo y la pendiente de dispersión, en las que intervienen las derivadas del índice de refracción con respecto a la longitud de onda. Se estudió también la influencia de la temperatura.

Al tratarse de materiales transparentes en el rango de longitudes de onda estudiado, las curvas que se obtienen corresponden a las esperadas en regiones con dispersión normal, disminuyendo el valor del índice de refracción conforme crece el de la longitud de onda. Se han observado variaciones usuales del índice de refracción en los extremos del espectro entre 0.02 y 0.03.

Con respecto a la variación de *Nc*, se observó que el índice de refracción aumenta con *Nc* en todos los casos (Grupos 1 y 2) excepto en aquellos líquidos que contienen el grupo sulfato en el anión (Subgrupo 3.1) que siguen la tendencia contraria. El incremento parece no depender de la longitud de onda. Para averiguar el origen de esta variación recurrimos a la ecuación de Lorentz-Lorenz que relaciona el índice de refracción con el volumen molar (V_m) y la refractividad molar, (R_m). Analizando los datos de densidad, se comprobó que el volumen molar es una función lineal de N_c, $V_m = V_0 + N_c \Delta V$; a partir de los datos de V_m y del índice de refracción, se constató también la linealidad de R_m con Nc, $R_m = R_0 + N_c \Delta R$. Sustituyendo estas expresiones en la ecuación de Lorentz-Lorenz concluimos que la relación entre $\Delta R/\Delta V$ y R_0/V_0 es la que determina el comportamiento del índice de refracción con N_c, donde ΔR y ΔV dan cuenta del cambio que se introduce en la refractividad y en el volumen molar, respectivamente, al añadir un grupo CH_2 a la cadena alquílica. $\Delta R/\Delta V > R_0/V_0$ implica un aumento del índice de refracción con *Nc* y $\Delta R/\Delta V < R_0/V_0$ una disminución del mismo. Esta modelización permite, además, realizar una predicción del índice de refracción de familias de líquidos iónicos que se diferencian en *Nc*, con sólo conocer el índice de refracción de dos de ellos (siempre que la adición de grupos CH_2 no genere anisotropías en el índice de refracción). Las diferencias entre los valores predichos y los experimentales son menores que 10^{-3}. Se calcularon también los valores límite del índice de refracción en todo el rango espectral que se

corresponde con Nc=0 y $Nc \rightarrow \infty$. Otra conclusión importante es que el efecto de la adición de grupos CH_2 en la cadena depende del entorno, es decir del catión y del anión del líquido iónico.

Se ha estudiado la influencia aniónica y se ha observado que el índice de refracción es muy dependiente de la naturaleza del anión; el índice de refracción crece de acuerdo con las siguiente series:

Grupo 3: $[BF_4]^- < [NTf_2]^- < [OTf]^- < [C_{Nc}SO_4]^-$

Grupo 4: $[BF_4]^- < [NTf_2]^- < [OTf]^- < [C_1SO_4]^- < [SCN]^-$

La adición de un nuevo grupo metilo o la sustitución del anillo imidazolio por un piperidinio causa un incremento del índice de refracción mientras que la sustitución del catión $[C_4MIm]^+$ por $[MOEMPL]^+$ causa una disminución; estos cambios inducidos en el índice de refracción no son homogéneos en todo el espectro, a diferencia de lo que ocurría con el incremento de grupos CH_2.

Una función basada en una ecuación de Sellmeier con una resonancia se ajustó a los datos experimentales. Los parámetros de ajuste se corresponden con la longitud de onda de la resonancia y con la fuerza de la resonancia. Se ha comprobado que la longitud de onda de la resonancia, λ_{uv}, es independiente de la temperatura y del número de carbonos Nc dentro de una misma familia; y que la dependencia de la fuerza de la resonancia con la temperatura se puede modelizar con una función lineal de ésta, $A+B\Delta T$, donde A y B dependen de Nc.

Demostrada la validez de este modelo, lo empleamos para calcular el coeficiente termoóptico (TOC), el índice de grupo (n_g), la dispersión de segundo orden a través del parámetro dispersión (D), y la dispersión de tercer orden a través de la pendiente de dispersión (S). Estas magnitudes apenas dependen de la temperatura, al menos en el rango estudiado, pero están influenciadas, unas más que otras, por la composición del líquido iónico (anión, catión, longitud de la cadena alquílica).

La dispersión del coeficiente termoóptico, que es negativo, es más importante en la región de longitudes de onda cortas que largas, zona en la que se reduce su valor absoluto. Con respecto a la influencia del anión, el TOC sigue una serie diferente a la observada en el índice de refracción en los grupos 3 y 4. El incremento de la cadena alquílica, tanto en el catión (Grupos 1 y 2) como en el anión (Subgrupo 3.1), produce un aumento del TOC en valor absoluto.

El parámetro de dispersión D no se ve afectado por cambios en *Nc*, y varía muy poco al modificar el tipo de catión; ejerce una mayor influencia, sin embargo, la parte aniónica del líquido especialmente en la zona de longitudes de onda corta. Los mayores valores de *D* (en valor absoluto) se encuentran en los líquidos iónicos que contienen átomos de azufre en el anión ($[C_{Nc}SO_4]^-$ o $[SCN]^-$). La longitud de onda caracterizada por *D*=0 se encuentra fuera del rango espectral disponible pero se estima que se sitúa en torno a 1.3 micras por comparación con la curva correspondiente del agua.

La pendiente de dispersión *S* tampoco se ve afectada por la adición de grupos CH_2 en la cadena alquílica de acuerdo con lo observado en los líquidos de los Grupos 1 y 2; se ha detectado una ligera variación al modificar el tipo de catión de forma que aumenta su valor de acuerdo con la serie: $[MOEMPL]^+<[C_4MPip]^+<C_4MIm]^+<[C_4MMIm]^+$. Este comportamiento es similar al observado en el valor absoluto de *D*. La influencia del anión también es pequeña siendo más importante en la zona de frecuencias altas; los mayores valores que se han obtenido en esta zona del espectro corresponden a aquellos líquidos iónicos que contienen átomos de azufre en el anión.

Los líquidos iónicos se han representado en un diagrama de Abbe. La mayoría de los líquidos tienen un índice de refracción en torno a 1.45 y un número de Abbe comprendido entre 45 y 65 con la excepción del líquido que contiene el anión $[SCN]^-$ y otros líquidos iónicos cuyo anión está constituido por complejos de coordinación integrados por un metal de transición y grupos $[NCS]^-$. El índice de refracción de éstos se encuentra en torno a 1.55 y el número de Abbe entre 30 y 36. Por otra parte se ha comprobado que el par coordenado (n_D, V_D) sigue un

comportamiento lineal con el incremento de temperatura y con *Nc*. Si se comparan estos resultados con los del agua, se observa que ésta tiene un índice de refracción menor y un número de Abbe mayor, por lo que estos líquidos son claramente más dispersivos. Por otra parte, la adición de un segundo grupo metilo en la posición 2 del anillo imidazolio del $[C_4MIm][NTf_2]$ causa un incremento del número de Abbe sin que varíe demasiado el índice de refracción. Por el contrario, los líquidos iónicos constituidos por los cationes $[C_4MPip]^+$ y $[MOEMPl]^+$ se caracterizan por un número de Abbe mayor que el del agua, siendo por lo tanto menos dispersivos.

El trabajo que se presenta para la obtención del título de doctor está organizado en cuatro capítulos. El primero de ellos se dedica a realizar una introducción al campo de los líquidos iónicos así como a las propiedades dispersivas derivadas del índice de refracción que han sido objeto de estudio. El segundo de los capítulos se destina a la descripción tanto de las técnicas y dispositivos de caracterización empleados como de los líquidos iónicos elegidos. En el tercer capítulo se analizan los resultados obtenidos y finalmente en el cuarto se exponen las conclusiones resultantes de esta investigación.

La investigación fue desarrollada en el marco de dos proyectos del Plan Nacional de I+D:

- Caracterización óptica de líquidos y geles iónicos para su aplicación en dispositivos fotónicos y electroquímicos (MAT2014-57943-C3-2-P).
- Materiales inteligentes para los retos electroquímicos y fotónicos: líquidos iónicos e ionogeles híbridos (MAT2017-89239-C2-1-P).

Mi contribución al primer proyecto se centró en la caracterización mediante REIBA y refractometría de Abbe de distintas familias de líquidos iónicos, y en el diseño de estrategias de preparación de muestras y de medida que garantizaran la repetibilidad de los datos obtenidos mediante estas técnicas.

Mi contribución al segundo proyecto se centró, por un lado, en la aplicación de un modelo analítico para describir el comportamiento del índice de refracción con la longitud de onda y temperatura, que permitió calcular con precisión diferentes propiedades relacionadas con el índice de refracción como son el coeficiente termoóptico, el índice de grupo o la dispersión de segundo y tercer orden; y, por otro, en la obtención de modelos simples que describieran el efecto de la longitud de cadena y la temperatura en el índice de refracción.

Acknowledgements

This thesis is the culmination of my journey of Ph.D., which was just like climbing a high peak step by step accompanied with encouragement, hardship, trust, and frustration. When I found myself at top experiencing the feeling of fulfillment, I realized though only my name appears on the cover of this dissertation, a great many people including my family members, my friends, colleagues, and various institutions have contributed to accomplishing this huge task.

At this moment of accomplishment, I would like to thank my professor supervisors Elena Lopez Lago and Raúl de la Fuente Carballo for giving me the opportunity to work with them, for their guidance, support, and mentorship. Elena and Raúl were always available to help me with the highest level of professionalism, as well as immaculate technical and theoretical knowledge.

I would also like to express my gratitude for all my colleagues in the group that helped me to succeed, Yago, Damián, and Hatem.

A massive thanks are due to all my friends that made me feel like I never left home; they will always have a place in my heart. Thanks for all the people that helped and supported me during the study.

I would like to thank my father, my mother; they are always there for me. They made me who I am today, and if was not for them, I would not be able to be where I am today. They are the ones that deserve my deepest gratitude. The end of this stage in my life is for them.

I would like to thank my brothers, Mohammad, Omar, Ali and Huthayfah, and my sisters, for supporting me spiritually throughout writing this thesis and my life in general.

And my biggest thanks to my small family for all the support you have shown me through this research, the culmination of five years of learning. For my children, Besan, Mariah, and Suhib, sorry for being even grumpier than normal while I wrote this thesis! And for my wife Sana'a, thanks for all your support, without which I would have stopped these studies a long time ago. Words would never say how grateful I am. I consider myself the luckiest in the world to have such a lovely and caring family, standing beside me with their love and unconditional support.

Contents

USC
UNIVERSIDADE
DE SANTIAGO
DE COMPOSTELA

USC
UNIVERSIDADE
DE SANTIAGO
DE COMPOSTELA

1 Introduction

1.1 IONIC LIQUIDS

Ionic liquid (IL) is the generic term for a kind of materials consisting entirely of oppositely charged ions that are in a liquid state below 100 ºC. The nature of the existing bonds leads to weak interactions resulting in their characteristic low melting points contrary to the observed in common inorganic salts.

The melting point is determined by the strength of a crystalline lattice, that depends on factors such as intermolecular forces (ionic bonds, hydrogen bonds,…), molecular symmetry or conformational degrees of freedom of a molecule, for example. The charge distribution on the ions and hydrogen bonding ability strongly influence melting points. The origin of the low melting points of ionic liquids lies fundamentally in the difference in the size of the ions that leads to weaker attractive forces between cations and anion and reduces the lattice energy. In fact, in ionic liquids, the charge is more spread out than in typical inorganic salts such as sodium chloride, which are solid at room temperature [1, 2]. This characteristic implies that many of the synthesized ionic liquids such as 1-butyl-3-methylimidazolium tetrafluoroborate or 1-Butyl-3-methylimidazolium Bis(trifluoromethylsulfonyl) imide, for example, are in liquid state at 298 K, that is why they are called room-temperature ionic liquids.

The first real inorganic molten salt (ionic salt) synthesis dates back from 1888 when ethanolammonium nitrate, with a melting point close to 323 K, was synthesized by S. Gabriel and J. Weiner [3]. Later, in

1914, P. Walden [1] created ethylammonium nitrate with a melting point of 285 K. In the 70s and 80s pyridinium cations combined with halogen anions were synthesized with the aim of being used as electrolytes in batteries [4, 5], or in catalytic reactions [6], like Diels−Alder reactions and alkylation of sodium β-naphthoxide [7, 8]. The reactions showed a strong preference and an acceleration of the reaction (greater than nonpolar organic solvents). Although the increased rate and selectivities were not as great as those seen in the water, the ionic liquid has the advantage that moisture-sensitive reagents may be used.

In the 90s more stable ionic liquids including the hexafluorophosphate anion and the boron tetrafluoride anion were synthesized, but even though the stability was greater, they were toxic [9, 10]. The advances in the field of synthesis lead in 2004 to the production of the first magnetic ionic liquid by Satoshi Ishii showing a strong response to magnetic fields; this has opened an entirely new field in magnetism of liquids[11]. It is currently known that, given the catalog of available anions/cations, trillions of ionic liquids may be synthesized.

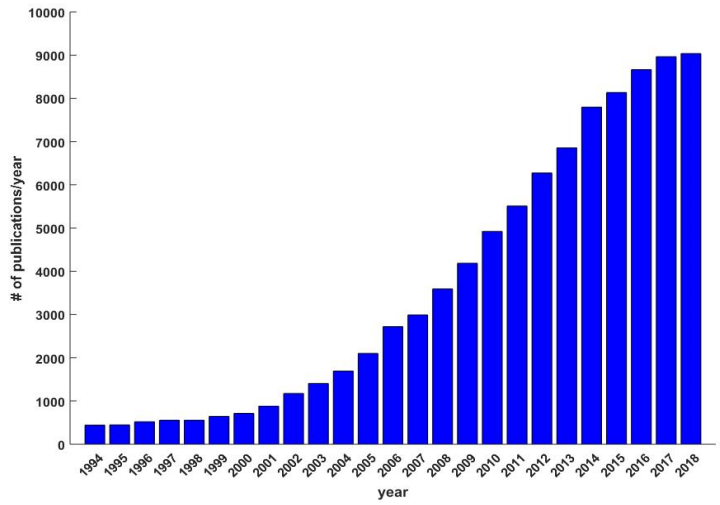

Figure 1.1 Scientific publications about ionic liquids per year in the past 25 years. (Data extracted from http://wcs.webofknowledge.com).

The growth rate of published papers related to ILs has increased quickly from 2004 until now as it is shown in Figure 1.1. During this time, the main aims of the researchers were to reduce the toxicity, making the ionic liquid environmentally friendly, and to increase the stability.

1.1.1 Thermophysical properties

The properties of these compounds are linked to their chemical composition so it is possible the design of an ionic liquid with desired properties by an adequate ionic combination [12]. The most valued properties are:

Low volatility: volatility measures the ability of a substance to evaporate; ionic liquids have practically negligible vapor pressure, less than 10^{-8} bar at ambient conditions or even 373 K, that means they do not evaporate [13, 14].

High thermal stability at high temperatures: the thermal stability is the ability of a compound to resist decomposing when heated. This characteristic joined to their low volatility, make them useful as thermal fluids [15].

High viscosity: viscosity measures the resistance of a fluid to flow; ionic liquids have high viscosity, usually greater than 100 cp, so molecules forming ILs have low mobility. The mobility increase with temperature so viscosity decrease with it [16].

High electrical conductivity: Electrical conductivity is related to the power of a material to conduct electricity. The ionic liquids have electrical conductivity higher than other liquids, so they are promising candidates as electrolytes in batteries, fuel cells, solar cells and capacitors [17-23].

Density: the density of the ionic liquids, greater than the density of water [17, 24, 25], depends strongly on temperature, as it is expected in liquids. The variation on density also induces changes in the refractive index.

Solvent capabilities: ILs have been used as a solvent for many types of reactions. Due to its ability to dissolve both polar and apolar substances, ILs let largely expand the catalog of solvents. The advantage of using ILs instead of common solvents is that the reaction rate is faster than that of a conventional organic solvent. Another advantage is that the mixture ILs catalyst used can be reused. Therefore, due the high probability that exists of being able to synthesize an ionic liquid with properties a priori determined, ILs have been recognized as designer-solvents [6, 26-28].

1.1.2 Applicability

ILs have been proposed for multiple applications in different fields such as chemistry, biotechnology, mineralogy, engineering, and pharmaceutical science. Some of these applications are:

- the use as solvents in non- aqueous reactions [29],
- to dissolve cellulose in wood processing [30, 31],
- to produce biofuel from algae [32],
- as absorbents for absorption heat pumps [33, 34],
- in radioactive nuclear waste processing [35],
- in carbon capture and storage [36, 37],
- in chemical processing as lubricants and in hydraulics [38],
- in metal processing,
- in separation and distillation processing[39],
- as electrolytes in the batteries [40, 41],
- as supercapacitor and solar cells [36, 42],
- as stationary phases for gas chromatography[43],

- as a filler between the glass/glass-ceramic grains, that enhances the ionic conductivity significantly. So they appear promising for Li^+ ion battery applications. [44],
- as compounds extraction for pharmaceutical, nutritional, and cosmetic applications [45-47].

Some ionic liquids play an important role in green chemistry which stands for high efficiency environmentally friendly processes with a reduced amount of toxic substances. A lot of studies about toxicity and ecotoxicity of ionic liquids that have been reported revealed that ionic liquids are good candidates as green solvents [48-53]; these properties have been evaluated through different models, even involving microorganisms.

Although they do not evaporate, most of them are toxic, for example, in the aquatic medium. The cytotoxic, environmental, and microbial toxicity of the most common ILs been studied [54-56]. Life-cycle analysis of ILs with more emphasis on recycling has been proposed by the research community. And, it is imperative to evaluate the toxic effects of ILs and determine their further consequences to environmental fate, to find ionic liquids efficient but eco-friendly.

On the other hand, ionic liquids are potential candidates to take part in tunable optics and photonic devices, because of their unique properties in particular as design solvents. The consideration of ionic liquids as optical materials requires precise knowledge of its optical behavior to ensure the optimal performance of a particular optical device. For example, an accurate measurement of fundamental properties as refractive index dispersion as well as optical absorption is essential for many applications in different fields such as optical imaging, optical communication, integrated optics, laser technology, optical sensing and so on. That even though ILs present high absorbance in the UV region, they are transparent in the visible and near IR region. So in this spectral range, the refractive index is very relevant optical parameter.

Along these years of study of ILs, the sensitivity of the refractive index to impurities, water content, or chemical processes that develop specifically in the ionic liquid, like hydrolysis, has been demonstrated. The water content that results from water absorption from the environment reduces significantly the refractive index value and makes impossible the reproducibility of the data since the water concentration varies with the passage of time. In order to avoid these disadvantages, it is necessary to work with high purity ionic liquids as well as to dry the liquids well and to measure with accuracy the amount of residual water that remains after the drying process.

1.1.3 Refractive index

The knowledge of the refractive index and its dependence with wavelength and temperature are crucial at the time of choosing ionic liquids for a given optical application. A lot of published papers deal with the measurement of the refractive index, in general, at a given wavelength; in fact, most of the commercial devices generally measure the refractive index at a single wavelength, commonly at the sodium *D* line (λ_D=589.3nm): for example, Kim *et al*. [57] measured the refractive indices of two pure ionic liquid in the temperature range of 298.2–323.2 K; Gomez *et al*. [58] measured the refractive indices for 1-hexyl-3-methylimidazolium chloride, and 1-methyl-3 octylimidazolium chloride in the temperature range of 298.15–343.15 K.; Pereiro *et al*. [59] measured the refractive indices of ionic liquids based on 1-alkyl-3- methylimidazolium cation and hexafluorophosphate in the temperature range of 278.15–343.15 K.

Seki *et al*. [60] measured the refractive index for 17 types of room-temperature ionic liquids in the temperature range between 283.15 and 353.15 K, and correlated them with the polarizability predicted by ab initio calculations; Deetlefs *et al*. [61] measured the refractive indices of some 1-alkyl- 3-methylimidazolium based ionic liquids containing polyhalide anions, which have high refractive

indices between 1.6 and 2.23, using optical microscopy and interferometry.

Other studies explore the relationship between the refractive index values and the structural parameters of the ionic liquids, like the cationic and the anionic part and analyze their dependence on temperature. Tariq *et al*. [62] measured the refractive indices of 17 ionic liquids based on 1-alkyl-3-methylimidazolium cation combined with different anions in the temperature range of 293–333 K and determined the effect of the temperature, the alkyl chain length of the 1-alkyl-3 methylimidazolium cation, and the nature of the anion. Bouzón-Capelo *et al*. [63] measured the refractive indices of alkylammonium nitrate-based ionic liquids (ethyl ammonium, propylammonium, and butylammonium nitrate) in the temperature range between 283 and 313 K and they studied the effect of the cationic chain length and showed the influence of the degree of hydrogen bonding.

Besides, other authors analyzed the mixture of ionic liquids with other solvents: Pereiro *et al*. [64] measured the refractive indices of the pure ionic liquid 1-hexyl-3-methylimidazolium hexafluorophosphate in the temperature range from 288.15 to 318.15 K; they also measured the refractive indices in terms of the molar fraction of the compounds of the binary mixtures involving dimethyl carbonate (DMC), diethyl carbonate (DEC), acetone, 2-butanone, 2-pentanone, methyl acetate, ethyl acetate, and butyl acetate + (1-hexyl-3-methylimidazolium hexafluorophosphate) at 298.15 K and atmospheric pressure. Rilo *et al*. [65] measured the refractive index of mixtures with different concentrations of 1-alkyl-3-methyl imidazolium tetrafluoroborate with water or ethanol. Rodil *et al*. [66] measured the refractive index of five ionic liquids (tributylmethylphosphonium and methylsulfate based ionic liquids) at a temperature range between 283.15 and 343.15 K at atmospheric pressure and investigated the effect of the ion composition and temperature on the thermophysical properties.

Nevertheless, to achieve a deeper understanding of these materials, a dispersion analysis is mandatory with a view to using them in optical applications. This property, that stands for the refractive index dependence with wavelength, is essential at the time of designing optofluidic devices such as liquid-core optical fibers, variable focus lenses or crystal analysis, for example [61, 67, 68].

Some studies concern with the measurement of the refractive index at several wavelengths and with the analysis of dispersion. Fröba *et al.* [69] determine the refractive index at the sodium line (589.3 nm) and the refractive index difference n_F- n_C for the Fraunhofer lines *F* (486.1 nm) and *C* (656.3 nm) at temperatures between 283.15 and 313.15 K. Calixto *et al.* [70] measured the refractive index at some specific wavelengths in the visible range at room temperature. Nóvoa-López *et al*. [71] calculated the refractive index values at six wavelengths between 475 - 680 nm and studied the influence of the structural parameters of alkyl-ammonium-based ILs and 1-butyl-3-methylimidazolium based ILs ($[C_{2,3,4,6}N][NO_3]$, $[C_3C_1Im][NO_3]$ $[C_{2,4,6}C1Im][NTf_2]$, $[C_2C_2C_1N][C_1SO_3]$, $[C_2C_2C_1N][OTf]$, $[C_2N][OF]$, $[C_4C_1Im][BF_4]$, $[C_4C_1Im][C_1SO_4]$) on the refractive index.

Chiappe *et al*. [72] determine the refractive index of 1-alkyl- 3-methylimidazolium based ionic liquids (alkyl = methyl, butyl and hexyl) combined with dimethyl phosphate, methyl phosphonate and methyl methylphosphonate, at five wavelengths (450, 532, 632.8, 964, 1551 nm) in the temperature range between 293 - 353 K. Arosa *et al*. [73] studied the refractive index of 14 ILs over a wide continuum Vis- NIR spectrum but at a constant temperature (300.15 K) by using a variant of Spectrally Resolved White Light Interferometry (SRWLI) assisted with an Abbe refractometer, that we call Refractive index spectroscopy by broadband interferomery (RISBI).

Parameters derived from the wavelength-dependent refractive index such as Abbe number, group velocity dispersion, third-order dispersion as well as their variation with temperature are crucial at the time of finding applications of these materials in fields such as ultrafast optics or optical communications.

Nevertheless, the great variety of synthesized ILs makes impracticable an experimental screening, so the development of predictive models to understand how structural and ambient parameters affect the optical properties are imposed. In a recent paper, [74] we report a model that describes the dependence of the refractive index as a function of wavelength and temperature of 1-alkyl-3-methylimidazolium-based ionic liquids with, tetrafluoroborate $[BF_4]^-$, bis(trifluoromethylsulfonyl)imide $[NTf_2]^-$ or trifluoromethanesulfonate $[OTf]^-$. The model, based on a single resonance Sellmeier equation, allows the identification, through the analysis of the fit parameters, of trends and behaviors that are related to the structure of the material. The developed model simplifies the determination of important macroscopic and microscopic wavelength-dependent properties such as the thermooptic coefficient, Abbe number or polarizability, in this case through the Lorentz-Lorenz equation [75].

1.1.4 Thermo-optic coefficient

Thermo-optic coefficient (TOC) is defined as the changing rate of the refractive index concerning temperature variation. The simultaneous measurements of temperature and refractive index are considered as being somewhat meaningful to investigate the optical properties of ILs because the refractive index of liquids is strongly dependent on the temperature [76]. There is a great variety of research about the ILs that study directly or indirectly this property at one wavelength, often at 589.3nm [77-80]. Although we know that the thermo-optic coefficient uses to be less dispersive than the refractive index, at least in the visible spectral region, it is interesting to study this behavior and spread the study to other spectral regions, such as the near-infrared region. Many researchers used the Z-scan technique [81] to characterize the thermal lens effect (TLE) caused by refractive index changes induced by irradiation with laser pulses [82], since starting from the strength of the thermal lens its is possible to determine the thermo-optic coefficient.

Tran *et al*. [83] have successfully demonstrated that ILs can be used as an attractive solvent for thermal lens measurements. It was found that ILs provide a better medium for thermal lens measurements than water, as they have relatively high solubility power. And they found that the substantial increase in their *dn/dT* values gives additional sensitivity enhancement. They used ionic liquids constituted the 1-butyl-3-methyl imidazolium cation, $[C_4MIm]^+$, combined with three anions ($[BF_4]^-$, $[NTf_2]^-$, $[PF_6]^-$) in their study. Souza *et al*. [84] studied experimentally nonlinear optical properties of thermal origin in two different ionic liquids (1-butyl-3-methylimidazolium tetrafluoroborate, [BMIm][BF_4], and 1-butyl-3-methylimidazolium hexafluorophosphate, [BMIm][PF_6]) by using the Z-scan technique for two excitation wavelengths, 514 and 810 nm, at room temperature, and also evaluated the thermo-optical coefficients of both compounds. Valencia –Loredo *et al*. [85] have studied the nonlinear optical characterization of four ionic liquids, namely [C_4MIm][BF_4], [C_2MIm][TF_2N], [C_2MIm][CF_3COO] and [C_4MIm][CF_3COO], by using Z-scan technique.

Santos *et al*. [86] have investigated the influence of the anionic and cationic parts on the nonlocal nonlinearity of ionic liquids by using the same technique, and they obtained the thermo-optical coefficients. Santos *et al*. [87] have also investigated the thermooptical effect under violet excitation at 410 nm for ionic liquids with the $[NTf_2]^-$ anion combined with four different imidazolium-based cations ($[C_{Nc}MIm]$, with *Nc* = 4, 6, 8, and 10). Nóvoa-López *et al*. [88] used the Z-scan technique to characterize the nonlinear refraction induced by a train of ultrashort laser pulses (80 fs, repetition-rate 80.75MHz, λ= 800 nm) for a set of ionic liquids as a function of the structural parameters such as cation, anion type, and alkyl chain length in the cation. They also measured linear absorption and thermal conductivity to determine the thermo-optic coefficient of ILs.

1.1.5 Abbe number

Abbe number (ν-number) is a measure of the material dispersion. It is a dimensionless parameter used to classify optical materials, the design of achromatic lenses and other applications. Abbe number take values from below 25 for very dense flint glasses and 75 to 90 for some fluorite and phosphate crown glasses [89]. High values of the Abbe number indicate low dispersion.

To calculate Abbe number, the refractive indices of optical materials must be measured at some specific wavelengths like blue hydrogen *F* line (486.1 nm), yellow sodium *D* line (589.3 nm), red hydrogen *C* line (656.3 nm). The Abbe number is usually defined for the *D* line as:

$$v_D = (n_D - 1)/(n_F - n_C) \qquad (1.1)$$

The difference between the refractive index at the blue hydrogen *F* line and the red hydrogen *C* line is called the principal dispersion[90].

Usually, Abbe number is plotted versus the corresponding values of refractive index; this plot is known as the Abbe diagram and it gives a qualitative idea about the chromatic dispersion of the liquids.

Calixto *et al*. [70] determined the Abbe number of six ionic liquids, ([C_2MIm][NTf_2], [C_2MIm][TA], [C_4Py] [NTf_2], [C_4MIm][NO_3], [C_4MIm][PF_6], and [C_1Pyrr][HSO_4]) with the object of fabricating variable focus liquid lenses.They plotted them in an Abbe diagram together with water and some glasses, showing that most of the ionic liquids have a lower refractive index than the common glasses.

Fröba *et al*. [69] characterized the principal dispersion of three pure -ethyl-3-methylimidazolium-based ionic liquids, [C_2MIm][NTf_2], [C_2MIm][C_2SO_4] and [C_2MIm] [$N(CN)_2$], as well as a tetraalkylammonium-based IL, [OMA][NTf_2]. Nóvoa-López *et al*. [88]

reported the characterization results of the refractive index of five alkylammonium-based ILs and five 1-butyl-3 methylimidazolium-based ILs together with the corresponding Abbe number. The measurement has been done by using the angle of minimum deviation technique and by multiwavelength Abbe refractometry at a temperature equal to 293 K.

Arosa *et al*. [73] plotted 14 ionic liquids in an Abbe diagram to study the optical effect that different anions have over the imidazolium-based cations.

1.1.6 Group velocity

The refractive index dependence on wavelength generates spectral and temporal effects on an optical pulse that lead to spectral broadening and chirp. Both of these effects play major roles in ultrafast optics and pulse propagation in optical fibers and waveguides. The role of the refractive index in these effects is that the dispersion causes the different spectral components of a polychromatic beam travel with different velocities.

In analogy to refractive index, group index n_g is defined as the ratio of the speed of light in a vacuum to the group velocity in a medium. The group velocity (v_g) of the pulse is the velocity with which the wave packet propagates through the medium. n_g is obtained from the refractive index value by using equation (1.2) where we expect that the value of the group refractive index in the visible or near-infrared spectral range is larger than the refractive index since the ionic liquids are transparent in this spectral range:

$$n_g = n - \lambda \frac{\partial n}{\partial \lambda} \qquad (1.2)$$

1.1.7 Group velocity dispersion

Group velocity dispersion (GVD) is the phenomenon that accounts for the dependence of the group velocity on the wavelength or, alternatively, frequency. It plays a determinant role in optical communication systems, femtosecond technology, and so on. It is usually quantified by two parameters D and β_2, defined as:

$$\beta_2 = \frac{\lambda^3}{2\pi c^2}\left(\frac{\partial^2 n}{\partial \lambda^2}\right) \tag{1.3}$$

$$D = \frac{1}{c}\left(\frac{\partial n_g}{\partial \lambda}\right) = -\left(\frac{2\pi c}{\lambda^2}\right)\beta_2 \tag{1.4}$$

The units of D are ps/nm/ km and the units of β_2 are usually s^2/m. GVD may be considered the main responsible for changes in the shape of the temporal pulse envelope.

The GVD of many liquids has been characterized by using different methods. Coello *et al*. [91] measured the second- and third-order dispersion of water, seawater, and ocular components in the range of 660–930 nm using a multiphoton intrapulse interference phase scan. Scarborough *et al*. [92] measured the group velocity dispersion(GVD) of water and methanol at 800 nm by using direct imaging methods.

Coello *et al*. [93] presented a number of multiphoton intrapulse interference phase scan (MIIPS) for directly measuring the second derivative of the spectral phase, and they also describe accurate spectral phase measurements. From these data they obtained the group-velocity dispersion (GVD) of water and seawater. It has been obtained with an accuracy comparable only to that of white-light interferometry. The measurements were carried out by transmitting an ultra broad-band width femtosecond laser (wavelength 620–1025 nm) through water-containing cuvettes. Wrzesinski *et al*. [94] measured the second- and

third-order dispersion values for nitrogen, oxygen, air, carbon dioxide, ethylene, acetylene, and propane within the 700–900 nm range by using an ultra-broadband-laser source. Up to our knowledge, these properties have not been reported for ionic liquids.

1.1.8 Third-order dispersion

Third-order dispersion (TOD) results from the frequency dependence of the Group velocity dispersion. Its effects use to be weaker than the produced by GVD except in the region where GVD is minimum, causing distortions in a pulse like, for example, an asymmetric temporal broadening in a symmetrical input pulse.

TOD became critical when the optical pulses become narrower to accommodate higher data rates since it is more susceptible to higher-order dispersion. The propagation of short pulses depends on managing the group velocity dispersion in the medium. Dispersion results in unwanted pulse broadening, so it is necessary to calculate Dispersion not only for the group delay dispersion but also for the third-order dispersion [95].

We can find the expression of the third-order dispersion (TOD) by deriving equation (1.3) to get the expression shown in equation (1.5):

$$TOD = \frac{\partial(GVD)}{\partial\lambda} \tag{1.5}$$

whose units in the international system are s^3/m, being *c* the speed of light. Related to TOD is the dispersion parameter *S* defined as:

$$S = \frac{\partial D}{\partial\lambda} \tag{1.6}$$

whose units are $ps/nm^2/km$.

1.1.9 Polarizability

Polarizability is a relevant magnitude at the time of explaining physicochemical processes that takes part in different material properties. It is an indicator of how easily the electronic cloud of an atom or molecule is distorted when an electric field is applied. Large and diffuse electronic clouds make the molecules more polarizable. Polarizability is proportional to molar refraction, R_m[96] that it is related to the refractive index, n, through the Lorentz-Lorenz equation:

$$\frac{n^2 - 1}{n^2 + 2} = \frac{R_m}{V_m} \tag{1.7}$$

Where V_m is the molar volume. Molar refraction can be estimated if the refractive index and molar volume are known. V_m can be easily calculated, starting from the values of the molar mass of a substance (M) and its density (ρ).

Computational simulations are often used to estimate the electronic polarizability of a compound and thus predict its refractive index. The experimental values of electronic polarizability obtained through experimental refractive index provide a test of the validity of these computational models. This is surely important for computational tuning of ionic liquids.

Scaife *et al*. [97] computed the values of the volume occupied per molecule V_m, and polarizability α_m per molecule of n-alkane liquids at different pressures and temperatures. Izgorodina *et al*. [98] calculated the electronic polarizabilities of 27 ionic liquid of different symmetry and size and used it to obtain the electronic polarization contribution to the dielectric constants of six ionic liquids. They concluded that a contribution from a form of ‘‘ionic polarization’’ must be present. Seki *et al*. [60] performed ab initio calculations to yield theoretical polarizability of the respective ionic liquid composing ions. They found a highly linear correlation between the experimental refractive index and the predicted polarizability normalized in terms of the molar volume.

Bica *et al*. [99] extracted the molar polarizability and molar volume of 71 ionic liquids and classify the ionic liquids in two classes, 1 or 2, depending on whether the value of ratio between the molar polarisability and molar volume is higher or lower than the corresponding ratio for CH_2 (0.0661 for λ=598.3nm), respectively. Class 1 comprises ionic liquids with highly polar anions such as sulfates or thiocyanates whose refractive index decrease as the alkyl chain does; whereas Class 2 comprises ionic liquids containing, for example, $[BF_4]^-$, $[NTf_2]^-$ and their refractive index increases when the alkyl chain does.

Díaz-Rodríguez *et al*. [100] used statistical models to estimate the refractive index of 72 imidazolium-based ionic liquids using the electronic polarizability of their ions as input data. They use two different mathematical methods: linear regression models and artificial neural networks (in the form of multi-layer perceptrons). They found that the multi-layer perceptron model has been shown to be a more accurate method.

Almost all the theoretical and experimental studies dealt with calculating the polarizability at a giving wavelength, λ_D=589.3 nm except the recent work of Arosa *et al*. [73] that report, for the first time, the electronic polarizability of 14 ILs by using the refractive index data measured over a wide spectral band from 400 to 1000 nm.

1.2 MOTIVATION:

In the development and optimization of ionic liquid-based optical devices for different applications such as optical imaging, optical guiding or ultrafast optics, the knowledge of optical and thermophysical properties of ILs is essential. Although the thermophysical properties of ionic liquids are, in general, well known, systematic optical studies are scarce. The efficiency of this kind of devices relies, among other factors, on the knowledge of properties such as density and refractive index and the influence of the environmental conditions. A depth study about refractive index can help the designers to choose the most appropriate compound for a given optical function. It must be highlighted that to achieve a deeper understanding of these materials; a dispersion analysis is mandatory. This property, which stands for the refractive index dependence with wavelength, is essential at the time of designing optofluidic devices, such as liquid-core optical fibers or variable focus lenses, and methods for refractive index crystal analysis, for example. Dispersion studies are also important for finding applications of these materials in fields such as ultrafast optics or optical communications.

A rigorous dispersion characterization requires to measure the refractive indices in a broad enough spectral range, not at single wavelengths as most of the published papers about this property report. The implementation in our laboratory of a system based in Refractive Index Spectroscopy by Brodband Interferometry (RISBI) designed for optical measurements propitiates the realization of these novel study in the field of ionic liquids. This technique allows measuring with high accuracy the refractive index as a quasi continuous function of the wavelength over a broad spectral band with a resolution less than 1 nm at several temperatures. More information about this technique is given in Chapter 2.

The great variety of synthesized ILs makes unfeasible an experimental screening, so the development of predictive models to describe how structural and ambient parameters affect the optical

properties is imposed. One of them, that is based on a single resonance Sellmeier equation, has been recently published by us [74]. It has been proven to describe with great accuracy the dependence of the refractive index on wavelength and temperature of 1-alkyl-3-methylimidazolium-based ionic liquids containing $[BF_4]^-$, $[NTf_2]^-$ or $[OTf]^-$ anions, but we consider that its use can be extended to other alkyl-methyl imidazolium ionic liquids. The existence of this model allows calculating the parameters derived from the temperature and wavelength dependence such as thermooptic coefficient (TOC), Abbe number (ν_D), group index (n_g), group velocity dispersion (GVD) or third-order dispersion (TOD),

On the other hand, it is well known the influence of the alkyl chain in the refractive index of ionic liquids, so if we are able to modelize this influence in the Lorentz-Lorenz equation through the molar volume and the molar refractivity, we expect to find a predictive model.

This Ph.D. thesis was carried out within the framework of two research projects:

Caracterización óptica de líquidos y geles iónicos para su aplicación en dispositivos fotónicos y electróquímico/ Optical characterization of ionic liquids and gels for application in photonic and electrochemical devices (MAT2014-57943-C3-2-P).

Materiales inteligentes para los retos electroquímicos y fotónicos: líquidos iónicos e ionogeles híbridos/ Smart materials for elecytchemical and photonic challenges: ionic liquids and hybrid ionogels (MAT2017-89239-C2-1-P).

The contribution to the first project was the characterization of a wide set of ionic liquids of different families and to assess the reproducibility of the data extracted by RISBI and Abbe refractometry. The contribution to the second project was, on the one side, the development and application of an analytical model that allows calculating with enough accuracy different properties related to the refractive index such as thermooptic coefficient, group index, and second and third-order dispersion; and, on the other side, the

development of simple models that allows to know how much the refractive index varies with the alkyl chain length.

This manuscript is structured in four chapters. The first one is an introductory chapter. In the second chapter, we present the materials under study together with relevant information for the recearch we want to carry out. This chapter is also devoted to the description of the commercial apparatus and standard techniques used as well as the non-commercial technique based on RISBI that allows determining the refractive indices over a large spectral band from 400 to 1000 nm.

In the third chapter, we present the results of the research developed during these years that was mainly centered on the characterization of the refractive index dependence with wavelength of 20 ionic liquids. Starting from these data we calculate other dispersive parameters: like Abbe number, group index, group velocity dispersion, third-order dispersion and the dispersion of the thermoptic coefficient. We applied a single resonance Sellmeier model to describe the refractive index and some of the parameters, and we check its validity. We use the Lorentz-Lorenz equation to build a simple model that describes the evolution of the refractive according to the increase of the number of carbons in the alkyl chain length. We analyze the ensemble of data to identify trends and behaviors that shed light on the influence of the structure of these materials in the studied optical properties.

Finally, in the last chapter, we summarize the conclusions reached with this analysis.

1.3 OBJECTIVES:

The main aim of this Ph.D. Thesis is to perform an experimental study of ionic liquids, through the analysis of several optical and thermophysical properties. Specific objectives of this Ph.D. Thesis are:

- To measure the refractive index in a wide set of ionic liquids by Abbe refractometry and RISBI as a function of wavelength and temperature. In a spectral interval comprising a range of wavelengths from 400 to 1000 nm at several temperatures between 298.15 and 323.15 K.

- To check the validation of a model based on the Sellmeier equation whose fitting parameters provide valuable physical information about the liquids.

- To calculate dispersive parameters that are relevant for several optical applications such as the Abbe number, group index, second and third-order dispersions as well as the Thermo optic coefficient.

- To analyze the influence of the structure of the ionic liquids (anion, cation, the number of carbons) in the refractive index and derived parameters.

- To derive a predictive model derived from the Lorentz Lorenz equation that stands for the dependence of the refractive index with the length of the alkyl chain that account.

1.4 REFERENCE:

[1] P. Walden, "Molecular weights and electrical conductivity of several fused salts," *Bull. Acad. Imper. Sci.(St. Petersburg),* vol. 1800, 1914.

[2] C. Reichardt, "Solvents and solvent effects: an introduction," *Organic process research & development,* vol. 11, no. 1, pp. 105-113, 2007.

[3] S. Gabriel and J. Weiner, "Ueber einige abkömmlinge des propylamins," *Berichte der deutschen chemischen Gesellschaft,* vol. 21, no. 2, pp. 2669-2679, 1888.

[4] K. M. Dieter, C. J. Dymek, N. E. Heimer, J. W. Rovang, and J. S. Wilkes, "Ionic structure and interactions in 1-methyl-3-ethylimidazolium chloride-aluminum chloride molten salts," *Journal of the American Chemical Society,* vol. 110, no. 9, pp. 2722-2726, 1988.

[5] J. S. Wilkes, J. A. Levisky, R. A. Wilson, and C. L. Hussey, "Dialkylimidazolium chloroaluminate melts: a new class of room-temperature ionic liquids for electrochemistry, spectroscopy and synthesis," *Inorganic Chemistry,* vol. 21, no. 3, pp. 1263-1264, 1982.

[6] T. Welton, "Room-temperature ionic liquids. Solvents for synthesis and catalysis," *Chemical reviews,* vol. 99, no. 8, pp. 2071-2084, 1999.

[7] M. Badri, J.-J. Brunet, and R. Perron, "Ionic liquids as solvents for the regioselective O-alkylation of C/O ambident nucleophiles," *Tetrahedron letters,* vol. 33, no. 31, pp. 4435-4438, 1992.

[8] D. A. Jaeger and C. E. Tucker, "Diels-Alder reactions in ethylammonium nitrate, a low-melting fused salt," *Tetrahedron Letters,* vol. 30, no. 14, pp. 1785-1788, 1989.

[9] H. C. áDe Long, "Structure of 1-ethyl-3-methylimidazolium hexafluorophosphate: model for room temperature molten salts," *Journal of the Chemical Society, Chemical Communications,* no. 3, pp. 299-300, 1994.

[10] J. S. Wilkes and M. J. Zaworotko, "Air and water stable 1-ethyl-3-methylimidazolium based ionic liquids," *Journal of the Chemical Society, Chemical Communications*, no. 13, pp. 965-967, 1992.
[11] S. Hayashi and H.-o. Hamaguchi, "Discovery of a magnetic ionic liquid [bmim] FeCl4," *Chemistry Letters*, vol. 33, no. 12, pp. 1590-1591, 2004.
[12] M. Freemantle, *An introduction to ionic liquids*. Royal Society of chemistry, 2010.
[13] D. Kuang, P. Wang, S. Ito, S. M. Zakeeruddin, and M. Grätzel, "Stable mesoscopic dye-sensitized solar cells based on tetracyanoborate ionic liquid electrolyte," *Journal of the American Chemical Society*, vol. 128, no. 24, pp. 7732-7733, 2006.
[14] S.-Y. Ku and S.-Y. Lu, "Inexpensive room temperature ionic liquids for low volatility electrolytes of dye-sensitized solar cells," *Int. J. Electrochem. Sci*, vol. 6, no. 11, pp. 5219-5227, 2011.
[15] V. Kamavaram and R. G. Reddy, "Thermal stabilities of di-alkylimidazolium chloride ionic liquids," *International Journal of Thermal Sciences*, vol. 47, no. 6, pp. 773-777, 2008.
[16] A. Pensado, M. Comunas, and J. Fernández, "The pressure–viscosity coefficient of several ionic liquids," *Tribology Letters*, vol. 31, no. 2, pp. 107-118, 2008.
[17] J. Fernández and F. Gaciño, "Properties and Green Aspects of Ionic Liquids," *Ionic Liquids in Separation Technology, Elsevier*, pp. 3-12, 2014.
[18] A. Lewandowski and A. Świderska-Mocek, "Ionic liquids as electrolytes for Li-ion batteries—an overview of electrochemical studies," *Journal of Power sources*, vol. 194, no. 2, pp. 601-609, 2009.
[19] H. Ohno, *Electrochemical aspects of ionic liquids*. John Wiley & Sons, 2005.
[20] T. Tamura, T. Hachida, K. Yoshida, N. Tachikawa, K. Dokko, and M. Watanabe, "New glyme–cyclic imide lithium salt complexes as thermally stable electrolytes for lithium batteries,"

Journal of Power Sources, vol. 195, no. 18, pp. 6095-6100, 2010.

[21] M. Gorlov and L. Kloo, "Ionic liquid electrolytes for dye-sensitized solar cells," *Dalton Transactions,* no. 20, pp. 2655-2666, 2008.

[22] C. Pinilla, M. G. Del Pópolo, R. M. Lynden-Bell, and J. Kohanoff, "Structure and dynamics of a confined ionic liquid. Topics of relevance to dye-sensitized solar cells," *The Journal of Physical Chemistry B,* vol. 109, no. 38, pp. 17922-17927, 2005.

[23] T. Yasuda and M. Watanabe, "Protic ionic liquids: fuel cell applications," *MRS bulletin,* vol. 38, no. 7, pp. 560-566, 2013.

[24] F. l. M. Gaciño, T. Regueira, L. Lugo, M. a. J. Comuñas, and J. Fernández, "Influence of molecular structure on densities and viscosities of several ionic liquids," *Journal of Chemical & Engineering Data,* vol. 56, no. 12, pp. 4984-4999, 2011.

[25] T. Regueira, L. Lugo, and J. Fernández, "Influence of the pressure, temperature, cation and anion on the volumetric properties of ionic liquids: New experimental values for two salts," *The Journal of Chemical Thermodynamics,* vol. 58, pp. 440-448, 2013.

[26] T. Méndez-Morales, J. s. Carrete, O. s. Cabeza, O. Russina, A. Triolo, L. J. Gallego, and L. M. Varela, "Solvation of lithium salts in protic ionic liquids: a molecular dynamics study," *The Journal of Physical Chemistry B,* vol. 118, no. 3, pp. 761-770, 2014.

[27] J. N. Canongia Lopes, M. F. Costa Gomes, and A. A. Pádua, "Nonpolar, polar, and associating solutes in ionic liquids," *The Journal of Physical Chemistry B,* vol. 110, no. 34, pp. 16816-16818, 2006.

[28] A. Triolo, O. Russina, H.-J. Bleif, and E. Di Cola, "Nanoscale segregation in room temperature ionic liquids," *The Journal of Physical Chemistry B,* vol. 111, no. 18, pp. 4641-4644, 2007.

[29] V. P. Böhm and W. A. Herrmann, "Nonaqueous Ionic Liquids: Superior Reaction Media for the Catalytic Heck-Vinylation of

Chloroarenes," *Chemistry–A European Journal,* vol. 6, no. 6, pp. 1017-1025, 2000.

[30] A. Pinkert, K. N. Marsh, S. Pang, and M. P. Staiger, "Ionic liquids and their interaction with cellulose," *Chemical reviews,* vol. 109, no. 12, pp. 6712-6728, 2009.

[31] H. Wang, G. Gurau, and R. D. Rogers, "Ionic liquid processing of cellulose," *Chemical Society Reviews,* vol. 41, no. 4, pp. 1519-1537, 2012.

[32] V. Piemonte, L. Di Paola, G. Iaquaniello, and M. Prisciandaro, "Biodiesel production from microalgae: ionic liquid process simulation," *Journal of cleaner production,* vol. 111, pp. 62-68, 2016.

[33] M. Lorenzo, M. Vilas, P. Verdia, M. Villanueva, J. Salgado, and E. Tojo, "Long-term thermal stabilities of ammonium ionic liquids designed as potential absorbents of ammonia," *RSC Advances,* vol. 5, no. 51, pp. 41278-41284, 2015.

[34] M. Villanueva, J. Parajó, P. B. Sánchez, J. García, and J. Salgado, "Liquid range temperature of ionic liquids as potential working fluids for absorption heat pumps," *The Journal of Chemical Thermodynamics,* vol. 91, pp. 127-135, 2015.

[35] S. H. Ha, R. N. Menchavez, and Y.-M. Koo, "Reprocessing of spent nuclear waste using ionic liquids," *Korean Journal of Chemical Engineering,* vol. 27, no. 5, pp. 1360-1365, 2010.

[36] D. R. MacFarlane, N. Tachikawa, M. Forsyth, J. M. Pringle, P. C. Howlett, G. D. Elliott, J. H. Davis, M. Watanabe, P. Simon, and C. A. Angell, "Energy applications of ionic liquids," *Energy & Environmental Science,* vol. 7, no. 1, pp. 232-250, 2014.

[37] M. Smiglak, J. Pringle, X. Lu, L. Han, S. Zhang, H. Gao, D. MacFarlane, and R. Rogers, "Ionic liquids for energy, materials, and medicine," *Chemical Communications,* vol. 50, no. 66, pp. 9228-9250, 2014.

[38] F. Zhou, Y. Liang, and W. Liu, "Ionic liquid lubricants: designed chemistry for engineering applications," *Chemical Society Reviews,* vol. 38, no. 9, pp. 2590-2599, 2009.

[39] J. F. Brennecke and E. J. Maginn, "Ionic liquids: innovative fluids for chemical processing," *AIChE Journal,* vol. 47, no. 11, pp. 2384-2389, 2001.

[40] A. V. Puga, "Líquidos iónicos como electrolitos estables para baterías de litio y otros dispositivos de almacenamiento de energía," in *Anales de Química,* 2012, vol. 108, no. 4.

[41] M. A. Navarra, "Ionic liquids as safe electrolyte components for Li-metal and Li-ion batteries," *MRS bulletin,* vol. 38, no. 7, pp. 548-553, 2013.

[42] A. C. Forse, J. M. Griffin, C. l. Merlet, P. M. Bayley, H. Wang, P. Simon, and C. P. Grey, "NMR study of ion dynamics and charge storage in ionic liquid supercapacitors," *Journal of the American Chemical Society,* vol. 137, no. 22, pp. 7231-7242, 2015.

[43] C. F. Poole and S. K. Poole, "Ionic liquid stationary phases for gas chromatography," *Journal of separation science,* vol. 34, no. 8, pp. 888-900, 2011.

[44] M. Rathore, A. Dalvi, A. Kumar, W. Ślubowska, and J. Nowinski, "Ionic liquid dispersed Li+ ion oxide glasses and glass-ceramics: Assessment of electrical transport and thermal stability," *Solid State Ionics,* vol. 282, pp. 76-81, 2015.

[45] J. Stoimenovski, D. R. MacFarlane, K. Bica, and R. D. Rogers, "Crystalline vs. ionic liquid salt forms of active pharmaceutical ingredients: a position paper," *Pharmaceutical research,* vol. 27, no. 4, pp. 521-526, 2010.

[46] M. Moniruzzaman and M. Goto, "Ionic liquids: future solvents and reagents for pharmaceuticals," *Journal of chemical engineering of Japan,* pp. 1103310164-1103310164, 2011.

[47] J. Azmir, I. Zaidul, M. Rahman, K. Sharif, A. Mohamed, F. Sahena, M. Jahurul, K. Ghafoor, N. Norulaini, and A. Omar, "Techniques for extraction of bioactive compounds from plant materials: a review," *Journal of Food Engineering,* vol. 117, no. 4, pp. 426-436, 2013.

[48] K. R. Seddon, "Ionic liquids for clean technology," *Journal of Chemical Technology & Biotechnology: International Research*

in Process, Environmental AND Clean Technology, vol. 68, no. 4, pp. 351-356, 1997.

[49] D. Coleman and N. Gathergood, "Biodegradation studies of ionic liquids," *Chemical Society Reviews,* vol. 39, no. 2, pp. 600-637, 2010.

[50] A. Jordan and N. Gathergood, "Biodegradation of ionic liquids–a critical review," *Chemical Society Reviews,* vol. 44, no. 22, pp. 8200-8237, 2015.

[51] M. Amde, J.-F. Liu, and L. Pang, "Environmental application, fate, effects, and concerns of ionic liquids: a review," *Environmental science & technology,* vol. 49, no. 21, pp. 12611-12627, 2015.

[52] M. Matzke, S. Stolte, K. Thiele, T. Juffernholz, J. Arning, J. Ranke, U. Welz-Biermann, and B. Jastorff, "The influence of anion species on the toxicity of 1-alkyl-3-methylimidazolium ionic liquids observed in an (eco) toxicological test battery," *Green Chemistry,* vol. 9, no. 11, pp. 1198-1207, 2007.

[53] M. Matsumoto, K. Mochiduki, and K. Kondo, "Toxicity of ionic liquids and organic solvents to lactic acid-producing bacteria," *Journal of Bioscience and Bioengineering,* vol. 98, no. 5, pp. 344-347, 2004.

[54] K. M. Docherty and C. F. Kulpa Jr, "Toxicity and antimicrobial activity of imidazolium and pyridinium ionic liquids," *Green Chemistry,* vol. 7, no. 4, pp. 185-189, 2005.

[55] R. P. Swatloski, J. D. Holbrey, S. B. Memon, G. A. Caldwell, K. A. Caldwell, and R. D. Rogers, "Using Caenorhabditis elegans to probe toxicity of 1-alkyl-3-methylimidazolium chloride based ionic liquids," *Chemical Communications,* no. 6, pp. 668-669, 2004.

[56] F. Stock, J. Hoffmann, J. Ranke, R. Störmann, B. Ondruschka, and B. Jastorff, "Effects of ionic liquids on the acetylcholinesterase–a structure–activity relationship consideration," *Green Chemistry,* vol. 6, no. 6, pp. 286-290, 2004.

[57] K.-S. Kim, B.-K. Shin, H. Lee, and F. Ziegler, "Refractive index and heat capacity of 1-butyl-3-methylimidazolium bromide and

1-butyl-3-methylimidazolium tetrafluoroborate, and vapor pressure of binary systems for 1-butyl-3-methylimidazolium bromide+ trifluoroethanol and 1-butyl-3-methylimidazolium tetrafluoroborate+ trifluoroethanol," *Fluid Phase Equilibria,* vol. 218, no. 2, pp. 215-220, 2004.

[58] E. Gomez, B. Gonzalez, Á. Domínguez, E. Tojo, and J. Tojo, "Dynamic viscosities of a series of 1-alkyl-3-methylimidazolium chloride ionic liquids and their binary mixtures with water at several temperatures," *Journal of Chemical & Engineering Data,* vol. 51, no. 2, pp. 696-701, 2006.

[59] A. B. Pereiro, J. L. Legido, and A. Rodrı, "Physical properties of ionic liquids based on 1-alkyl-3-methylimidazolium cation and hexafluorophosphate as anion and temperature dependence," *The Journal of Chemical Thermodynamics,* vol. 39, no. 8, pp. 1168-1175, 2007.

[60] S. Seki, S. Tsuzuki, K. Hayamizu, Y. Umebayashi, N. Serizawa, K. Takei, and H. Miyashiro, "Comprehensive refractive index property for room-temperature ionic liquids," *Journal of Chemical & Engineering Data,* vol. 57, no. 8, pp. 2211-2216, 2012.

[61] M. Deetlefs, M. Shara, and K. R. Seddon, "Refractive indices of ionic liquids," *Ionic Liquids IIIA: Fundamentals, Progress, Challenges, and Opportunities,* pp. 219-233, 2005.

[62] M. Tariq, P. Forte, M. C. Gomes, J. C. Lopes, and L. Rebelo, "Densities and refractive indices of imidazolium-and phosphonium-based ionic liquids: Effect of temperature, alkyl chain length, and anion," *The Journal of Chemical Thermodynamics,* vol. 41, no. 6, pp. 790-798, 2009.

[63] S. B. Capelo, T. Méndez-Morales, J. Carrete, E. López Lago, J. Vila, O. Cabeza, J. Rodriguez, M. Turmine, and L. Varela, "Effect of temperature and cationic chain length on the physical properties of ammonium nitrate-based protic ionic liquids," *The journal of physical chemistry B,* vol. 116, no. 36, pp. 11302-11312, 2012.

[64] A. Pereiro, E. Tojo, A. Rodrıguez, J. Canosa, and J. Tojo, "Properties of ionic liquid HMIMPF6 with carbonates, ketones and alkyl acetates," *The Journal of Chemical Thermodynamics,* vol. 38, no. 6, pp. 651-661, 2006.

[65] E. Rilo, M. Domínguez-Pérez, J. Vila, L. Segade, M. García, L. Varela, and O. Cabeza, "Easy prediction of the refractive index for binary mixtures of ionic liquids with water or ethanol," *The Journal of Chemical Thermodynamics,* vol. 47, pp. 219-222, 2012.

[66] E. Rodil, A. Arce, and A. Soto, "Measurements of the density, refractive index, electrical conductivity, thermal conductivity and dynamic viscosity for tributylmethylphosphonium and methylsulfate based ionic liquids," *Thermochimica Acta,* 2018.

[67] X. Hu, S. Zhang, C. Qu, Q. Zhang, L. Lu, X. Ma, X. Zhang, and Y. Deng, "Ionic liquid based variable focus lenses," *Soft Matter,* vol. 7, no. 13, pp. 5941-5943, 2011.

[68] K. Kieu, L. Schneebeli, R. Norwood, and N. Peyghambarian, "Integrated liquid-core optical fibers for ultra-efficient nonlinear liquid photonics," *Optics Express,* vol. 20, no. 7, pp. 8148-8154, 2012.

[69] A. P. Fröba, H. Kremer, and A. Leipertz, "Density, refractive index, interfacial tension, and viscosity of ionic liquids [EMIM][EtSO4],[EMIM][NTf2],[EMIM][N (CN) 2], and [OMA][NTf2] in dependence on temperature at atmospheric pressure," *The Journal of Physical Chemistry B,* vol. 112, no. 39, pp. 12420-12430, 2008.

[70] S. Calixto, M. Rosete-Aguilar, F. J. Sanchez-Marin, O. L. Torres-Rocha, E. M. M. Prado, and M. Calixto-Solano, "Optofluidic compound lenses made with ionic liquids," in *Applications of Ionic Liquids in Science and Technology*: IntechOpen, 2011.

[71] J. A. N. López, H. Michinel, and E. L. Lago, "Optical Properties of Ionic Liquids," in *Ionic Liquids in Separation Technology*: Elsevier, 2014, pp. 24-34.

[72] C. Chiappe, P. Margari, A. Mezzetta, C. S. Pomelli, S. Koutsoumpos, M. Papamichael, P. Giannios, and K.

Moutzouris, "Temperature effects on the viscosity and the wavelength-dependent refractive index of imidazolium-based ionic liquids with a phosphorus-containing anion," *Physical Chemistry Chemical Physics,* vol. 19, no. 12, pp. 8201-8209, 2017.

[73] Y. Arosa, C. D. R. Fernández, E. L. Lago, A. Amigo, L. M. Varela, O. Cabeza, and R. de la Fuente, "Refractive index measurement of imidazolium based ionic liquids in the VIS-NIR," *Optical Materials,* vol. 73, pp. 647-657, 2017.

[74] Y. Arosa, B. S. AlGnamat, C. D. Rodríguez Fernández, E. Lopez Lago, L. M. Varela, and R. de la Fuente, "Modeling the Temperature Dependent Material Dispersion of Imidazolium Based Ionic Liquids in the Vis-NIR," *The Journal of Physical Chemistry C,* 2018.

[75] M. A. Iglesias-Otero, J. Troncoso, E. Carballo, and L. Romaní, "Density and refractive index in mixtures of ionic liquids and organic solvents: Correlations and predictions," *The Journal of Chemical Thermodynamics,* vol. 40, no. 6, pp. 949-956, 2008.

[76] G. Ghosh, "Sellmeier coefficients and dispersion of thermo-optic coefficients for some optical glasses," *Applied optics,* vol. 36, no. 7, pp. 1540-1546, 1997.

[77] A. B. Pereiro, P. Verdía, E. Tojo, and A. Rodríguez, "Physical properties of 1-butyl-3-methylimidazolium methyl sulfate as a function of temperature," *Journal of Chemical & Engineering Data,* vol. 52, no. 2, pp. 377-380, 2007.

[78] B. Mokhtarani, M. M. Mojtahedi, H. R. Mortaheb, M. Mafi, F. Yazdani, and F. Sadeghian, "Densities, refractive indices, and viscosities of the ionic liquids 1-methyl-3-octylimidazolium tetrafluoroborate and 1-methyl-3-butylimidazolium perchlorate and their binary mixtures with ethanol at several temperatures," *Journal of Chemical & Engineering Data,* vol. 53, no. 3, pp. 677-682, 2008.

[79] A. N. Soriano, B. T. Doma Jr, and M.-H. Li, "Measurements of the density and refractive index for 1-n-butyl-3-methylimidazolium-based ionic liquids," *The Journal of Chemical Thermodynamics,* vol. 41, no. 3, pp. 301-307, 2009.

[80] E. Vercher, F. J. Llopis, M. V. González-Alfaro, and A. Martínez-Andreu, "Density, speed of sound, and refractive index of 1-ethyl-3-methylimidazolium trifluoromethanesulfonate with acetone, methyl acetate, and ethyl acetate at temperatures from (278.15 to 328.15) K," *Journal of Chemical & Engineering Data,* vol. 55, no. 3, pp. 1377-1388, 2009.

[81] M. Sheik-Bahae, A. A. Said, T.-H. Wei, D. J. Hagan, and E. W. Van Stryland, "Sensitive measurement of optical nonlinearities using a single beam," *IEEE journal of quantum electronics,* vol. 26, no. 4, pp. 760-769, 1990.

[82] R. Leite, R. Moore, and J. Whinnery, "Low absorption measurements by means of the thermal lens effect using an He–Ne laser," *Applied Physics Letters,* vol. 5, no. 7, pp. 141-143, 1964.

[83] C. D. Tran, S. Challa, and M. Franko, "Ionic liquids as an attractive alternative solvent for thermal lens measurements," *Analytical chemistry,* vol. 77, no. 22, pp. 7442-7447, 2005.

[84] R. Souza, M. Alencar, M. Meneghetti, J. Dupont, and J. Hickmann, "Nonlocal optical nonlinearity of ionic liquids," *Journal of Physics: Condensed Matter,* vol. 20, no. 15, p. 155102, 2008.

[85] C. V. Loredo, K. Barrera-Rivera, M. Trejo-Durán, E. Alvarado-Méndez, A. Martínez-Richa, and J. Andrade-Lucio, "Nonlinear optical characterization of ionics liquids," in *Photonics North 2009*, 2009, vol. 7386, p. 738610: International Society for Optics and Photonics.

[86] C. E. Santos, M. A. Alencar, P. Migowski, J. Dupont, and J. M. Hickmann, "Anionic and cationic influence on the nonlocal nonlinear optical response of ionic liquids," *Chemical Physics,* vol. 403, pp. 33-36, 2012.

[87] C. E. Santos, M. A. Alencar, P. Migowski, J. Dupont, and J. M. Hickmann, "Nonlocal nonlinear optical response of ionic liquids under violet excitation," *Advances in Materials Science and Engineering,* vol. 2013, 2013.

[88] J. Nóvoa-López, E. L. Lago, M. Domínguez-Pérez, J. Troncoso, L. Varela, R. De La Fuente, O. Cabeza, H. Michinel, and J. Rodríguez, "Thermal refraction in ionic liquids induced by a train of femtosecond laser pulses," *Optics & Laser Technology*, vol. 61, pp. 1-7, 2014.

[89] M. J. Weber, *Handbook of optical materials*. CRC press, 2018.

[90] D. Malacara and B. J. Thompson, *Handbook of optical engineering*. Marcel Dekker New York, 2001.

[91] Y. Coello, B. Xu, T. L. Miller, V. V. Lozovoy, and M. Dantus, "Group-velocity dispersion measurements of water, seawater, and ocular components using multiphoton intrapulse interference phase scan," *Applied optics*, vol. 46, no. 35, pp. 8394-8401, 2007.

[92] T. D. Scarborough, C. Petersen, and C. J. Uiterwaal, "Measurements of the GVD of water and methanol and laser pulse characterization using direct imaging methods," *New Journal of Physics*, vol. 10, no. 10, p. 103011, 2008.

[93] Y. Coello, V. V. Lozovoy, T. C. Gunaratne, B. Xu, I. Borukhovich, C.-h. Tseng, T. Weinacht, and M. Dantus, "Interference without an interferometer: a different approach to measuring, compressing, and shaping ultrashort laser pulses," *JOSA B*, vol. 25, no. 6, pp. A140-A150, 2008.

[94] P. J. Wrzesinski, D. Pestov, V. V. Lozovoy, J. R. Gord, M. Dantus, and S. Roy, "Group-velocity-dispersion measurements of atmospheric and combustion-related gases using an ultrabroadband-laser source," *Optics express*, vol. 19, no. 6, pp. 5163-5170, 2011.

[95] G. Chen, T. Wang, C. Donnelly, and D. Tan, "Second and third order dispersion generation using nonlinearly chirped silicon waveguide gratings," *Optics express*, vol. 21, no. 24, pp. 29223-29230, 2013.

[96] X. Zhao, X. Wang, H. Lin, and Z. Wang, "Electronic polarizability and optical basicity of lanthanide oxides," *Physica B: Condensed Matter*, vol. 392, no. 1-2, pp. 132-136, 2007.

[97] W. Scaife and C. Lyons, "Density and Dielectric Polarizability of n-Alkane Liquids," *Berichte der Bunsengesellschaft für physikalische Chemie,* vol. 94, no. 7, pp. 758-765, 1990.

[98] E. I. Izgorodina, M. Forsyth, and D. R. MacFarlane, "On the components of the dielectric constants of ionic liquids: ionic polarization?," *Physical chemistry chemical physics,* vol. 11, no. 14, pp. 2452-2458, 2009.

[99] K. Bica, M. Deetlefs, C. Schröder, and K. R. Seddon, "Polarisabilities of alkylimidazolium ionic liquids," *Physical Chemistry Chemical Physics,* vol. 15, no. 8, pp. 2703-2711, 2013.

[100] P. Díaz-Rodríguez, J. C. Cancilla, N. V. Plechkova, G. Matute, K. R. Seddon, and J. S. Torrecilla, "Estimation of the refractive indices of imidazolium-based ionic liquids using their polarisability values," *Physical Chemistry Chemical Physics,* vol. 16, no. 1, pp. 128-134, 2014.

2 Material and experimental method

2.1 INTRODUCTION

This chapter is devoted to introducing the ionic liquids and the experimental techniques used in this work. In section 2.2, basic information about the studied ionic liquids such as name, short name, CAS number, and chemical structure is presented. The description of the commercial apparatus and techniques used for the ionic liquid characterization are described in section 2.3, including the vacuum system, to dry the ionic liquids; the Mettler Toledo Karl-Fisher coulometer, to measure the water content; the multiwavelength ATAGO DR-M2 Abbe refractometer, to determine the refractive index at five wavelengths; and the Anton Paar DSA-5000M vibrating tube density and sound velocity meter, that was used to determine the density of ionic liquids. Section 2.3 also describes a noncommercial technique RISBI, that has allowed to determine the refractive indices of ionic liquids over a large spectral band from 400 to 1000 nm.

2.2 MATERIALS

Twenty ionic liquids have been selected for this study. Abbreviations, CAS numbers, and chemical structures for these materials are shown in Table 2.1.

Table 2.1. Ionic liquid

	Name	Abbreviation	Chemical structure	CAS number
1	1-Ethyl-3-methylimidazolium tetrafluoroborate	$[C_2MIm][BF_4]$	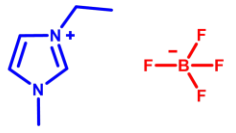	143314-16-3
2	1-Propyl-3-methylimidazolium tetrafluoroborate	$[C_3MIm][BF_4]$	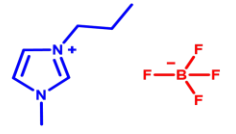	244193-48-4
3	1-Butyl-3-methylimidazolium tetrafluoroborate	$[C_4MIm][BF_4]$	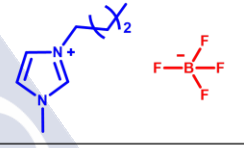	174501-65-6
4	1-Hexyl-3-methylimidazolium tetrafluoroborate	$[C_6MIm][BF_4]$	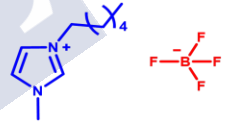	244193-50-8
5	1-Octyl-3-methylimidazolium tetrafluoroborate	$[C_8mim][BF_4]$	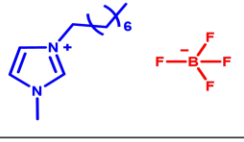	244193-52-0

	Name	Abbreviation	Chemical structure	CAS number
6	1-Ethyl-3-methylimidazolium Bis(trifluoromethylsulfonyl)imide	$[C_2MIm][NTf_2]$		174899-82-2
7	1-Propyl -3-methylimidazolium Bis(trifluoromethylsulfonyl)imide	$[C_3MIm][NTf_2]$		216299-72-8
8	1- Butyl -3-methylimidazolium Bis(trifluoromethylsulfonyl)imide	$[C_4MIm][NTf_2]$		174899-83-3
9	1- Hexyl -3-methylimidazolium Bis(trifluoromethylsulfonyl)imide	$[C_6MIm][NTf_2]$		382150-50-7
10	1-Ethyl-3-methylimidazolium triflate	$[C_2MIm][OTf]$		145022-44-2

	Name	Abbreviation	Chemical structure	CAS number
11	1-Butyl-3-methylimidazolium triflate	[C_4MIm][OTf]		174899-66-2
12	1-Ethyl-3-methylimidazolium hydrogen sulfate	[C_2MIm][$HySO_4$]		412009-61-1
13	1-Ethyl-3-methylimidazolium methyl sulfate	[C_2MIm][C_1SO_4]		516474-01-4
14	1-Ethyl-3-methylimidazolium ethyl sulfate	[C_2MIm][C_2SO_4]		342573-75-5
15	1-Ethyl-3-methylimidazolium hexyl sulfate	[C_2MIm][C_6SO_4]		942916-86-1

	Name	Abbreviation	Chemical structure	CAS number
16	1- Butyl -3-methylimidazolium methyl sulfate	$[C_4MIm][C_1SO_4]$	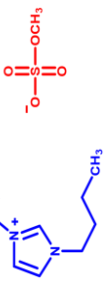	401788-98-5
17	1-Butyl-3-methylimidazolium thiocyanate	$[C_4MIm][(SCN)]$	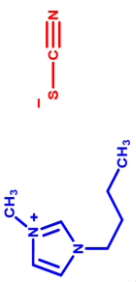	344790-87-0
18	1-Butyl-1-methylpiperidinium bis(trifluoromethylsulfonyl)imide	$[C_4MPiP][NTF_2]$	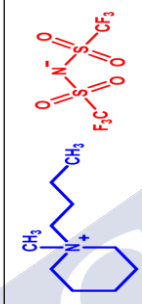	623580-02-9
19	1-(2-methoxyethyl)-1 methylpyrrolidinium bis-(trifluoromethylsulfonyl)imide	$[MOEMPL][NTF_2]$		757240-24-7
20	1- Butyl -dimethylimidazolium Bis(trifluoromethylsulfonyl)imide	$[C_4MMIm][NTF_2]$	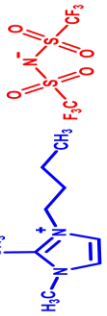	350493-08-2

2.3 EXPERIMENTAL TECHNIQUES

2.3.1 Preparing the sample

2.3.1.1 Vacuum system

Ionic liquids are highly hygroscopic and absorb water easily from the environment. In order to avoid water impurities, all the liquids were vacuum dried under pressure less than 10^{-3} atm before the measurements, for more than 48 h at room temperature. A photograph of the Vacuum system is shown in Figure 2.1, where the key elements have been labelled in order to facilitate a novel user the understanding of the description of its handling.

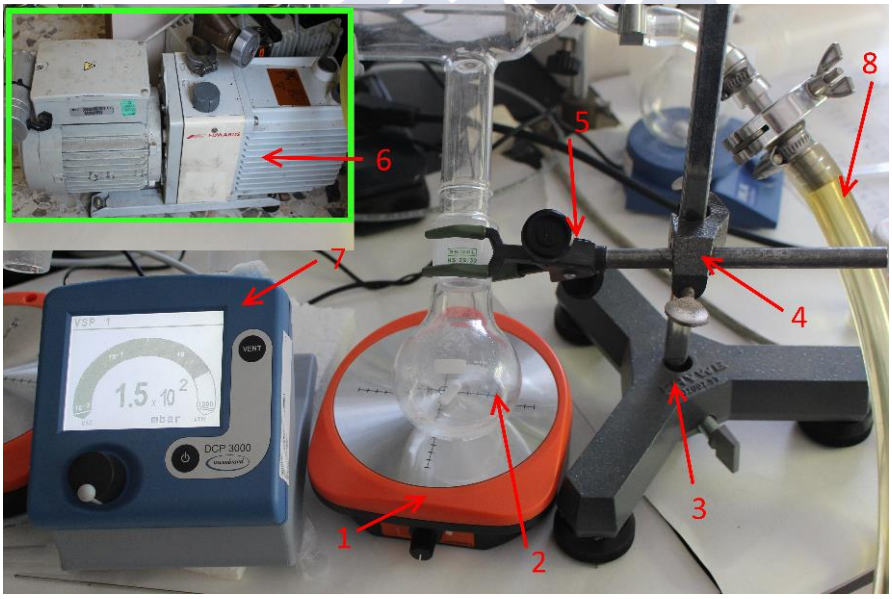

Figure 2.1. Sample in the vacuum system: 1- Hot plate magnetic stirrer, 2- Evaporation flask, 3- Retort stand, 4- Boss, 5- Clamp, 6- Vacuum pump, 7- Digital pressure gauge, Vacuum 8- Rubber housing.

The use of the vacuum system requires to follow the next steps:

The apparatus was connected, as shown in Figure 2.1. Then the liquid sample was transferred inside the flask by using a syringe. Next, a magnetic stirrer par is introduced in the evaporation flask. The speed should be adjusted until saw the regular circulation. The reduced pressure is applied by switching on the vacuum pump, so the water content in the IL starts to boil. Samples use to be left under the vacuum more than 48 h at room temperature to eliminate the water content as much as possible. After this procedure, the water content of the dried ILs is determined by using a Mettler Toledo Karl-Fisher coulometer (Figure 2.2).

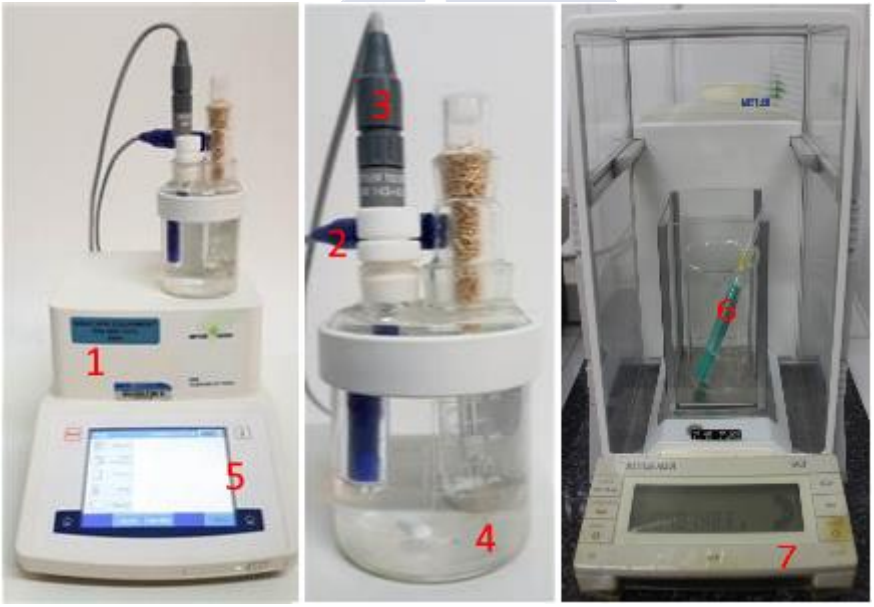

Figure 2.2. Karl-Fischer coulometer c20. The main elements are 1- system with commercial software. 2- Cable for generator electrode. 3- Cable for measure electrode. 4- Magnetic stirrer bar. 5- Touch screen. 6- syringe. 7- analytical balance.

2.3.1.2 Karl Fischer coulometer

The Karl Fischer coulometer combines fast and precise water content determination with very simple operation and the need for a little amount of sample [1, 2]. The main elements are an analytical balance, cable for generator electrode, cable for measure electrode, a system with commercial software, touch screen; syringe, magnetic stirrer bar, draining tube.

The amount of the sample is collected with a syringe, and after, syringe and sample are weighed on the scale. Next, the needle is inserted through the septum, and a few drops are injected just below the surface of the solvent. Then, the syringe is removed and weighed again. The difference of weight is manually entered by the commercial software that it's incorporated in the system. The device, then, calculates the water content by using titration.

Titration, the principle of the device proposed by the German chemist Karl Fischer in 1934, is based on the Bunsen Reaction between iodine and sulfur dioxide in an aqueous medium. He found that this reaction could be modified to be used for the fixing of water in a non-aqueous medium. In the device, iodine is created electrochemically in situ during the titration.

Water and iodine are consumed in a 1:1 ratio in the reaction. When all of the water content is consumed, the remaining iodine is measured by using the titrator's indicator electrode. Water is quantified based on the overall charge (the value of the charge is proportional to the concentration of iodine) passed according to the following relation: 1 mg H_2O = 10.72 C.

Once the measurement is done, the ILs were kept in glass vials and closed with screw caps fitted with a silicone septum to ensure a secure seal and prevent their contact with air moisture.

The water content of the dried ILs was found to be less than 500 ppm; that is value inside the range of the measurement of the apparatus that goes from 1ppm to 5%; for example we have obtained 194, 167,

216, 482 and 374 ppm for $[C_2MIm][BF_4]$, $[C_4MIm][NTf_2]$, $[C_2MIm][OTf]$, $[C_2MIm][C_1SO_4]$ and $[C_4MIm][SCN]$ respectively. These quantities are not high enough to have an appreciable influence on the measure of the refractive index and its associated parameters.

2.3.2 Refractive index measurement

2.3.2.1 Abbe refractometer

Abbe refractometer is a standard instrument for measuring the refractive index, n, of a sample in the visible and near-infrared range (Figure 2.3) by using the optical phenomena of total internal reflection. It can operate at a single wavelength, usually 589 nm, or in multiwavelength mode. The model used in this work is a multiwavelength ATAGO DR M2 refractometer that allows measuring refractive indices of solids and liquid samples. Table 2.2 shows the measurement range of the refractive index at different wavelengths.

Table 2.2. The measurement range of the refractive index of DR-M2 varies depending on wavelength.

Wavelength (nm)	Refractive index
450	1.3277-1.7379
589	1.3000-1.7100
680	1.2912-1.7011

The operation principle of an Abbe refractometer is described as following [3, 4]:

The sample is placed between two prisms, the illuminating prism, and the secondary prism. Its refractive index should be smaller than the refractive index of the secondary prism.

The upper prism or illuminating prims has a rough surface allowing light to scatter in all directions, that is why it is called illuminating prism.

When the light crosses the interface between the liquid and secondary prism, it is refracted with an angle α. When this angle is higher than the critical angle, α_c, for the secondary prism, then total internal reflection takes place at the exit interface of the prism; then an observer looking at the exit of the prism can distinguish a dark and an illuminated area and the position of the boundary line allows determining the value of α_c. The refractive index of the sample can be calculated by using the relation $n = n_p \cdot \sin \alpha_c$ being n_p the refractive index of the refracting prism.

As α_c depends on the wavelength of the light, a filter should be inserted in the interference filter insertion slot of the light source. The available interference filters are centered at λ= 486, 546, 589, 633, and 680 nm.

The refractive index of liquids depends on temperature. The temperature in the refractometer was controlled by using a circulation pump connected with constant temperature water bath within ± 0.1 K stability. The maximum temperature interval that can be achieved with this device ranges from 278.15 to 323.15 K. The refractometer is also equipped with a thermometer that measures the temperature of the sample when we take the measurement.

2.3.2.1.1 Equipment

The main parts of our Multi-wavelength Abbe refractometer are shown in Figure 2.3.

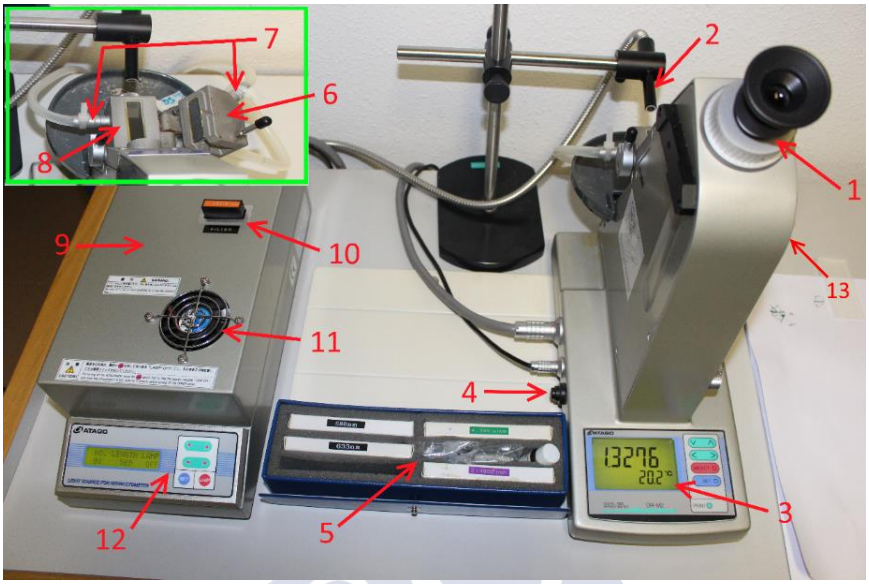

Figure 2.3. Abbe refractometer. 1-Eyepiece 2-Optical fiber. 3-Display panel of the refractometer[1]. 4-Power switch of the refractometer. 5-Set of interference filters at 486, 546, 589, 633, 680 nm. 6-Main prism or Illuminating prism. 7-Constant temperature water circulating nozzles. 8-Secondary prism or Refracting prism. 9-Light source unit. 10-Interference filter insertion slot. 11-Cooling fan. 12-Display panel of the light source unit. 13-Wheel.

2.3.2.1.2 Cleaning and Calibration

To proceed with the measurement, we must follow the next steps:

-Cleaning: Remove properly with a soft paper wiped with water or ethanol any material that could be on the surface of both prisms, before each use of the device.

-Calibration: the calibration needs to be carried out carefully following the instruction manual using distilled water at a temperature of 293 K and at a wavelength of 589 nm. The water sample is directly injected into the prism assembly of the instrument using a syringe (without needle). The drop must be just enough to

[1] The Display panel of refractometer gives information about function mode number, refractive index, temperature, wavelength, abbe number.

cover the surface completely but forming a homogeneous thin film.

2.3.2.1.3 Measurement

After cleaning and drying the prims, a second drop of the sample under study is placed between the two prisms. After setting the temperature and inserting the interference filter (λ= 486, 546, 589, 633 or 680 nm), we turn the wheel until the half of the field of view is dark, and so the boundary line splits the field of vision into two regions of equal surface, a bright and a dark region. The refractometer has a digital display so the refractive index can be found directly as a digit number on the screen. Each sample was measured three or four times to calculate the average value. Refractive indices were measured with uncertainty about ± 0.0002 units.

Keeping the same temperature, we change the interference filter and measure the refractive index at the corresponding wavelength. Next, we increase the temperature every five degrees and repeat the procedure at the five wavelengths.

In Table 2.3, we show the measured refractive indices of ethanol and acetone at 295 K, together with previously reported values [5]. The refractive indices of the ILs measured by us and the ones given by other authors are listed in Table 2.4.

Table 2.3. Refractive index at 295 K.

	Ethanol		Acetone	
Wavelength (nm)	Literature value [5]	Measured value	Literature value [5]	Measured value
486	1.3660	1.3657	1.3638	1.3635
546	1.3631	1.3629	1.3607	1.3604
589	1.3616	1.3615	1.3591	1.3590
633	1.3604	1.3602	1.3578	1.3577
680	1.3594	1.3592	1.3567	1.3565

Table 2.4. Refractive index at D-line 589 nm.

	$[C_4MIm][BF_4]$		$[C_2MIm][NTf_2]$	
Temperature (K)	Measured value	literature value	Measured value	literature value
298	1.4213	1.4215 [6] 1.4219 [7] 1.4217 [8]	1.4225	1.4225 [6] 1.4230 [9]
303	1.4200	1.4206 [7] 1.4200 [10] 1.4203 [8]	1.4211	1.4210 [10] 1.4215 [9]
308	1.4187	1.4189 [8]	1.4196	1.4201 [9]
313	1.4173	1.4174 [6] 1.4180 [10] 1.4175 [8]	1.4181	1.4185 [10] 1.4184 [6] 1.4186 [9]
318	1.4160	1.4162 [8]	1.4167	1.4172 [9]
323	1.4146	1.4160 [10] 1.4155 [7] 1.4149 [8]	1.4152	1.4160 [10] 1.4157 [9]

2.3.2.2 Refractive Index Spectroscopy by Brodband Interferometry (RISBI)

Refractive Index Spectroscopy by Brodband Interferometry, **RISBI** was used to measure the refractive index dispersion of the ILs listed in Table 2.1 in a wide and continuous spectral range from 400 nm to 1000 nm. It incorporates a temperature controller system covering a range from 298.15 to 323.15 K [11]. The measurements were taken at the atmospheric pressure, and the humidity was between 60-80 %.

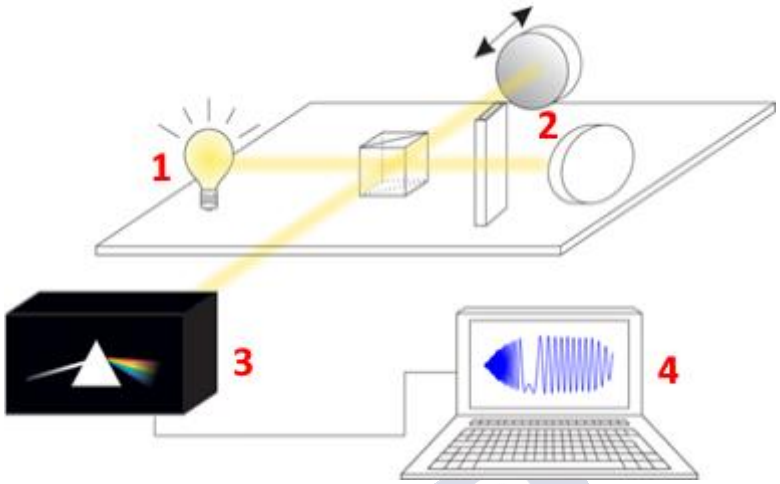

Figure 2.4. Schematic design of the experimental set-up of RISBI [12]: 1- White light source. 2- Michelson interferometer. 3- Homemade prism spectrometer. 4- Processing unit.

2.3.2.2.1 Equipment

A schematic representation of the RISBI device is shown in Figure 2.4. The main parts of the equipment are:

A white light source: the source of illumination is a stabilized halogen lamp with 150W of electrical power, with a black body like emission spectrum. The beam is collimated by using convex lenses, and the intensity is spectrally homogenized by a filter.

A Michelson interferometer: The main elements beam- splitter (1), moving mirror (2), and fixed mirror (3) are identified in Figure 2.5. The light beam hits the beam splitter (1), and it is split into two beams that travel different ways, that are known as the reference arm and the test arm. One of the beams is reflected in the moving mirror (2) located in the reference arm. The moving mirror may be displaced by a lever (5) connected to a micrometer screw (4). The second beam is reflected in the fixed mirror (3) placed in the test arm, where the sample is inserted. Both beams were recombined on the beam splitter to produce an interference pattern. The light exiting the beam splitter is coupled to

an optical fiber. The sample is inside a quartz cell, Hellma 100-QS 1mm, located on the cell holder. The temperature of the cell holder is controlled by a circulating water bath.

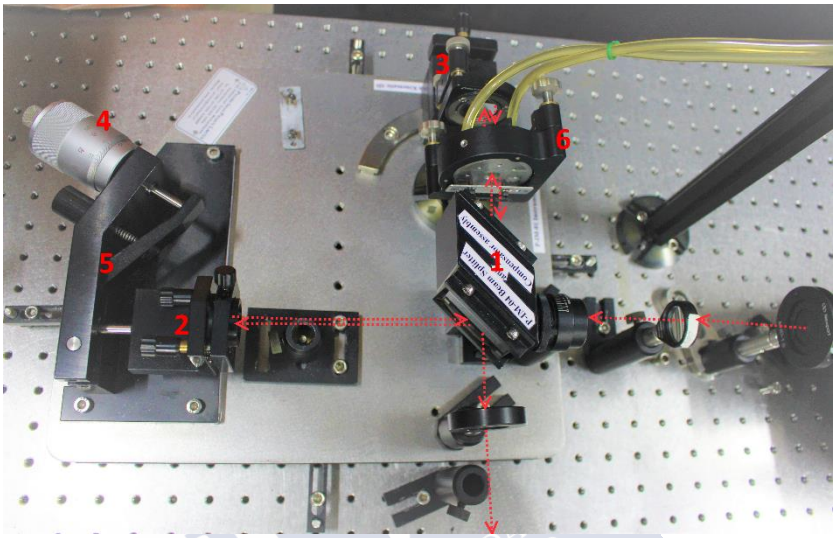

Figure 2.5. A Michelson interferometer: 1-Beam- splitter, 2- Moving mirror, 3- Fixed mirror, 4- Micrometer screw, 5- Lever, 6- Cell holder.

Figure 2.6. Circulating water bath.

A homemade prism spectrometer. It is more suitable in the visible range since its resolution increases as the wavelength decreases. The elements of the spectrometer, that covers a spectral range from 400 to 1000 nm, are a entrance slit, a dispersive prism made of F2 optical glass, three flat mirrors M1-M3, a collimating lens L1 and a focusing lens L2, with 315 mm focal length and a linear Mightex CCD camera with 3648 pixels (sensor area: 8 x 200 μm^2), as shown in Figure 2.7.

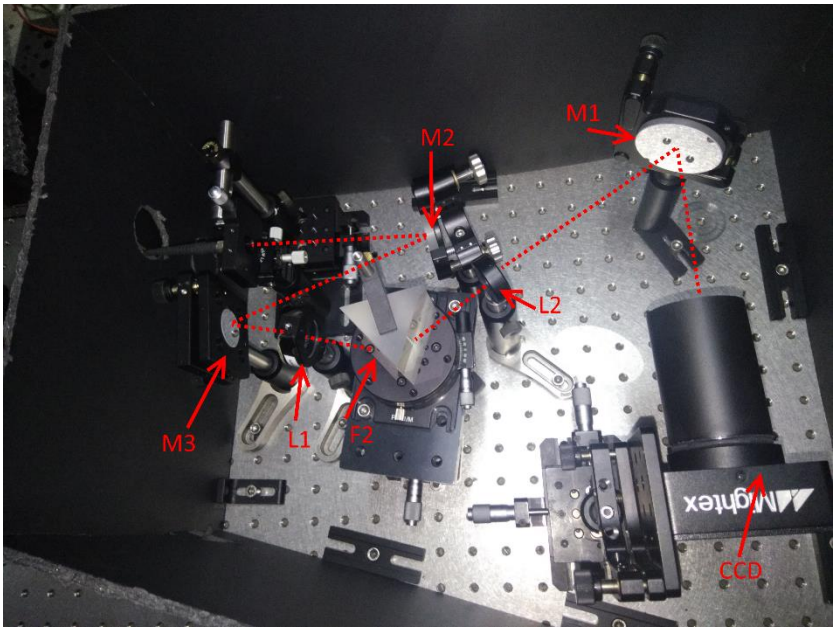

Figure 2.7. A homemade prism spectrometer. Diffraction prism (F2). Linear CCD camera (CCD). Mirrors (M1, M2, M3). Lens (L1, L2).

A commercial Czerny-Turner spectrometer: It is used to determine with great accuracy the relative displacement between the mirrors of the Michelson interferometer. We opted by high-resolution commercial spectrometer better than 0.01 nm model SpectralPro-500i from Acton Research. The main elements are identified in Figure 2.8.

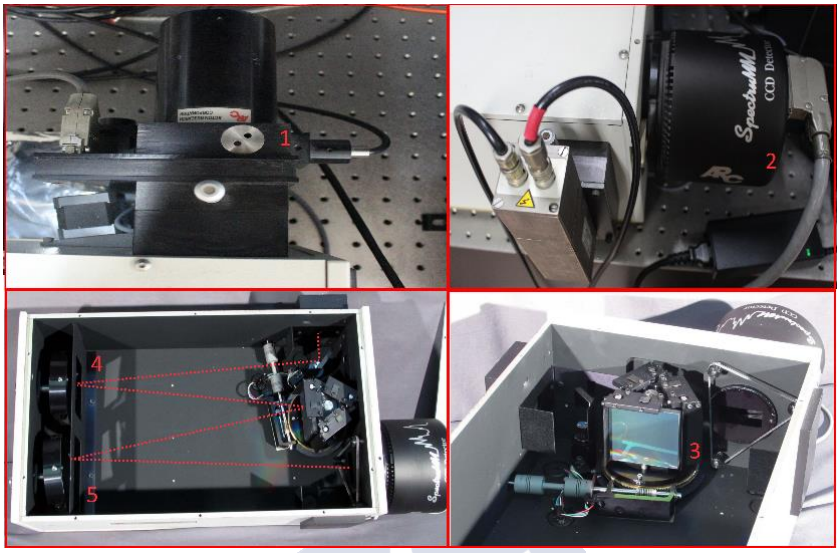

Figure 2.8. Commercial Czerny-Turner spectrometer: 1-entrance slit, 2-CCD camera with 1024x128 pixels, 3- 1200 lines/mm rotating grating, 4-collimating mirror, 5- focusing mirror.

2.3.2.2.2 Theory

The technique is based on the interferometric pattern that produces a Michelson interferometer illuminated with white light. The interferometer's output intensity as a function of the wavelength (λ) is described by the expression:

$$I(\lambda) = I_0(\lambda)[1 + v\,(\lambda)cos(\frac{4\pi}{\lambda}\Lambda(\lambda))] \qquad (2.1)$$

Where I_0 is the background intensity of the interferometer arm, v is the visibility function, and $\varphi=(4\pi\Lambda/\lambda)$ is the phase difference produced by the optical path (Λ) between the interferometer arms. This phase is wavelength dependent and carries information about the relative position of the interferometer mirrors and the optical properties of any material inserted in one of the arms.

When a sample with refractive index $n(\lambda)$ and thickness d is placed in one arm, the resulting phase is:

$$\varphi(\lambda) = \frac{4\pi}{\lambda}[d(n(\lambda) - 1) - L] \quad (2.2)$$

Where L is the relative displacement between the mirrors on the interferometer's arms. This phase can be resolved over the spectrum to be analyzed with an appropriate spectrometer. Since our aim is to obtain the refractive index of our samples, it seems direct to extract it from eq.(2.2) when the thickness of the sample and the mirrors' relative displacement are known. However, that is not so easy due to the multivalued nature of the cosine, which introduces an ambiguity in the phase. That means that the extracted phase is:

$$\varphi(\lambda)exp = \varphi(\lambda) - 2k\pi \quad (2.3)$$

This $2k\pi$ factor (where k is an integer) produces an error on the refractive index when it is directly determined from the phase:

$$n'(\lambda) = \frac{(\varphi(\lambda) - 2k\pi)\lambda}{4\pi d} + 1 + \frac{L}{d} \quad (2.4)$$

The difference between the real refractive index (n) and the unsuccessfully calculated one (n') can be obtained using eq.(2.2) and (2.4).

$$\Delta n = n' - n = \frac{k\lambda}{2d} \quad (2.5)$$

Hopefully, this deviation between the real and the first estimated index can be avoided, if the value of the refractive index at a given wavelength λ_0 is known. Comparing the real and the inaccurate indices, the value of k can be extracted as:

$$k = \frac{2d}{\lambda_0}[n'(\lambda_0) - n(\lambda_0)] \qquad (2.6)$$

Usually, due to experimental uncertainties, the calculated value of k is not an integer as it should be, in that case, we round it to the nearest integer [11]. Once the value of k determined, the real refractive index n can be obtained by rewriting eq.(2.4**)** as:

$$n(\lambda) = \frac{(\varphi(\lambda)_{exp} + 2k\pi)\lambda}{4\pi d} + 1 + \frac{L}{d} \qquad (2.7)$$

2.3.2.2.3 Experimental procedure

A quartz cell (Hellma 100-QS 1 mm) filled with a liquid sample was placed in the test arm of the interferometer (at the front of the fixed mirror). A temperature controller system was used to stabilize the sample temperature allowing variation within ± 0.1 K. To compensate the extra optical path difference resulting from quartz cell walls; a 2mm quartz plate was placed in the reference arm. Both cell and plate were adjusted until their faces are normal to the incidence direction of the respective beams.

It is necessary to evaluate the background intensity (I_0) at the output of the interferometer with the sample placed in the test arm in order to subtract its contribution to eq.(2.1). Once it is determined, the mirror is moved micrometrically until the phase stationary point[2] is visualized in the interferogram near the green region where the visibility is greater. An image of the intensity (I) (interferometric pattern) was taken at a certain temperature. An example of the initial intensity images (I_0) and the intensity (I) for deionized water is shown in Figure 2.9.

[2] Phase stationary point appears when the group index verifies $n_g(\lambda_{st}) = 1 + \frac{L}{d}$
It is an extremal point of the phase and a minimum for normal dispersion materials.

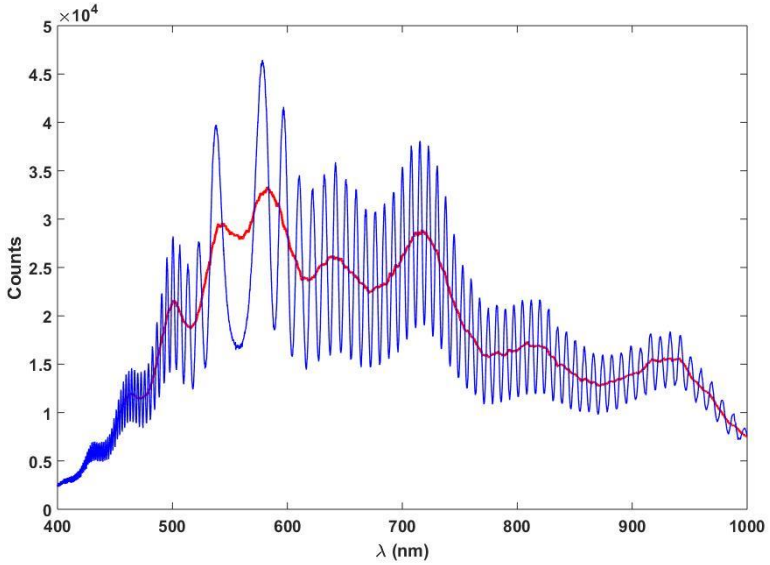

Figure 2.9. Example of I_0 (red line) and I (blue line) for a deionized water sample.

To calculate the phase φ, I_0 was subtracted in eq.(2.1), and the lower and upper envelopes of the resulting graph were determined by interpolation of minima and maxima, respectively. The visibility was calculated subtracting the two envelopes, and the phase was retrieved from the spectrogram by inverting the cosine function. The images with the empty cell where taken to extract the background phase, and subtract it from the phase obtained with the cell filled with the sample [13].

As it was previously mentioned, to measure the displacement L between mirrors, a grating spectrometer with a greater wavelength resolution ($\Delta\lambda$ <0.01 nm) was used [14]. As well as, to avoid the phase ambiguity error, we measure the value of refractive index at five wavelengths by using the Abbe refractometer, previously described. One of them is used to determine k in eq.(2.6) and the others help us to check the reliability of the results provided by RISBI.

In Figure 2.10 we show the calculated values of *k* from eq.(2.6) and highlight the corresponding to the five wavelengths of the Abbe refractometer for a sample of deionized water.

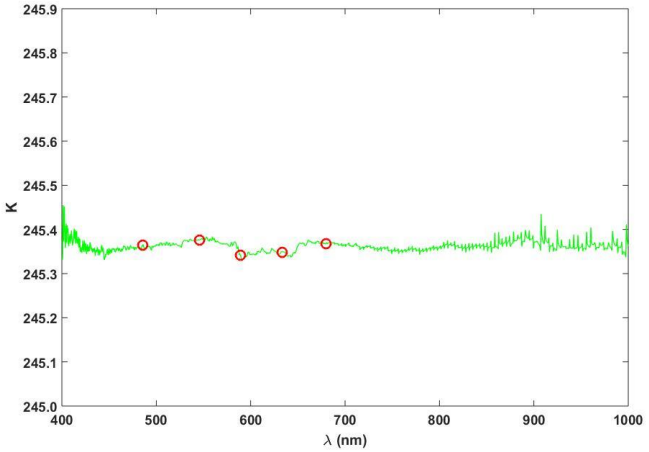

Figure 2.10. Calculated values of k for deionized water from eq (2.6) versus wavelength (green line); particular values of *k* at 486, 546, 589, 633 and 680 nm (red open circles).At temperature 298.15 K.

One critical parameter is the inner width of the cell, *d*. In order to calculate it, we use different liquids whose refractive index is well known. Once *L*, *d*, and *k* are precisely known the refractive index is calculated using eq.(2.7). The resulting noisy refractive is fitted to fulfill a relation as the given by Cauchy or Sellmeir dispersion formula.

Before measuring the refractive indices of ionic liquids, the refractive index of well-characterized substances was measured at different temperatures to find how precisely these can be retrieved. In Figure 2.11, the refractive indices of deionized water obtained with RISBI at 298 and 323K are plotted together with the values given by Abbe refractometry. In Figure 2.11 b, the deviations between the values retrieved by the two techniques are shown. The deviations are smaller than 10^{-4}.

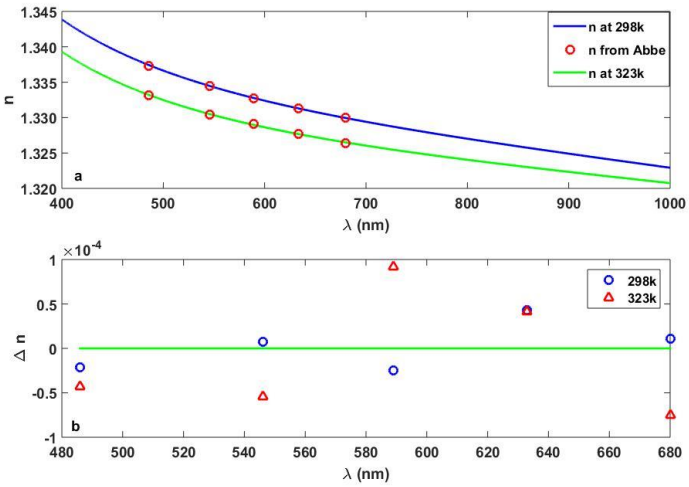

Figure 2.11. (a) Refractive index of deionized water measured by RISBI at a 298 K(blue curve) and 323 K (green curve); corresponding refractive index of deionized water measuring by Abbe refractometer(red open circle). (b) Deviations of the Abbe refractive index values with respect to calculated values

2.3.3 Density measurement

The density of the ionic liquids was automatically measured using a vibrating tube digital densimeter, and sound speed analyzer, Anton Paar DSA 5000; the procedure is based on the vibrating tube densimetry (VTD) that is one of the best-stablished methods used for density measurement since it is a fast and accurate technique.

2.3.3.1 Equipment

Figure 2.12 shows a picture of the commercial device used in this work in which we mark the main elements:

1- Waste vessel.
2- Syringe 2 ml Luer.
3- Injection Adapter Luer.
4- Hose 3 x 5 mm silicone.
5- The measuring cell.

6- LC display that shows date and time, density with automatic viscosity correction, speed of sound, measuring cell temperature, state of the measurement.
7- Green light indicates power-on.
8- "LIGHT" key for lighting up the display.
9- "PUMP" key for switching on the air pump.
10- Soft keys.

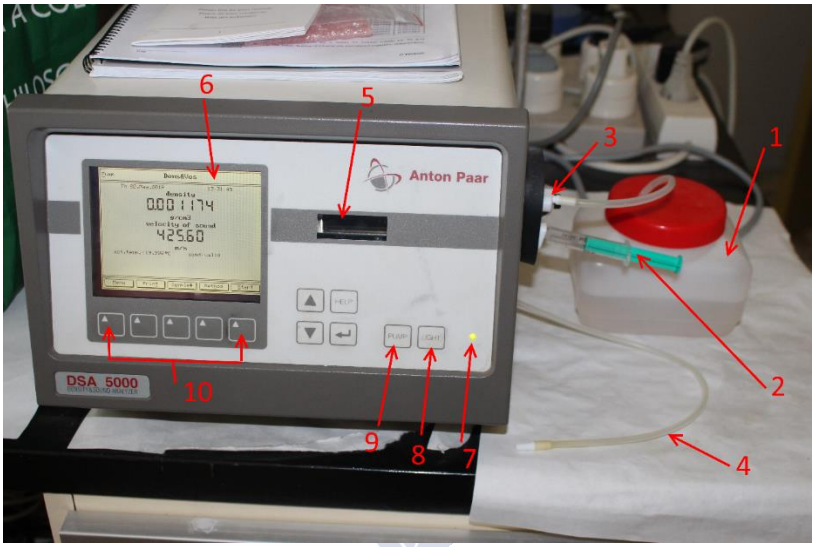

Figure 2.12. Density and speed of sound analyzer (Anton Paar DSA 5000): 1-Waste vessel; 2-Syringe 2 ml Luer; 3-Injection adapter Luer; 4-Hose 3 x 5 mm silicone; 5-Measuring cell; 6-LC display; 7-Green light indicates power-on; 8-"LIGHT" key; 9-"PUMP" key and 10-Soft keys.

The instrument is equipped with a U-shaped density cell and a pulse-echo speed of sound cell (see Figure 2.13). Both the cells (5) are temperature controlled by a built-in Peltier thermostat (pt-100) The device has a built-in thermostat to maintain the temperature at desired value between 0 -70 °C.

The principle of a vibrating tube densimeter involves the phenomenon in which the U-shaped sample tube, completely filled with the sample liquid (to be sure that no air bubbles remain inside the tube), is excited to a continuous oscillation at its natural

frequency using a magneto-electrical excitation system.

The oscillation frequency is related to the density of the liquid inside the tube (the tube was isolated from the external vibrations). When the density of the sample in the tube modifies by changing the temperature or by replacing the sample, the resonant frequency of the tube also changes. At a frequency equal to that of the vibrating tube, the frequency counter analyzes the signal from the pick-up coil and measures the resonance frequency of the tube.

An acoustic signal gives information about the completion of the measurement of density and speed of sound of the ionic liquids. The results are automatically converted so the density can be known directly as a digit number on the screen, and we can save the results in the memory of the device.

Before each series of measurements, three steps were done: firstly, the measuring cell was cleaned and dried; secondly, the apparatus was adjusted and finally, the apparatus was calibrated by measuring the density of distilled water and dry air at all desired temperatures and at atmospheric pressure according to the manual instructions. The overall precision in experimental density measurements for all samples was found to be better than $\pm 2 \times 10^{-6}$ g·cm^{-3}.

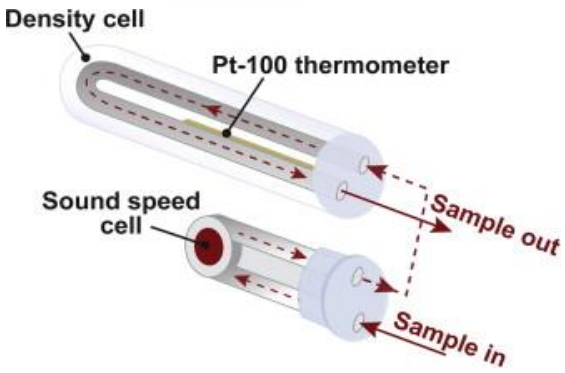

Figure 2.13. Schematic diagram of U-shaped density cell and sound speed cell [15].

2.3.3.2 Cleaning and Drying the Measuring Cell

The measuring cell needs to be cleaned and dried. Cleaning is performed with acetone and distilled water; acetone dissolves and removes residues, distilled water removes acetone, and it is easily evaporated by a stream of dry air, in order to accelerate the drying in the cell.

The first step consists on filling the measuring cell with acetone using a syringe (2) with Luer tip (3) (see Figure 2.14); the plunger of the syringe was moved in and out several times. This action creates gas bubbles that improve the cleaning action. Then the acetone was removed out from the measuring cell.

After that, the measuring cell was filled with distilled water and the procedure carry out with acetone is repeated. Finally, the tube was dried by attaching the air hose (4) to the injection adapter Luer (3), using the dry air that is let blow through the measuring cell for approximately 10 minutes.

2.3.3.3 Adjustment of the apparatus

The apparatus is adjusted to bringing it into a suitable state for use by setting or modify the instrument constants. This process is performed by using dry air and distilled water.

The density values of dry air and distilled water at a specific atmospheric pressure are stored in the memory of the apparatus for the complete temperature range. The dry air and distilled water adjustments for the entire temperature range take approximately 2 hours.

The first adjustment is performed using dry air at 20°C; the complete procedure takes 5 to 10 minutes. The measuring cell is filled with dry air by attaching the air hose to the injection adapter, Luer. For air adjustment, the current air pressure must be entered as it influences the air density. The adjustment starts by selecting it from the menu key. Once finished, the adjustment can be saved, stored, and printed.

After the adjustment, the density of dry air was found around

0.001169 g/cm^3 at a temperature of 20 ºC and at atmospheric pressure of 980 mbar, close values to those reported in the manual (ρ_{air}=0.001165 g/cm^3).

All the previous procedures are repeated to the adjustment by distilled water whose density was found around 0.998211 g/cm^3 at a temperature of 20 ºC and at atmospheric pressure of 980 mbar, close values to those reported in the manual (ρ_{water}=0.998203 g/cm^3) [16].

2.3.3.4 Calibration of the apparatus

The apparatus is calibrated by measuring the density of distilled water and dry air at temperatures from 20 ºC to 60 ºC at atmospheric pressure according to the manual of instructions and comparing the measured values with theoretical ones. The overall precision in experimental density measurements for all samples was found to be better than $\pm 2 \times 10^{-6}$ g·cm^{-3}.

2.3.3.5 Measurements

To precisely determine the density of the ionic liquids, the device is set to measure the density at a temperature interval starting from 298.15 K to 323.15 K, at every 5 K. The measuring cell is slowly filled with 2 ml of the sample by using the syringe attached to the injection adapter Luer.

After the filling procedure, the syringe must be kept in the filling position, in order to prevent sample leakage (see Figure 2.14). We must ensure that there are no gas bubbles in the measuring cell by looking through the inspection window and observing the filling of the measuring cell.

When the sample attains constant temperature, the acoustic signal gives information about the completion of the measurement; the value of density including temperature, sample name, and date can be shown on the programmable LC display and saved automatically in the memory of the device. After that, the temperature will start to increase until reaching the next one.

Figure 2.14. Side view shows injection adapter Luer, syringe and Placing of the waste vessel.

Finally, the sample is removed out by using the syringe, and the inside tube is cleaned and dried by using acetone, water, and dry air.

2.4 REFERENCE

[1] C. A. De Caro, A. Aichert, and C. M. Walter, "Efficient, precise and fast water determination by the Karl Fischer titration," *Food Control*, vol. 12, no. 7, pp. 431-436, 2001.

[2] M. Margreth, R. Schlink, and A. Steinbach, "Water determination by Karl Fischer titration," *Pharmaceutical Sciences Encyclopedia: Drug Discovery, Development, and Manufacturing*, pp. 1-34, 2010.

[3] A. García-Valenzuela and H. Contreras-Tello, "Optical model enabling the use of Abbe-type refractometers on turbid suspensions," *Optics letters*, vol. 38, no. 5, pp. 775-777, 2013.

[4] D. Malacara, *Geometrical and instrumental optics*. Academic Press, 1989.

[5] J. Rheims, J. Köser, and T. Wriedt, "Refractive-index measurements in the near-IR using an Abbe refractometer," *Measurement Science and Technology*, vol. 8, no. 6, p. 601, 1997.

[6] M. Tariq, P. Forte, M. C. Gomes, J. C. Lopes, and L. Rebelo, "Densities and refractive indices of imidazolium-and phosphonium-based ionic liquids: Effect of temperature, alkyl chain length, and anion," *The Journal of Chemical Thermodynamics*, vol. 41, no. 6, pp. 790-798, 2009.

[7] G. Vakili-Nezhaad, M. Vatani, M. Asghari, and I. Ashour, "Effect of temperature on the physical properties of 1-butyl-3-methylimidazolium based ionic liquids with thiocyanate and tetrafluoroborate anions, and 1-hexyl-3-methylimidazolium with tetrafluoroborate and hexafluorophosphate anions," *The Journal of Chemical Thermodynamics*, vol. 54, pp. 148-154, 2012.

[8] C. M. Neves, K. A. Kurnia, J. o. A. Coutinho, I. M. Marrucho, J. N. C. Lopes, M. G. Freire, and L. P. N. Rebelo, "Systematic study of the thermophysical properties of imidazolium-based ionic liquids with cyano-functionalized anions," *The Journal of Physical Chemistry B*, vol. 117, no. 35, pp. 10271-10283, 2013.

[9] R. G. Seoane, E. J. González, and B. González, "1-Alkyl-3-methylimidazolium bis (trifluoromethylsulfonyl) imide ionic liquids as solvents in the separation of azeotropic mixtures," *The Journal of Chemical Thermodynamics,* vol. 53, pp. 152-157, 2012.

[10] M. Montalban, C. Bolivar, F. G. Díaz Baños, and G. Villora, "Effect of temperature, anion, and alkyl chain length on the density and refractive index of 1-alkyl-3-methylimidazolium-based ionic liquids," *Journal of Chemical & Engineering Data,* vol. 60, no. 7, pp. 1986-1996, 2015.

[11] Y. Arosa, E. L. Lago, L. M. Varela, and R. de la Fuente, "Spectrally resolved white light interferometry to measure material dispersion over a wide spectral band in a single acquisition," *Optics express,* vol. 24, no. 15, pp. 17303-17312, 2016.

[12] Y. Arosa, B. S. AlGnamat, C. D. Rodríguez Fernández, E. Lopez Lago, L. M. Varela, and R. de la Fuente, "Modeling the Temperature Dependent Material Dispersion of Imidazolium Based Ionic Liquids in the Vis-NIR," *The Journal of Physical Chemistry C,* 2018.

[13] P. Hlubina and J. Olszewski, "Phase retrieval from spectral interferograms including a stationary-phase point," *Optics communications,* vol. 285, no. 24, pp. 4733-4738, 2012.

[14] L. M. Smith and C. C. Dobson, "Absolute displacement measurements using modulation of the spectrum of white light in a Michelson interferometer," *Applied Optics,* vol. 28, no. 16, pp. 3339-3342, 1989.

[15] T. J. Fortin, A. Laesecke, M. Freund, and S. Outcalt, "Advanced calibration, adjustment, and operation of a density and sound speed analyzer," *The Journal of Chemical Thermodynamics,* vol. 57, pp. 276-285, 2013.

[16] F. Spieweck and H. Bettin, "Solid and liquid density determination/Übersicht: Bestimmung der Dichte von Festkörpern und Flüssigkeiten," *Tm-Technisches Messen,* vol. 59, no. 7-8, pp. 285-292, 1992.

USC
UNIVERSIDADE
DE SANTIAGO
DE COMPOSTELA

3 Results and discussion

3.1 INTRODUCTION

In this chapter, we present the results of the research developed during these years that was mainly centered on the characterization of the refractive index wavelength dependence of a set of 20 ionic liquids. By RISBI, we calculate other dispersive parameters that are relevant for several optical applications such as optical imaging, optical guiding or ultrafast optics; Abbe number, group index, group velocity dispersion, third-order dispersion and the dispersion of the thermoptic coefficient are some examples.

Using the Lorentz-Lorentz approach density and refractive index data, we demonstrate from empirical results the linear variation of the molar volume and molar refraction with the number of carbons in the alkyl chain for each family of ionic liquids, integrated by ILs that different only on the length of the alkyl chain, *Nc*; this linear relation is used to give a prediction of the refractive index of ionic liquids of the same family, whenever the addition of CH_2 groups does not lead to anisotropies in the refractive index.

In order to simplify the analysis, the ionic liquids have been classified into five groups (see Table 3.1) according to common structural characteristics. Groups 1 and 2 comprise ILs with alkyl-methylimidazolium cations paired with $[BF_4]^-$ and $[NTf_2]^-$ anions, respectively. Groups 3 and 4 contain the ionic liquids sharing the $[C_2MIm]^+$ and the $[C_4MIm]^+$ cations, respectively, combined with different anions. The ILs resulting from the combination of the $[C_2MIm]^+$ cation with alkyl sulfate anions will also object of a particular

study due to their singular behavior. We will refer to them as Subgroup 3.1. Finally, a fifth group, composed of four ionic liquids sharing the $[NTf_2]^-$ anion but combined with cations other than alkyl-methyl imidazolium, is also considered.

Table 3.1. Ionic Liquids classified in each one of the five identified groups. Subgroup 3.1 is formed by the underlined ionic liquids

Group 1		Group 2		Group 3		Group 4		Group 5	
Cation	Anion	Cation	Anion	Cation	Anion	Cation	Anion	Cation	Anion
C_2MIm C_3MIm C_4MIm C_6MIm C_8MIm	BF_4	C_2MIm C_3MIm C_4MIm C_6MIm	NTf_2	C_2MIm	BF_4 NTf_2 OTf $\underline{H_ySO_4}$ $\underline{C_1SO_4}$ $\underline{C_2SO_4}$ $\underline{C_6SO_4}$	C_4MIm	BF_4 NTf_2 OTf C_1SO_4 SCN	C_4MIm C_4MMIm C_4MPip MOEMPl	NTf_2

3.2 REFRACTIVE INDEX

As it has been previously announced in Chapter 2, the refractive index is determined in a wide spectral band covering a range of 600 nm, from 400 nm to 1000 nm. The corresponding data are obtained by RISBI assisted with Abbe refractometry, that is used to remove the phase ambiguity. As it was previosly mentioned, the Abbe refractometer used in this work allows the measurement at five wavelengths; one of them is used for the ambiguity removal, and the other four serve to check the validity of the system.

It must be noted that there is a great dispersion between the refractive index values measured by different researchers; in Table 3.2 we show the refractive index at 589.3 nm of the ionic liquids object of this study that has been published in the last years together with ours. We also show a curious result: the average value of the data are rather close to the value provided by us. An example can be seen in Figure 3.1 for [C4MIm] [BF4] where we plot the mean value (red circles) and the standard deviation of those reported data [1-16] together with the values measured by us at different temperatures. Notice that the mean values and our values show a great concordance. The observed differences in

literature, sometimes greater than 10^{-3}, have been traditionally attributed to different degrees of purity, water content or systematic errors due to the measurement conditions, for example. In the past, the purity of ionic liquids studied by researchers appears to be a somewhat neglected issue in view of the differences encountered between the values of different physical properties that have been reported for the same ionic liquid. However, in the last years researchers make efforts to develop synthesis processes that guarantee the preparation of samples with a high degree of purity.

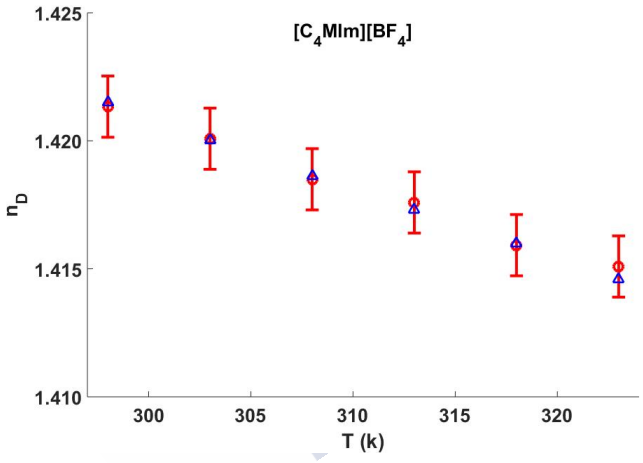

Figure 3.1. Red circles: averaged refractive index value of the n_D data reported for [C_4MIm] [BF_4] at different temperatures [1-16] Red bars: standard deviation. Blue triangles: refractive index values obtained by us.

Refractive index, as well as optical absorption or electrical conductivity, for example, depends strongly on the purity. That is why we have been very careful during all the measurement procedure, guaranteeing minimal contamination of the samples that cannot alter the results. Measurements have been repeated periodically, and the high degree of compatibility of the data confirms that the sample preparation process and the storage conditions are adequate, reinforcing the confidence in the high repeatability of RISBI.

Established this confidence in the characterization method, we proceed to analyze the trends and behaviors observed in the selected set of ionic liquids. We pay special attention to the influence of the length of the aliphatic chain in anion and cation, the anionic influence and also how the functionalization of the cation alters the refractive index and its derived parameters.

Table 3.2. The refractive index at 589.3 nm, n_D, of the ionic liquids object of this study and the average of the refractive index values measured by different researchers.

Ionic liquid	T (K)	n_D	Average	References
$[C_2MIm][BF_4]$	298	1.4116	1.4128	[1-16]
	303	1.4103	1.4099	
	308	1.4090	1.4091	
	313	1.4077	1.4074	
$[C_3MIm][BF_4]$	298	1.4174	1.4165	
	303	1.4161	1.4153	
	308	1.4148	1.4142	
	313	1.4135	1.4132	
$[C_4MIm][BF_4]$	298	1.4213	1.4213	
	303	1.4200	1.4201	
	308	1.4186	1.4185	
	313	1.4173	1.4176	
	318	1.4160	1.4159	
	323	1.4146	1.4151	
$[C_6MIm][BF_4]$	298	1.4275	1.4276	
	303	1.4261	1.4258	
	308	1.4248	1.4251	
	313	1.4234	1.4236	
$[C_8MIm][BF_4]$	298	1.4328	1.4329	
	303	1.4314	1.4309	
	308	1.4300	1.4292	
	313	1.4286	1.4278	
$[C_2MIm][NTf_2]$	298	1.4225	1.4228	[5, 7-9, 12, 14-21]
	303	1.4211	1.4214	
	308	1.4196	1.4201	
	313	1.4181	1.4183	
	318	1.4167	1.4172	
	323	1.4152	1.4157	
$[C_3MIm][NTf_2]$	298	1.4246	1.4253	
	303	1.4231	1.4238	
	308	1.4217	1.4222	

	313	1.4202	1.4205	
	318	1.4187	1.4193	
	323	1.4172	1.4178	
$[C_4MIm][NTf_2]$	298	1.4265	1.4267	
	303	1.4250	1.4249	
	308	1.4235	1.4234	
	313	1.4220	1.4222	
	318	1.4204	1.4201	
	323	1.4189	1.4183	
$[C_6MIm][NTf_2]$	298	1.4292	1.4300	
	303	1.4277	1.4289	
	308	1.4261	1.4271	
	313	1.4245	1.4258	
	318	1.4229	1.4239	
	323	1.4214	1.4228	
$[C_2MIm][OTf]$	298	1.4339	1.4333	[5, 12, 18, 21-26]
	303	1.4325	1.4315	
	308	1.4311	1.4305	
	313	1.4298	1.4290	
	318	1.4284	1.4274	
	323	1.4270	1.4265	
$[C_4MIm][OTf]$	298	1.4371	1.4375	
	303	1.4357	1.4355	
	308	1.4343	1.4347	
	313	1.4330	1.4323	
	318	1.4316	1.4319	
	323	1.4302	1.4298	

3.2.1 Effect of the aliphatic chain

The refractive index of ionic liquids that belong to the same group (i.e. ionic liquids of Groups 1, 2 and those of Subgroup 3.1) experiences a monotonic variation, increase or decrease, as the number of carbons of the alkyl chain, N_c, increases as it can be seen in Figure 3.2, Figure 3.3 and Figure 3.4.

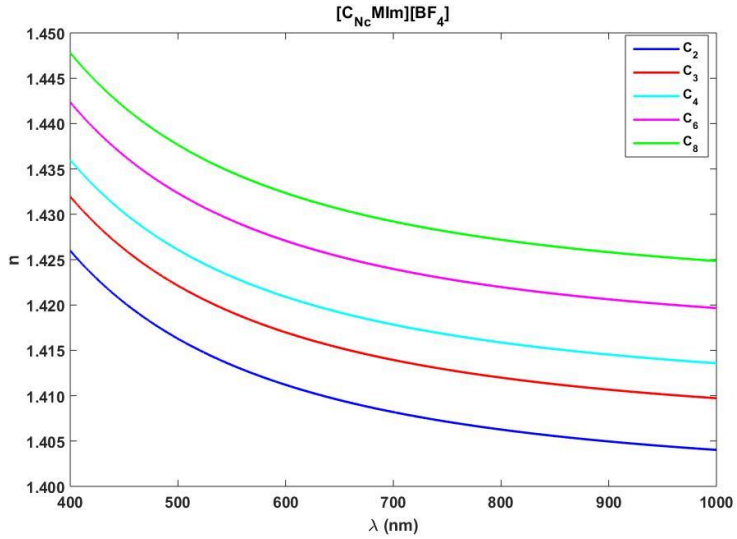

Figure 3.2. Refractive index dispersion of ionic liquids of Group 1, $[C_{Nc}MIm][BF_4]$ (N_c = 2, 3, 4, 6, 8).

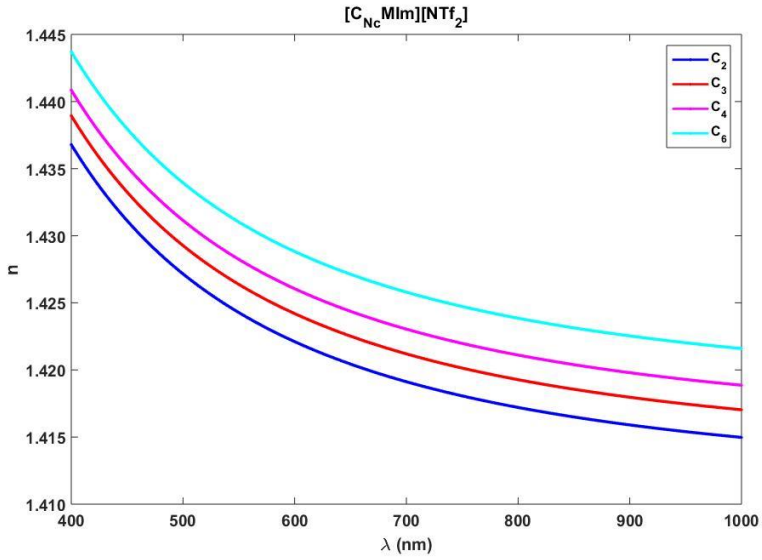

Figure 3.3. Refractive index dispersion of ionic liquids of Group 2, $[C_{Nc}MIm][NTf_2]$ (N_c= 2, 3, 4, 6).

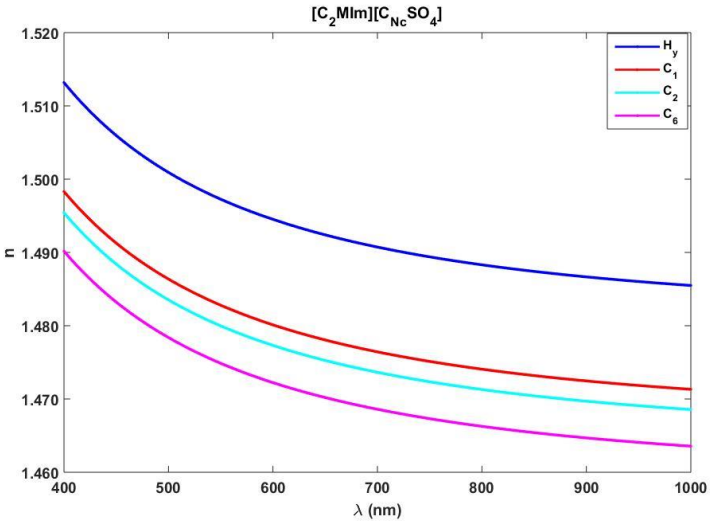

Figure 3.4.Refractive index dispersion of ionic liquids of Subgroup 3.1, $[C_2MIm][C_{Nc}SO_4]$ (N_c = 0, 1, 2, 6). The curves labeled with Hy corresponds to the ionic liquid $[C_2MIm][H_ySO_4]$.

In Table 3.3, we show the difference between the refractive index of the ionic liquid with the shortest chain and the refractive index of the ionic liquid with the longest chain in Groups 1, 2 and Subgroup 3.1, for three different wavelengths (400, 700 and 1000 nm). The refractive index change resulting from the increasing of N_c is barely dependent on wavelength in particular in the case of ionic liquids of Group 2. The results showed that the experienced change is slightly higher for blue wavelengths than for NIR wavelengths. The addition of a CH_2 group has fewer effects in the refractive index as longer is the chain as can be deduced from data of Table 3.4.

Table 3.3.Maximum refractive index change detected inside Group 1, Group 2 and Subgroup 3.1 at T=298.15 K.

GROUP	Δn400	Δn700	Δn1000
Group 1	-0.0218	-0.0210	-0.0208
Group 2	-0.0069	-0.0067	-0.0066
Subgroup 3.1	0.0230	0.0221	0.0219

Table 3.4. Refractive index change due to the addition of 1 or 2 CH_2 groups to the alkyl chain of ionic liquids of the same group at T=298.15K.

GROUP 1	Δn400	Δn700	Δn1000
C_3MIm- C_2MIm	0.0060	0.0058	0.0057
C_4MIm- C_3MIm	0.0040	0.0039	0.0039
C_6MIm- C_4MIm	0.0064	0.0061	0.0061
C_8MIm- C_6MIm	0.0054	0.0052	0.0052
GROUP 2			
C_3MIm- C_2MIm	0.0022	0.0021	0.0021
C_4MIm- C_3MIm	0.0019	0.0018	0.0018
C_6MIm- C_4MIm	0.0029	0.0028	0.0027
SUBGROUP 3.1			
C_1SO_4-H_ySO_4	-0.0149	-0.0143	-0.0142
C_2SO_4- C_1SO_4	-0.0029	-0.0028	-0.0028
C_6SO_4 - C_2SO_4	-0.0052	-0.0051	-0.0050

3.2.2 Lorentz–Lorenz equation

This behavior of the refractive index value, n, is determined by the changes induced in the molar volume, V_m, and in the molar refraction, R_m, due to the addition of CH_2 groups in the alkyl chain. The Lorentz–Lorenz equation relates these three magnitudes at a given wavelength (notice that n and R_m are dispersive properties):

$$\frac{n^2-1}{n^2+2}=\frac{R_m}{V_m} \qquad (3.1)$$

V_m can be easily calculated starting from the values of the molar mass, M, and the density, ρ, of the compound that can be determined experimentally.

$$V_m = \frac{M}{\rho N_A} \tag{3.2}$$

R_m is proportional to the molar polarizability, α_m, [27-29] that gives an idea of how easily an electromagnetic field can distort the electronic cloud of a chemical compound:

$$R_m = N_A \frac{\alpha_m}{3\varepsilon_0} V_m \tag{3.3}$$

Where N_A is the Avogadro number and ε_0 is the permittivity in the free space. R_m can be estimated if the refractive index and molar volume are known.

In order to calculate the molar volume, the density of the ionic liquids has been measured at several temperatures between 298.15 and 323.15 K every five degrees. The obtained values of density at T=298.15 K together with the corresponding molar mass, M, and the calculated molar volume are shown in Table 3.5.

The density values of the ionic liquids at different temperatures, as well as the coefficients of a linear fit over-temperature, are accessible in Appendix (Tables A2 and A3).

Table 3.5.The molar mass, density, and molar volume of the ionic liquid at T=298.15 K.

GROUP 1	Molas Mass(M) g/mol	Density (ρ) g/cm^3	Molar volumen(V_m) cm^3/mol
[C_2MIm] [BF_4]	197.97	1.284912	154.073
[C_3MIm] [BF_4]	212.00	1.237089	171.370
[C_4MIm] [BF_4]	226.02	1.201029	188.189
[C_6MIm] [BF_4]	254.08	1.145176	221.870
[C_8MIm] [BF_4]	282.13	1.104262	255.492
GROUP 2			
[C_2MIm] [NTf_2]	392.31	1.518490	258.355
[C_3MIm] [NTf_2]	405.34	1.474690	274.865
[C_4MIm] [NTf_2]	419.36	1.436639	291.904
[C_6MIm] [NTf_2]	447.42	1.372197	326.061
SUBGROUP 3.1			
[C_2MIm] [$HySO_4$]	208.24	1.370980	151.891
[C_2MIm] [C_1SO_4]	222.26	1.288246	172.529
[C_2MIm] [C_2SO_4]	236.29	1.237665	190.916
[C_2MIm] [C_6SO_4]	292.38	1.130178	258.703

The behaviour of V_m with the number of carbons of the aliphatic chain (quantity that we have called N_c) for ionic liquids belonging to Groups 1, 2 and Subgroup 3.1, is shown in Table 3.5 and plotted in Figure 3.5 at a temperature of 298.15 K. All the curves display a linear variation of V_m with N_c The dashed line corresponds to the fitted function $V_m=V_0+N_c\Delta V$ whose slope, ΔV, depends on the anion as can be clearly appreciated in Table 3.6.

The tax of molar volume growth is similar in ionic liquids of Groups 1 and 2 although the molar volume ionic of liquids sharing the $[NTf_2]^-$ anion is greater. The ionic liquids of Subgroup 3.1 have an intermediate size, and a higher growth rate than the experienced by ionic liquids of the other studied two groups.

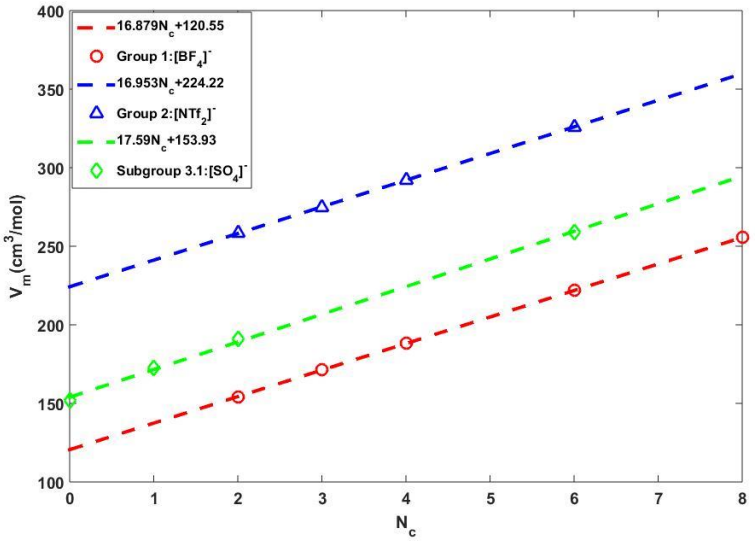

Figure 3.5. The behavior of V_m with N_c for ionic liquids of Groups 1, 2, and Subgroup 3.1 at 298.15 K.

In the groups under study in this subsection, ΔR and ΔV come from the addition of a CH_2 group to the alkyl chain; the influence of this group is modulated for the type of anion paired with de alkyl-methyl-imidazolium cation.

Assuming this linear behavior within each family, we can rewrite equation (2.1):

$$\frac{n^2 - 1}{n^2 + 2} = \frac{R_0 + N_c \Delta R}{V_0 + N_c \Delta V} \tag{3.4}$$

And we can reorganize it to obtain the expression of the refractive index:

$$n^2 = \frac{1 + 2\frac{R_0 + N_c\Delta R}{V_0 + N_c\Delta V}}{1 - \frac{R_0 + N_c\Delta R}{V_0 + N_c\Delta V}} \qquad (3.5)$$

If we take limits when *Nc* tends to 0 and to ∞ in equation (3.5), we determine the extreme values for n^2:

$$\lim_{N_c\to\infty} n^2 = \frac{1 + 2\frac{\Delta R}{\Delta V}}{1 - \frac{\Delta R}{\Delta V}} = n_\infty^2 \qquad (3.6)$$

$$\lim_{N_c\to 0} n^2 = \frac{1 + 2\frac{R_0}{V_0}}{1 - \frac{R_0}{V_0}} = n_0^2 \qquad (3.7)$$

The behavior of n with Nc depends on the relation between $\frac{\Delta R}{\Delta V}$ and $\frac{R_0}{V_0}$. If $\frac{\Delta R}{\Delta V} > \frac{R_0}{V_0}$, then the refractive index increases with N_c, whereas if it verifies the opposite relation, the refractive index decreases with N_c. The values for the three groups of liquids are shown in Table 3.6 for λ=589.3 nm at T=298.15 K. The limit values, those achieved when N_c tends to zero or infinite, are denoted as n_0 and n_∞ in Table 3.6.

Table 3.6. R_0, V_0, ΔR, ΔV, R_0/V_0, R_0/V_0, n_0 and n_∞ values that characterize the ionic liquids of Group 1 ([C_{Nc}MIm][BF_4]), Group 2 ([C_{Nc}MIm][NTf_2]) and Subgroup 3.1 ([C_2MIm][$C_{Nc}SO_4$]). The wavelength is 589.3nm and the temperature is T=298.15 K.

	[C_{Nc}MIm][BF_4]	[C_{Nc}MIm][NTf_2]	[C_2MIm][$C_{Nc}SO_4$]
R_0 (cm^3/mol)	29.06	56.49	44.42
V_0 (cm^3/mol)	120.55	224.22	153.93
ΔR (cm^3/mol)	4.666	4.601	4.700
ΔV (cm^3/mol)	16.879	16.953	17.59
R_0/V_0	0.241	0.252	0.289
$\Delta R/\Delta V$	0.276	0.271	0.267
n_0	1.3975	1.4178	1.4888
n_∞	1.4650	1.4552	1.4470

So, the asymptotic value of the refractive index is given by n_∞. But we must take into account, at the time of prediction, that long alkyl tails can give rise to ionic liquids crystals (ILCs). These liquid crystal phases can arise in pure ionic liquids or may need the addition of a certain amount of water depending on the combination of cation and anion [30-32]. ILCs present anisotropies in the refractive index; in this situation, an *a priori* determination of the refractive index requires the knowledge of the ordinary and the extraordinary refractive indices. The discussed model does not apply to this situation.

In Figure 3.6a, b, c we plot the refractive index dispersion of the ILs of Groups 1 (a), 2 (b) and Subgroup 3.1(c) together with both limit values, given by n_0 and n_∞.

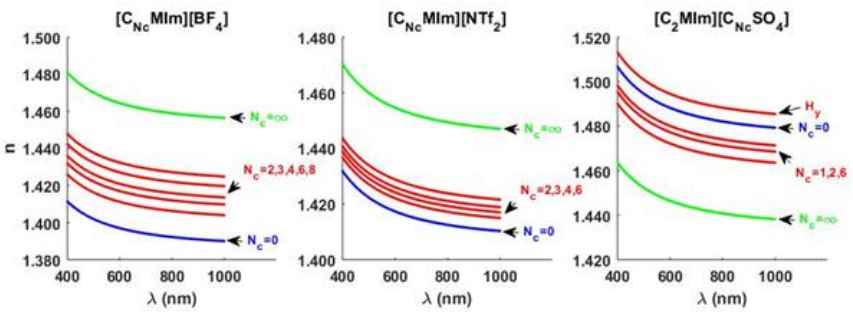

Figure 3.6. Refractive index dispersion of the ILs of Group 1 (a), Group 2 (b) and Subgroup 3.1(c) together with both limit values, given by n_0 and n_∞. at T=298.15 K.

Equation (3.5) allows estimating the refractive index value at any wavelength of an ionic liquid if we know the refractive index and density of two liquids of the same family. At the time of prediction, we must take into account that, although RISBI is a very accurate technique, equation (3.5) is an approximated expression derived by Lorentz-Lorenz equation where we have assumed the linear variation of R_m and V_m with N_c, too.

The experimental and predicted values of the refractive index at specific wavelengths for ionic liquids belonging to Groups 1, 2, and Subgroup 3.1, are shown in Table 3.7 and Table 3.8.

Table 3.7. The experimental (n) and predicted (n_e) value of refractive index for ionic liquids belonging to Groups 1, 2, and Subgroup 3.1, at 400, 700 and 1000 nm. The temperature is T=298.15 K.

GROUP 1	n_{400}	n_{400e}	n_{700}	n_{700e}	n_{1000}	n_{1000e}
$[C_2MIm]$ $[BF_4]$	1.4262	____	1.4083	____	1.4037	____
$[C_3MIm]$ $[BF_4]$	1.4322	1.4316	1.4140	1.4136	1.4093	1.4090
$[C_4MIm]$ $[BF_4]$	1.4361	____	1.4180	____	1.4133	____
$[C_6MIm]$ $[BF_4]$	1.4424	1.4430	1.4241	1.4247	1.4192	1.4200
$[C_8MIm]$ $[BF_4]$	1.4477	1.4481	1.4293	1.4297	1.4245	1.4249
GROUP 2						
$[C_2MIm]$ $[NTf_2]$	1.4372	____	1.4190	____	1.4140	____
$[C_3MIm]$ $[[NTf_2]$	1.4391	1.4391	1.4212	1.4211	1.4166	1.4162
$[C_4MIm]$ $[[NTf_2]$	1.4408	1.4409	1.4231	1.4229	1.4188	1.4181
$[C_6MIm]$ $[[NTf_2]$	1.4438	____	1.4259	____	1.4214	____
SUBGROUP 3.1						
$[C_2MIm]$ $[H_ySO_4]$	1.5134	1.5014	1.4908	1.4791	1.4851	1.4737
$[C_2MIm]$ $[C_1SO_4]$	1.4983	____	1.4765	____	1.4712	____
$[C_2MIm]$ $[C_2SO_4]$	1.4951	1.4958	1.4737	1.4744	1.4683	1.4690
$[C_2MIm]$ $[C_6SO_4]$	1.4891	____	1.4688	____	1.4634	____

Table 3.8. The experimental (*n*)and predicted (n_e)value of refractive index for ionic liquids belonging to Groups 1, 2 and Subgroup 3.1, at some Fraunhofer lines A (759.37 nm), B (686.72 nm), C (656.28 nm), D (589.29 nm), E (527.04 nm), F (486.13 nm) and G (430.80 nm) at T=298.15 K.

GROUP 1		A	B	C	D	E	F	G
$[C_2MIm]$ $[BF_4]$	n	1.4070	1.4086	1.4095	1.4118	1.4147	1.4174	1.4224
	n_e	-----	-----	-----	-----	-----	-----	-----
$[C_3MIm]$ $[BF_4]$	n	1.4127	1.4144	1.4152	1.4176	1.4206	1.4233	1.4284
	n_e	1.4123	1.4140	1.4148	1.4171	1.4201	1.4228	1.4278
$[C_4MIm]$ $[BF_4]$	n	1.4167	1.4183	1.4192	1.4215	1.4245	1.4272	1.4323
	n_e	-----	-----	-----	-----	-----	-----	-----
$[C_6MIm]$ $[BF_4]$	n	1.4227	1.4244	1.4253	1.4276	1.4307	1.4334	1.4386
	n_e	1.4234	1.4251	1.4259	1.4283	1.4314	1.4341	1.4393
$[C_8MIm]$ $[BF_4]$	n	1.4279	1.4296	1.4305	1.4328	1.4359	1.4387	1.4438
	n_e	1.4284	1.4301	1.4309	1.4333	1.4364	1.4392	1.4444
GROUP 2								
$[C_2MIm]$ $[NTf_2]$	n	1.4177	1.4194	1.4203	1.4226	1.4257	1.4284	1.4334
	n_e	-----	-----	-----	-----	-----	-----	-----
$[C_3MIm]$ $[NTf_2]$	n	1.4199	1.4216	1.4224	1.4247	1.4277	1.4303	1.4353
	n_e	1.4197	1.4214	1.4223	1.4246	1.4276	1.4303	1.4354
$[C_4MIm]$ $[NTf_2]$	n	1.4219	1.4234	1.4242	1.4265	1.4294	1.4320	1.4370
	n_e	1.4215	1.4232	1.4240	1.4264	1.4294	1.4320	1.4371
$[C_6MIm]$ $[NTf_2]$	n	1.4246	1.4262	1.4270	1.4293	1.4323	1.4349	1.4400
	n_e	-----	-----	-----	-----	-----	-----	-----
SUBGROUP 3.1								
$[C_2MIm]$ $[H_ySO_4]$	n	1.4892	1.4912	1.4923	1.4951	1.4989	1.5022	1.5086
	n_e	1.4776	1.4795	1.4805	1.4833	1.4870	1.4902	1.4964
$[C_2MIm]$ $[C_1SO_4]$	n	1.4750	1.4769	1.4779	1.4807	1.4843	1.4875	1.4936
	n_e	-----	-----	-----	-----	-----	-----	-----
$[C_2MIm]$ $[C_2SO_4]$	n	1.4722	1.4741	1.4751	1.4778	1.4814	1.4846	1.4907
	n_e	1.4729	1.4748	1.4758	1.4785	1.4821	1.4853	1.4913
$[C_2MIm]$ $[C_6SO_4]$	n	1.4673	1.4692	1.4701	1.4728	1.4763	1.4794	1.4852
	n_e	-----	-----	-----	-----	-----	-----	-----

As a graphical evidence, we show in Figure 3.7, Figure 3.8 and Figure 3.9 the predicted values of refractive index along the Vis-NIR spectra for ionic liquids belonging to Groups 1, 2 and Subgroup 3.1 as together with the measured ones. Besides, we plot the difference between them that remains below $8 \cdot 10^{-4}$ except the case of the ionic liquid $[C_2MIm][H_ySO_4]$. The result obtained for this ionic liquid suggests that it could not be considered to be part of Subgroup 3.1.

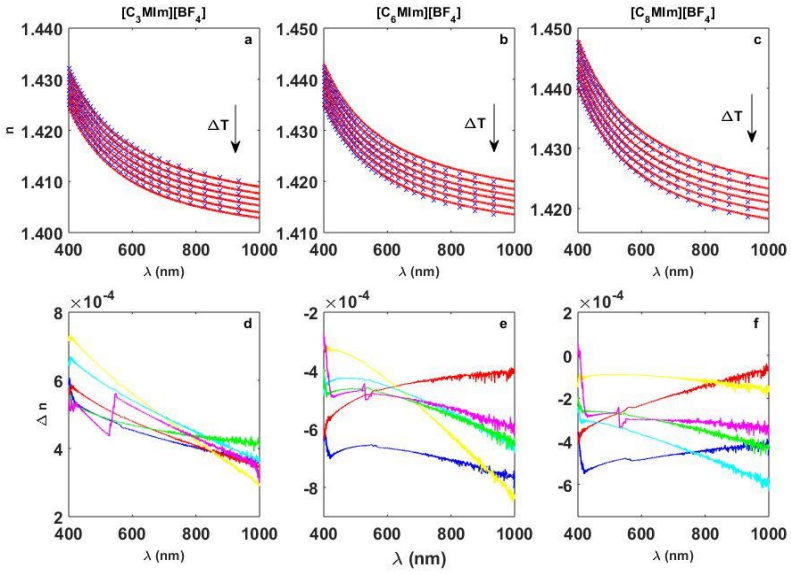

Figure 3.7. Experimental (cross blue mark) and predicted (red curve) values of refractive index using eq. (3.5) versus wavelength at temperatures from 298.15 to 323.15 K at every five degrees: (a) $[C_3MIm][BF_4]$,(b) $[C_6MIm][BF_4]$; (c) $[C_8MIm][BF_4]$; (d), (e) and (f) show the difference between experimental and predicted values. This prediction was made starting from the refractive index and density data of the ionic liquids $[C_2MIm][BF_4]$ and $[C_4MIm][BF_4]$.

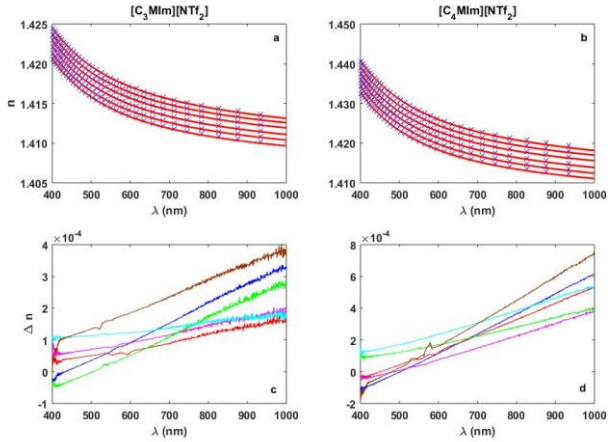

Figure 3.8. Experimental (cross blue mark) and predicted (red curve) values of *n* using eq. (3.5) versus wavelength at temperatures from 298.15 to 323.15 K at every 5 degrees. (a) $[C_3MIm][NTf_2]$,(b) $[C_4MIm][NTf_2]$; (c) and (d) show the difference between experimental and predicted values. This prediction was made starting from the *n* and *ρ* of ILs $[C_2MIm][NTf_2]$ and $[C_6MIm][NTf_2]$.

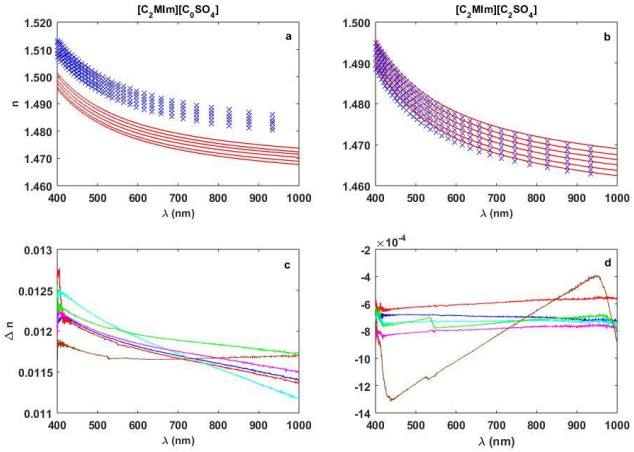

Figure 3.9. Experimental (cross blue mark) and predicted (red curve) values of *n* using eq. (3.5) versus wavelength at temperatures from 298.15 to 323.15 K at every 5 degrees. (a) $[C_2MIm][H_ySO_4]$,(b) $[C_2MIm][C_2\ SO_4]$; (c) and (d) show the difference between experimental and predicted values. This prediction was made starting from the *n* and *ρ* of ILs $[C_2MIm][\ C_1SO_4]$ and $[C_2MIm][\ C_6SO_4]$.

In order to show a second example, as we have measured the values of the refractive index and density of two liquids from [OTf] family with Nc equal to 2 and 4, we used them to predict the refractive index for ionic liquids with *Nc* equal to 6 and to 8; Figure 3.10 shows the values. We can see in Figure 3.11a the plot of the predicted values of the refractive index (blue circles) with those reported in the literature [33, 34] at different temperatures. Figure 3.11b shows the differences between them that keep below 10^{-3}, result that demonstrates the consistency of the prediction.

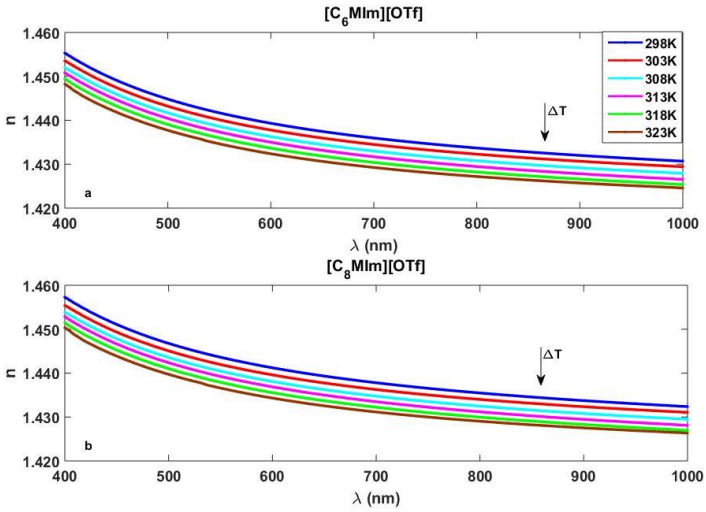

Figure 3.10. Predicted values of refractive index using eq (3.5) versus wavelength at temperatures from 298.15 to 323.15 K every five degrees: (a) [C_6MIm][OTf] ,(b) [C_8MIm][OTf]. This prediction was made starting from the refractive index and density data of [C_2MIm][OTf] and [C_4MIm][OTf].

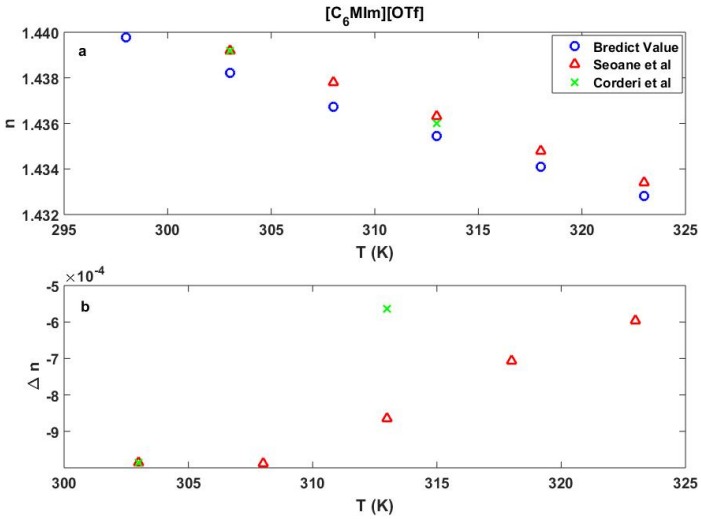

Figure 3.11. (a) Predicted values of the refractive index (blue circles) together with those previously reported data in the literature (red triangles from [33], green crosses from [34]). (b) Difference between predicted and reported values (red triangles [33], green crosses [34]).

A study trying to predict the trend of the refractive index with *Nc* was published some years ago by Bica *et al*. [27]; they defined two groups of 1-alkyl-3-methylimidazolium- based ionic liquids, Class 1 and Class 2, as function of the ratio α_{mol}/ V_{mol}, being α_{mol} the molar polarizability of the ionic liquid at λ=589.3nm, that is proportional to R_m. Class 1 comprises ionic liquids with highly polar anions such as sulfates or thiocyanates, and their refractive indices decrease when the number of CH_2 groups in the alkyl chain increases; whereas Class 2 ionic liquids are those containing $[BF_4]^-$, $[NTf_2]^-$ or [OTf]$^-$, for example, whose refractive index follows the opposite behavior. According to this classification, among the studied set of 20 ionic liquids, only those containing the sulfate or thiocyanate anions belong to Class 1. The other ionic liquids belong to Class 2, a conclusion that agrees with the observed behavior of the refractive index.

The value of the ratio delimiting the boundary between the two groups is just corresponding to the one of a CH_2 group (α_{mol}/ V_{mol} = 0.0661 for λ=589.3nm). This quantity has been obtained by

deconstructing the molar polarizabilities and molar volumes into atomic contributions starting from a numerous set of ionic liquids and, under the used approach, it is independent of the environment of the CH_2 group. Although this result works well for the classification of ionic liquids, actually our research confirms that the environment influences the value of α_{mol}/ V_{mol} of the CH_2 group (notice that α_{mol} is proportional to ΔR and V_{mol} to ΔV).

3.2.3 Effect of the cation

In Figure 3.12, we show how other structural changes in the cation modified the chromatic dispersion curves with respect to the $[C_4MIm][NTf_2]$ one. These changes consist on: the addition of a new methyl functional group at the position two in the imidazolium ring, $[C_4MMIm]^+$; the substitution of the imidazolium ring by a piperidinium, $[C_4MPip]^+$; and the complete substitution of the $[C_4MIm]^+$ cation by a $[MOEMPl]^+$ one. Although the four curves follow the trend expected in the normal dispersion regime since they are transparent in the range of available wavelengths, the magnitude of the respectively induced variations of the refractive index are higher than the caused by changing in one unity the carbon number in the longer alkyl chain (compare with data of Figure 3.3 taking as reference the curve corresponding to $[C_4MIm][NTf_2]$).

The addition of a new methyl functional group leads to the highest refractive index value. The replacement of cation $[C_4MIm]^+$ by $[C_4MPip]^+$ increases the refractive index of the IL, being the difference more noticeable in the red edge of the spectrum. On the contrary, the replacement of cation $[C_4MIm]^+$ by cation $[MOEMPl]^+$ causes a decrease on this magnitude along with the studied spectral range, slightly more evident for short wavelengths than for long wavelengths.

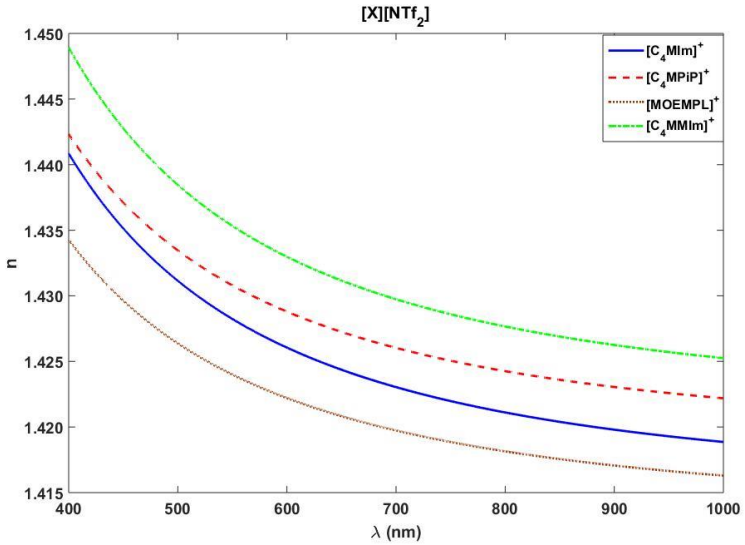

Figure 3.12. Refractive index dispersion of ionic liquids sharing the $[NTf_2]^-$ anion paired with different cations at T=298.15 K.

We can use eq (3.5) to try to elucidate the origin of the refractive index change. In Table 3.9 we show the molar mass, density, V_m and the R_m of each ionic liquid at T=298.15 K, we specify the values of this last quantity at three different wavelengths:

Table 3.9. Molar mass (M), density (ρ), Molar volume (V_m) and the Molar refractivity (R_m) of each ionic liquid at T=298.15 K.

Ionic liquid	M (g/mol)	ρ (g/cm^3)	V_m (cm^3/mol)	R_m (cm^3/mol) (400nm)	R_m (cm^3/mol) (700nm)	R_m (cm^3/mol) (1000nm)	(V_m/R_m - 1)
$[C_4MIm][NTf_2]$	419.36	1.436639	291.904	77.046	74.346	73.677	2.789
$[C_4MMIm][NTf_2]$	433.39	1.418644	305.496	81.875	78.899	78.057	2.731
$[C_4MPip][NTf_2]$	436.43	1.382353	315.715	83.501	80.932	80.170	2.781
$[MOEMPl][NTf_2]$	424.38	1.453158	292.040	76.069	73.874	73.284	2.839

In Table 3.10 show the variation of V_m and R_m calculated for $[C_4MMIm][NTf_2]$, $[C_4MPip][NTf_2]$, $[C_4MPip][NTf_2]$ with respect to the corresponding values of $[C_4MIm][NTf_2]$.

Table 3.10. Variation of V_m and R_m calculated for [C_4MMIm][NTf_2], [C_4MPip][NTf_2], [C_4MPip][NTf_2] with respect to the corresponding values of [C_4MIm][NTf_2], at T=298.15 K.

Ionic liquid	ΔV_m	ΔR_m (400nm)	ΔR_m (700)	ΔR_m (1000nm)
[C_4MIm][NTf_2]	-------	--------	---------	----------
[C_4MMIm][NTf_2]	13.592 (4.66%)	4.829 (6.27%)	4.552 (6.12%)	4.379 (5.94%)
[C_4MPip][NTf_2]	23.811 (8.16%)	6.455 (8.38%)	6.585 (8.86%)	6.492 (8.81%)
[MOEMPl][NTf_2]	00.136 (0.01%)	-0.977 (-1.27%)	0.472 (-0.06%)	0.393 (-0.05%)

In view of these results, we can conclude that the refractive index change is mainly due to changes in both of V_m and R_m, not just one of them. Nevertheless, the values are highly cation dependent without any evident relationship between them (the order of the cations based on the increase in V_m or R_m does not match with their increase in refractive index). From this point of view, equation (3.1) can be rearranged to be expressed in terms of the free molar volume[3]:

$$n^2 - 1 = \frac{3}{\left(\frac{V_m}{R_m} - 1\right)} \qquad (3.8)$$

this equation shows that n^2-1 is inversely proportional to the reduced molar free volume (V_m/R_m -1). Thus increasing the reduced molar free volume reduces n, behaviour that agrees with our results, as can be seen in Table 3.9.

3.2.4 Effect of the anion

Figure 3.13 shows the dispersion curves of ionic liquids resulting by the imidazolium cation 1-ethyl-3-methylimidazolium combined with different anions: $[C_1SO_4]^-$, $[C_2SO_4]^-$, $[C_6SO_4]^-$, $[HySO_4]^-$, $[OTf]^-$, $[NTf_2]^-$ and $[BF_4]^-$. The curves have the same qualitative behavior for all the anions and are nearly parallel. The refractive index values vary from 1.4000 to 1.5100 throughout the studied spectral range, and they

[3] Free molar volume is a measurement of the molar volume which does not interact with light and equal (V_m/R_m).

are highly dependent on the anion. The anions can be ordered according to the refractive index magnitude to which they give rise, resulting the following series: $[HySO_4]^-$ > $[C_1SO_4]^-$ > $[C_2SO_4]^-$ > $[C_6SO_4]^-$ > $[OTf]^-$ > $[NTf_2]^-$ > $[BF_4]^-$. The first inspection of Figure 3.13a allows us to distinguish two groups of well-differentiated curves: ionic liquids containing anions with the SO_4 functional group and the others. The first one is characterized by higher values of the refractive index between 1.4600 and 1.5100 in the whole spectral interval that diminishes as increases the number of carbons in the anion; whereas the other group presents lower refractive index values, between 1.4200 and 1.4500 at T=308.15 K.

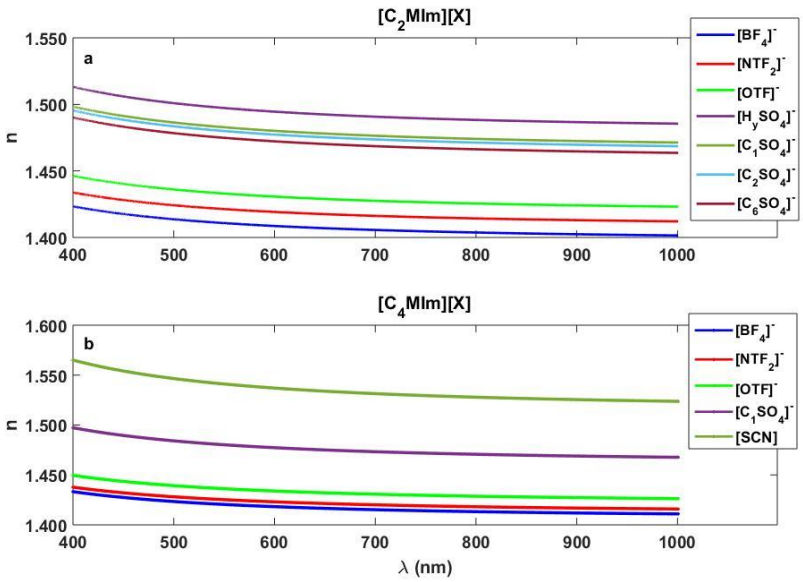

Figure 3.13. Effect of the anion in the refractive index dispersion of (a) 1-ethyl-3-methylimidazolium and (b) 1-butyl-3-methylimidazolium-based ionic liquids. Data were taken at T=308.15 K.

Similar characteristics are observed in Figure 3.13b, where the chromatic dispersion curves for ionic liquids sharing the $[C_4MIm]^+$ cation are depicted. $[SCN]^-$ and $[C_1SO_4]^-$ anions give rise to ionic liquids with higher refractive index than $[OTf]^-$,$[NTf_2]^-$ and $[BF_4]^-$. The

values of V_m and R_m for three different wavelengths at T=298.15 K are shown in Table 3.11.

Table 3.11 Values of Molar mass (*M*), density (ρ) , Molar volume(V_m) and Molar refractivity (R_m) for three different wavelengths at T=298.15 K of ethyl-methylimidazolium (a) and butyl-methylimidazolium-based ionic liquids.

Ionic liquid	*M* (g/mol)	(*ρ*) (g/cm^3)	V_m (Cm^3/mol)	R_m 400 (nm)	R_m 700 (nm)	R_m 1000 (nm)	(V_m/R_m -1)
[C_2MIm][H_ySO_4]	208.24	1.370980	151.891	45.684	43.977	43.542	2.325
[C_2MIm] [C_1SO_4]	222.26	1.288246	172.529	50.597	48.709	48.237	2.410
[C_2MIm] [C_2SO_4]	236.29	1.237665	190.916	55.682	53.627	53.101	2.429
[C_2MIm] [C_6SO_4]	292.38	1.130178	258.703	74.683	72.018	71.311	2.464
[C_2MIm] [BF_4]	197.97	1.284912	154.073	39.490	38.034	37.654	2.902
[C_2MIm] [NTf_2]	392.31	1.518490	258.355	67.713	65.250	64.565	2.815
[C_2MIm] [OTf]	260.23	1.382060	188.291	50.521	48.670	48.197	2.727
[C_4MIm][SCN]	197.30	1.069328	184.508	60.191	57.104	56.448	2.065
[C_4MIm][C_1SO_4]	250.32	1.212159	206.508	60.406	57.997	57.252	2.419
[C_4MIm] [BF_4]	226.02	1.201029	188.189	49.212	47.423	46.954	2.824
[C_4MIm] [NTf_2]	419.36	1.436639	291.904	77.046	74.346	73.677	2.789
[C_4MIm] [OTf]	288.29	1.297670	222.160	60.012	57.803	57.213	2.702

Given these results, the behavior observed when the anion changes are similar to the observed when the cation changes. In view of these results, we conclude that the variation induced in the refractive index when the anion change is caused by the simultaneous variations in V_m and R_m; we have not any evidence for assigning a dominant role to one of them.

3.3 THE EFFECT OF TEMPERATURE ON THE REFRACTIVE INDEX

Figure 3.14, a-c, show the linear variation of the refractive index, n_D, with temperature in all the compounds. The slope, which is known as a thermo-optic coefficient (TOC) is always negative and, its absolute value increases when the cationic or anionic alkyl chain length does, as it is shown in Figure 3.14d. Taking as reference the ILs containing the sulfate group, the absolute value of the slope is smaller for compounds sharing the $[BF_4]^-$ anion and greater for compounds sharing the $[NTf_2]^-$ anion. Measured values of refractive index at selected Fraunhofer lines and temperatures are provided in the Appendix (Table A1).

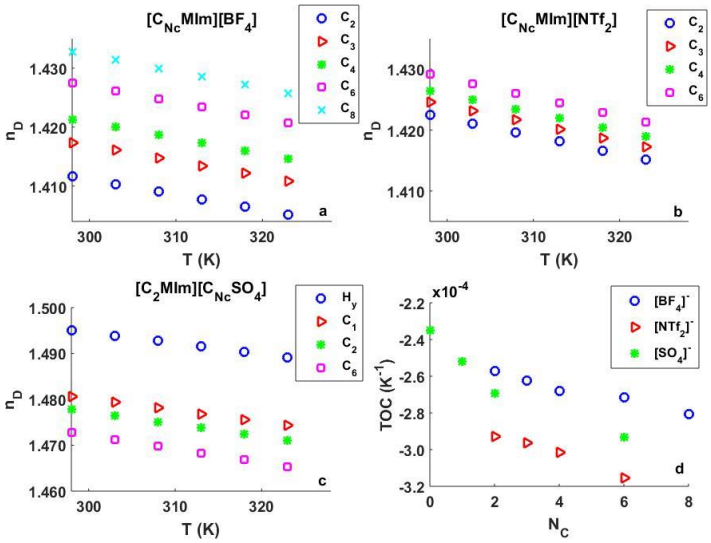

Figure 3.14. Refractive index versus temperature at 589.3 nm: (a) $[C_{Nc}Mim]$ $[BF_4]$ (*Nc* = 2, 3, 4, 6, 8); (b) $[C_{Nc}Mim]$ $[NTf_2]$ (*Nc*= 2, 3, 4, 6); (c) $[C_2Mim]$ $[C_{Nc}SO_4]$ (*Nc* = 0, 1, 2, 6); and (d) Variation of the thermooptic coefficient with the number of carbons *Nc*.

3.3.1 Molar volume and molar refraction

According to the Lorentz-Lorenz equation, changes in V_m or in R_m modify the refractive index values. In this subsection, we analyze the variation of V_m and R_m behind a change in refractive index induced by temperature. V_m variations are determined independently starting from changes in densities. In Table 3.12, we list the values of molar mass, density, V_m, R_m (the last three at 298.15 K and 318.15 K). We also calculate the percentage of variation of the last properties, quantities that we have called ΔV_T and ΔR_T, that are similar.

Table 3.12. Molar mass (M), density (ρ), Molar volume (V_m), and the Molar refractivity (R_m), the last three at T1=298.15 K and T2= 318.15 K.

Ionic Liquid	T (K)	ρ (g/cm^3)	V_m (Cm^3/mol)	R_m (589.3nm)	ΔV_T	V_{T2}/V_{T1} %	ΔR_T	R_{T2}/R_{T1}%
[C_2MIM] [BF_4]	298.15	1.284912	154.073	38.316	2.286	101.48	0.019	100.05
	318.15	1.266119	156.359	38.336				
[C_3MIm] [BF_4]	298.15	1.237089	171.370	43.145	2.566	101.50	0.029	100.07
	318.15	1.218832	173.937	43.174				
[C_4MIm] [BF_4]	298.15	1.201029	188.189	47.772	2.806	101.49	0.014	100.03
	318.15	1.183384	190.994	47.786				
[C_6MIm] [BF_4]	298.15	1.145176	221.870	57.038	3.350	101.51	0.037	100.07
	318.15	1.128139	225.220	57.076				
[C_8MIm] [BF_4]	298.15	1.104262	255.492	66.377	3.946	101.54	0.058	100.09
	318.15	1.087464	259.438	66.436				
[C_2MIm][NTf_2]	298.15	1.518490	258.355	65.736	4.332	101.67	0.073	100.11
	318.15	1.493448	262.687	65.810				
[C_3MIm][NTf_2]	298.15	1.474690	274.865	70.236	4.636	101.69	0.083	100.12
	318.15	1.450228	279.500	70.320				
[C_4MIm][NTf_2]	298.15	1.436639	291.904	74.862	4.902	101.68	0.061	100.08
	318.15	1.41291	296.805	74.924				

$[C_6MIm][NTf_2]$	298.15	1.372197	326.061	84.112	5.507	101.69	0.040	100.05
	318.15	1.349405	331.568	84.152				
$[C_4MMIm][NTf_2]$	298.15	1.418644	305.496	79.494	5.023	101.64	0.093	100.12
	318.15	1.395693	310.519	79.587				
$[C_4MPip][NTf_2]$	298.15	1.382353	315.715	81.457	4.935	101.56	0.067	100.08
	318.15	1.361075	320.651	81.525				
[MOEMPl] $[NTf_2]$	298.15	1.453158	292.039	74.311	4.775	101.64	0.067	100.09
	318.15	1.429778	296.815	74.379				
$[C_2MIm][H_ySO_4]$	298.15	1.370980	151.891	44.303	1.728	101.14	0.042	100.10
	318.15	1.355554	153.619	44.346				
$[C_2MIm]$ $[C_1SO_4]$	298.15	1.288246	172.529	49.069	2.277	101.32	0.099	100.20
	318.15	1.271462	174.806	49.168				
$[C_2MIm]$ $[C_2SO_4]$	298.15	1.237665	190.916	54.025	2.630	101.38	0.071	100.13
	318.15	1.220844	193.546	54.096				
$[C_2MIm]$ $[C_6SO_4]$	298.15	1.130178	258.703	72.547	3.796	101.47	0.090	100.13
	318.15	1.113832	262.499	72.638				
$[C_2MIm]$ [OTf]	298.15	1.382060	188.291	49.027	2.877	101.53	0.040	100.08
	318.15	1.361260	191.168	49.068				
$[C_4MIm][SCN]$	298.15	1.069328	184.508	57.659	2.564	101.39	0.105	100.18
	318.15	1.054670	187.072	57.764				
$[C_4MIm]$ [OTf]	298.15	1.297670	222.160	58.236	3.409	101.53	0.067	100.12
	318.15	1.278053	225.569	58.303				
$[C_4MIm][C_1SO_4]$	298.15	1.212159	206.508	58.487	2.861	101.39	0.056	100.10
	318.15	1.195593	209.369	58.544				

3.3.1.1 Groups 1, 2 and Subgroup 3.1

Special attention should be deserved to ionic liquids of groups 1, 2 and subgroup 3.1. In Table 3.13 the obtained values of V_0 and ΔV are shown for 298, 303, 308, 313, 318 and 323K.

Table 3.13 Values of V_0 , ΔV and the regression coefficients of the linear fit with ($V_m=V_0+\Delta VN_c$) to the molar volume data at different temperatures .

IL	T	V_0	ΔV	R^2
$[C_nMIm][BF_4]$	298 K	120.5547	16.8791	0.9999
	303 K	120.8902	16.9355	0.9999
	308 K	121.2319	16.9913	0.9999
	313 K	121.5833	17.0447	0.9999
	318 K	121.9336	17.0990	0.9999
	323 K	122.2826	17.1538	0.9999
$[C_nMIm][NTf_2]$	298 K	224.2205	16.9535	0.9999
	303 K	224.9687	17.0105	0.9999
	308 K	225.7170	17.0685	0.9999
	313 K	226.4675	17.1269	0.9999
	318 K	227.2177	17.1863	0.9999
	323 K	227.9685	17.2459	0.9999
$[C_2MIm][C_nSO_4]$ With H_y	298 K	153.9327	17.5898	0.9986
	303 K	154.3016	17.6577	0.9986
	308 K	154.6730	17.7248	0.9986
	313 K	155.0478	17.7894	0.9985
	318 K	155.4232	17.8540	0.9985
	323 K	155.7988	17.9196	0.9985

$[C_2MIm][C_nSO_4]$	298 K	155.9254	17.1524	0.9998
	303 K	156.3185	17.2150	0.9998
	308 K	156.7153	17.2766	0.9998
	313 K	157.1187	17.3348	0.9998
	318 K	157.5226	17.3932	0.9998
	323 K	157.9260	17.4527	0.9998

The plot of the data of Table 3.13 shows that V_0 and ΔV present a linear trend with the increase of temperature as it can be seen in Figure 3.15. The coefficients of the linear fit ($V_0=V_{00}+\alpha T$ and $\Delta V=\Delta V_0+\beta T$), together with the regression coefficient, is given in Table 3.14.

Table 3.14. Coefficients of the linear fit $V_0=V_{00}+\alpha T$ and $\Delta V=\Delta V_0+\beta T$ for ionic liquids of Group 1, Group 2 and Subgroup 3.1.

Group	V_{00}	a	r^2	ΔV_0	β	r^2
1 $[C_{Nc}MIm][BF_4]$	99.9	0.0693	0.99999	13.6	0.0110	0.99999
2 $[C_{Nc}MIm][NTf_2]$	180	0.1499	0.99999	13.5	0.0117	0.99999
3.1$[C_2MIm][C_{Nc}SO_4]$ With H_y	132	0.0747	0.99998	13.7	0.0132	0.99991
3.1$[C_2MIm][C_{Nc}SO_4]$	132	0.0801	0.99999	13.6	0.0120	0.99998

Notice that in Tables 3.13 and 3.14 the quality of the fit improves if we discard the ionic liquid $[C_2MIm][H_ySO_4]$.

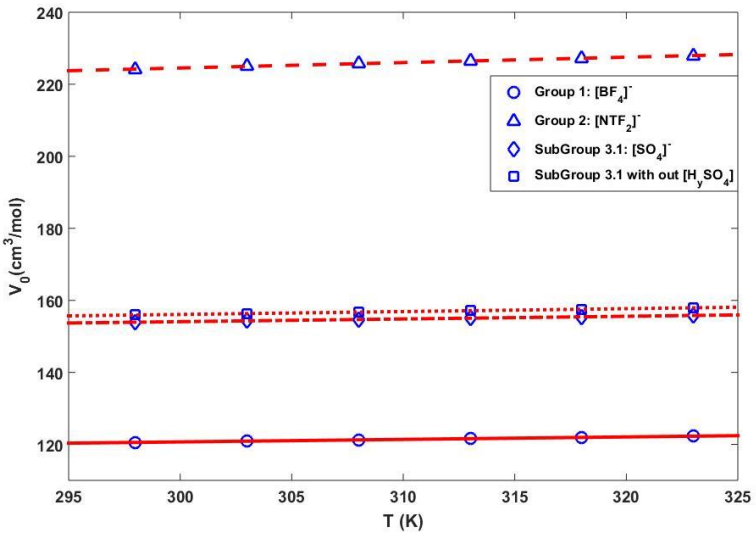

Figure 3.15. The linear variation of V_0 with temperature for ionic liquids of Groups 1, 2, and Subgroup 3.1.

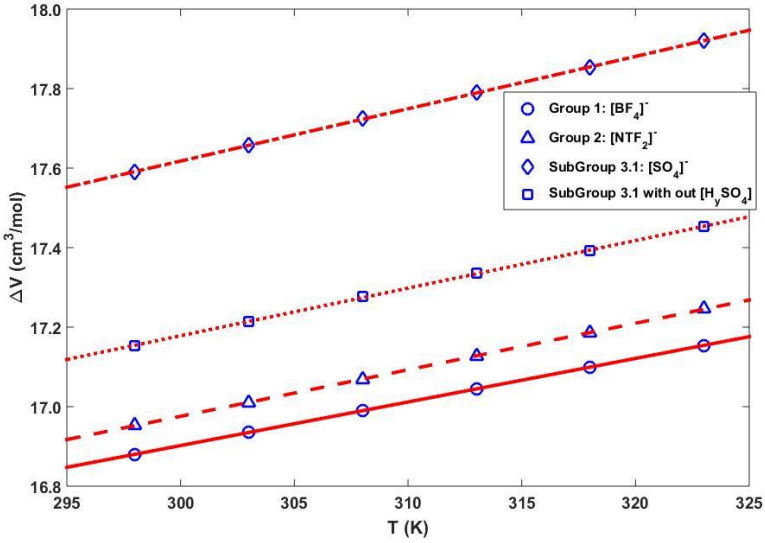

Figure 3.16. The value of ΔV with temperature for the ionic liquids of Groups 1, 2, and Subgroup 3.1.

The variation of R_m with *Nc* for the same three groups of ionic liquids at the Fraunhofer lines *D*=589.3 nm *F*=486.1 nm and *C*=656.3 nm at T=298.15 K. Notice that this relation is practically linear for every represented wavelength. The dashed line corresponds to the fit of the function $R_m=R_0+N_c\Delta R$ to the experimental data.

As we can see, the slopes of the linear fittings are almost the same for the curves of each Fraunhofer line. Thus, the molar refraction contribution of each carbon atom in the imidazolium cation is not strongly dependent on the wavelength at this spectral range.

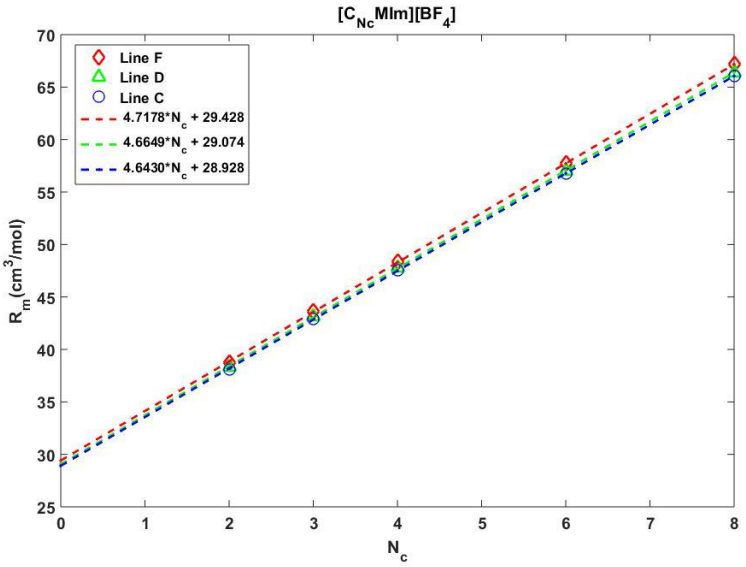

Figure 3.17. Variation of *Rm* with *Nc* for the $[C_{Nc}MIm][BF_4]$ at the Fraunhofer lines *D*=589.3 nm, *F*=486.1 nm, and *C* =656.3 nm at T=298.15 K.

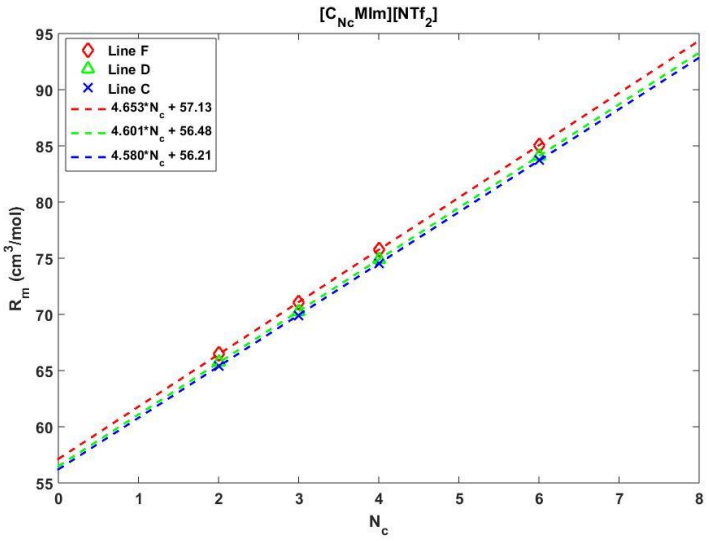

Figure 3.18. Variation of Rm with *Nc* for the [C_{Nc}MIm][NTf_2] at the Fraunhofer lines *D*=589.3 nm, *F*=486.1 nm, and *C* =656.3 nm at T=298.15 K.

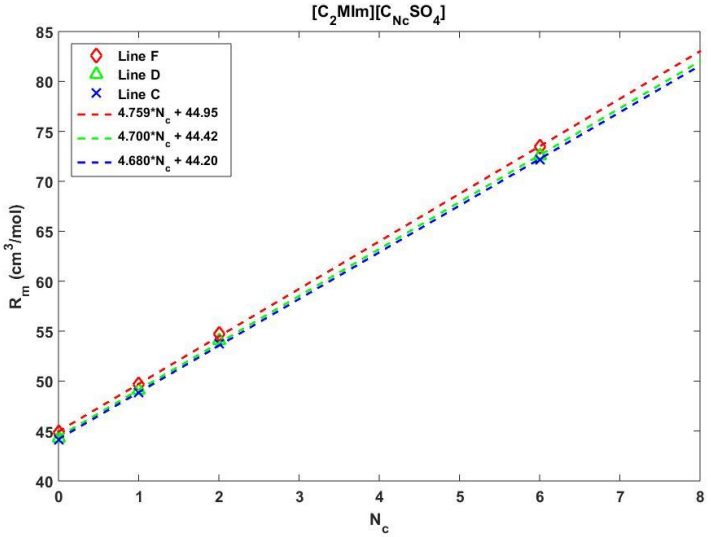

Figure 3.19. The variation of R_m with *Nc* for the [C_2MIm][$C_{Nc}SO_4$] at the Fraunhofer lines *D*=589.3 nm *F*=486.1 nm and *C* =656.3 nm at T=298.15 K.

In Table 3.15 we show the highly linear relation between molar refraction and the number of carbons in the cation chain $R = R_0 + \Delta R N_c$, for the sodium *D* line at different temperature. The slope of the fitting gives the molar refraction contribution of each carbon atom added to the alkyl chain. In average for the different studied temperature, the electronic polarizability contribution per carbon atom is 4.67 for Group 1, 4.59 for Group 2 and 4.68 for the Subgroup 3.1. The slope of the molar refraction changes little for the three studied groups. These changes mainly seem to be due to the increase in molar mass when adding a methyl group. The intercept value is related to the combination of the molar refraction of the imidazolium ring and the anions as well as their weight. As the imidazolium ring is the same in all the compounds, the main differences in molar refraction are related to the anions. Heavy and easily polarizable anions such as $[NTf_2]^-$ produce larger intercept values than light and less polarizable anions such as $[BF_4]^-$.

Table 3.15. The values of R_0 , ΔR and the regression coefficients of the fits ($R_m=R_0+N_c\Delta R$) at 589.3 nm.

IL	T	R_0	ΔR	R^2
$[C_{Nc}MIm][BF_4]$	298 K	29.0732	4.6649	0.99997
	303 K	29.0560	4.6702	0.99997
	308 K	29.0604	4.6710	0.99997
	313 K	29.0679	4.6703	0.99997
	318 K	29.0703	4.6722	0.99997
	323 K	29.0763	4.6711	0.99997
$[C_{Nc}MIm][NTf_2]$	298 K	56.4883	4.6002	0.99997
	303 K	56.5290	4.5950	0.99996
	308 K	56.5764	4.5867	0.99997
	313 K	56.5829	4.5860	0.99997
	318 K	56.5780	4.5892	0.99997
	323 K	56.5896	4.5905	0.99998
$[C_2MIm][C_{Nc}SO_4]$ With H_y	298 K	44.4126	4.7002	0.99986
	303 K	44.4285	4.7022	0.99985
	308 K	44.4433	4.7055	0.99986
	313 K	44.4539	4.7069	0.99986
	318 K	44.4633	4.7034	0.99985
	323 K	44.4776	4.7051	0.99986
$[C_2MIm][C_{Nc}SO_4]$	298 K	44.5177	4.6772	0.99987
	303 K	44.5408	4.6775	0.99986
	308 K	44.5515	4.6818	0.99987
	313 K	44.5688	4.6817	0.99988
	318 K	44.5800	4.6778	0.99987
	323 K	44.6042	4.6773	0.99989

3.3.2 Single resonance Sellmeier equation

We have recently shown in [35] that the behavior of the refractive index versus wavelength and temperature can be accurately described by using a temperature-dependent Sellmeier equation with a single resonance at the UV.

$$n^2_{(\lambda,\Delta T)} - 1 = \left(\frac{(A + B\,\Delta T)\lambda^2}{\lambda^2 - \lambda^2_{uv}}\right) \tag{3.9}$$

where λ_{uv} is a fitting coefficient that represents the effective resonance wavelength that lays in the UV region; λ is the wavelength in micrometers; and *A* and *B* are two fitting coefficients that provide the strength of the resonance for each temperature, that exhibit a linear dependence. ΔT is $T - T_0$ where T is the temperature of measurement, and T_0 is the temperature of reference (in this work we take T_0 = 310.65 K, the center of the measured temperature interval).

The values of coefficients *A*, *B*, and λ_{uv} that return the curve fitting are listed in Table 3.16 together with their uncertainty. To determine the values of the coefficients, firstly, we consider independent fits for the same compound at different temperatures. So we found that the value of the resonant wavelength independent of temperature, while the strength of the resonance varies linearly with the variation of temperature ($\Delta T = T - T_0$). The relation between refractive index and alkyl chain length for ILs sharing the same anion suggests that the resonance does not change with the cation alkyl chain length. Taking this into account, we fix the resonance wavelength for ionic liquids of Group 1 and Group 2; and Subgroup 3.1. Once the resonance is determined, we calculate the coefficients *A* and *B* in eq (3.9) by applying a linear least-squares method.

Table 3.16. Coefficients *A*, *B* and *λuv* resulting from the fit of the Sellmeier equation (3.9) to the refractive index data of each ionic liquid.

Ionic liquid	$(\lambda_{uv})^2$ (10^{-2} μm^2)	*A*	*B* (10^{-4} K^{-1})
$[C_2MiM][BF_4]$	1.1326 (12)	0.951517(10)	-7.010(11)
$[C_3MIm][BF_4]$		0.967156(12)	-7.179(14)
$[C_4MIm][BF_4]$		0.977712(11)	-7.355(13)
$[C_6MIm][BF_4]$		0.994587(14)	-7.483(16)
$[C_8MIm][BF_4]$		1.008824(11)	-7.763(13)
$[C_2MIm][NTf_2]$	1.1010 (10)	0.981064(23)	-8.049(27)
$[C_3MIm][NTf_2]$		0.986696(11)	-8.156(13)
$[C_4MIm][NTf_2]$		0.991628(15)	-8.309(18)
$[C_6MIm][NTf_2]$		0.998811(11)	-8.701(13)
$[C_2MIm][OTf]$	1.1450 (10)	1.011677(12)	-7.701(14)
$[C_4MIm][OTf]$		1.020564(15)	-7.589(18)
$[C_2MIm][H_ySO_4]$	1.2114 (14)	1.183607(16)	-6.769(18)
$[C_2MIm][C_1SO_4]$		1.141701(11)	-7.181(13)
$[C_2MIm][C_2SO_4]$		1.133079(13)	-7.668(16)
$[C_2MIm][C_6SO_4]$		1.117789(19)	-8.312(22)
$[C_4MIm][C_1SO_4]$	1.3288 (56)	1.128929(39)	-7.877(46)
$[C_4MIm][SCN]$	1.6497 (35)	1.288674(30)	-9.057(35)
$[C_4$ MPip$][NTf_2]$	1.0066 (38)	1.002586(23)	-7.799(27)
$[MOEMPL][NTf_2]$	0.9151 (12)	0.986706(10)	-7.981(11)
$[C_4MMIm][NTf_2]$	1.1657 (29)	1.009041(17)	-8.218(21)

As has just been reported, ionic liquids of Group 1 ([C_{Nc}MIm][BF_4], *Nc*=2,3,4,6,8) are characterized for a λ_{uv}=0.1064 µm that is independent of *Nc*, whereas *A* and *B* show a continuous increase. A similar behavior is observed in ionic liquids of Group 2 ([C_{Nc}MIm][NTf_2], *Nc*=2,3,4,6) being λ_{uv}=0.1049 µm [35]. On the contrary, coefficients *A* and *B* of ionic liquids [C_{Nc}MIm][OTf] (*Nc*=2, 4) decrease as *Nc* increases whereas λ_{uv} remains equal to 0.1070 nm in both liquids.

On the contrary, in the case of ionic liquids containing an alkyl sulfate anion, the addition of a CH_2 group manifests itself in a decrease of *A* and a growth of *B* whereas the resonance remains the same.

In order to highlight the quality of the fit, the deviations between the experimental chromatic dispersion curves for each temperature and the ones obtained by using eq (3.9) were calculated. These differences keep always below 3 10^{-4} for all the measured liquids being larger at the edges of the spectrum, they are a little higher than the resolution device.

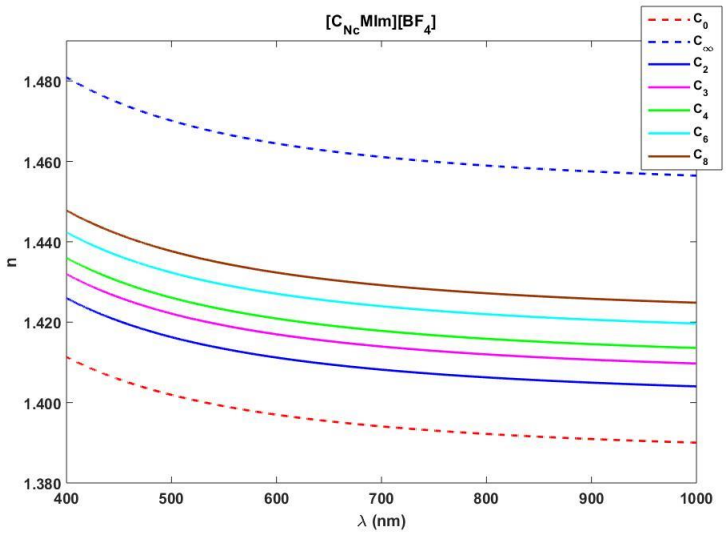

Figure 3.20. Values of n_0 and n_∞ for [C_{Nc}MIm][BF_4] at T=298.15 K together with the refractive index values of the ionic liquid of Group 1 between 400 and 1000 nm.

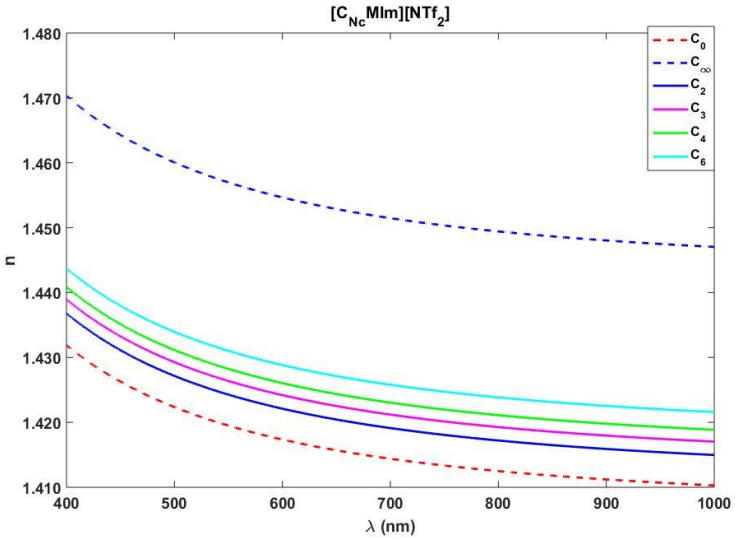

Figure 3.21. values of n_0 and n_∞ for [C_{Nc}MIm][NTF2] at T=298.15 K together with the refractive index values of the ionic liquid of the Group 2 between 400 and 1000 nm.

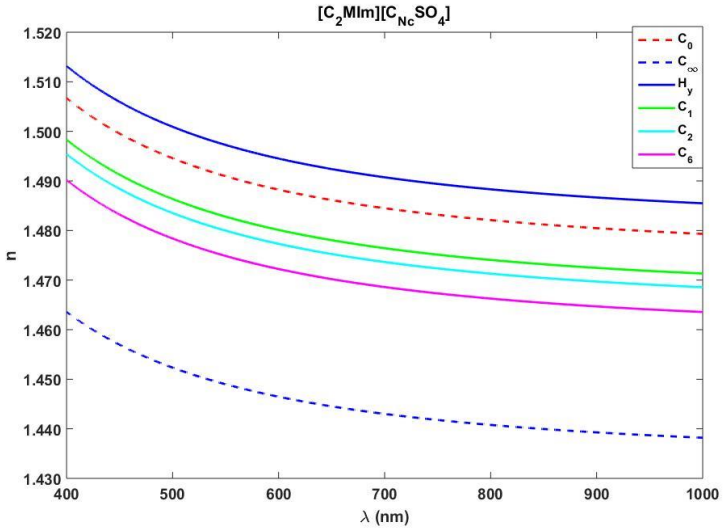

Figure 3.22.values of n_0 and n_∞ for [C_2MIm][$C_{Nc}SO_4$] at T=298.15 K together with the refractive index values of the ionic liquid of the Subgroup 3.1 between 400 and 1000 nm.

Another important final consideration related to the predictive model described by eq.(3.5) in section 3.2.2 is that R_0, V_0, ΔR and ΔV vary with temperature and that R_0 and ΔR are also wavelength-dependent. So, the limit values for the refractive index n_0 and n_∞ are also wavelength and temperature-dependent.

In Figure 3.20, Figure 3.21 and Figure 3.22 we plot the values n_0 and n_∞ estimated along the spectral range comprising 400- 1000 nm for the Group 1, 2 and Subgroup 3.1. The fit of the temperature-dependent single resonance Sellmeier equation returns the following values for the function parameters (coefficients *A*, *B*, and λ^2_{uv}) listed in Table 3.17 :

Table 3.17. Coefficients *A*, *B* and λ_{uv} resulting from the fit of the Sellmeier equation (3.9) to the refractive index limit values (n_0 and n_∞) of Group 1 ([C_{Nc}MIm] [BF_4]), Group 2 ([C_{Nc}MIm] [NTf_2]) and Subgroup 3.1([C_2MIm] [$C_{Nc}SO_4$]).

n_∞	[C_{Nc}MIm] [BF_4]	[C_{Nc}MIm] [NTf_2]	[C_2MIm] [$C_{Nc}SO_4$]
$\lambda^2_{uv}(10^{-2}\ \mu m^2)$	1.1350	1.1021	1.2134
A	1.097334	1.067642	1.042758
$B(10^{-4}k^{-1})$	-8.959	-11.378	-10.162
n_0			
$\lambda^2_{uv}(10^{-2}\ \mu m^2)$	1.1336	1.1010	1.2114
A	0.913425	0.968649	1.165418
$B(10^{-4}k^{-1})$	-6.529	-7.504	-6.848

Table 3.18. λ_{uv} resulting from the fit of the Sellmeier equation (3.9) to n0 and n_∞ values of Group 1, 2 and Subgroup 3.1 compared to those shown in Table 3.16.

		[C_{Nc}MIm] [BF_4]	[C_{Nc}MIm] [NTf_2]	[C_2MIm] [$C_{Nc}SO_4$]
$\lambda^2_{uv}(10^{-2}\ \mu m^2)$	n_0	1.1336	1.1010	1.2114
	n_∞	1.1350	1.1021	1.2134
	Table(3.16)	1.1326	1.1010	1.2114

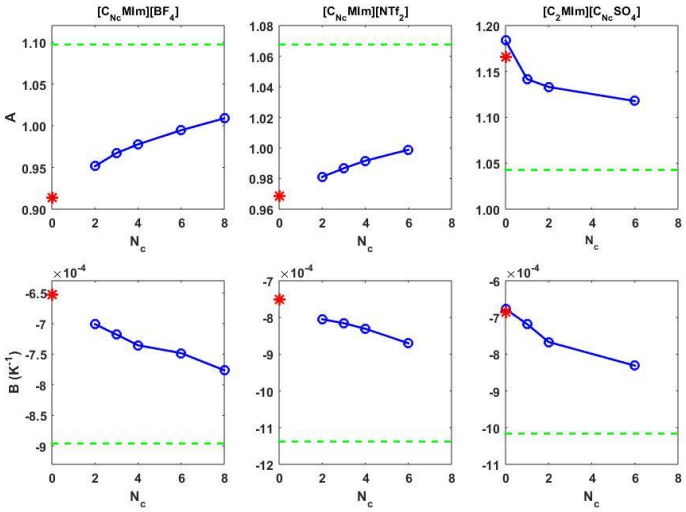

Figure 3.23. Values of the coefficients *A* and *B* as a function of the number of carbons (N_c) for ionic liquids of Group 1 ($[C_{Nc}MIm][BF_4]$), Group 2 ($[C_{Nc}MIm][NTf_2]$) and Subgroup 3.1 ($[C_2MIm][C_{Nc}SO_4]$).The asterisk represents the asymptotic limit when *Nc* tends to 0, and the dashed lines represent the value at the infinite.

Taking into account that the Lorentz-Lorenz equation is an approximation, we can say that the values of the coefficients of the Sellmeier equation that describes the behavior of n_0 and n_∞ follow the trend observed for the corresponding group. As we can see in Table 3.18, the fit of the Sellmeier model to the n_0 data corresponding to Group 2 and Subgroup 3.1 returns a value of λ_{uv} equal to the listed ones in Table 3.16 for the same groups. Although the obtained value of n_0 of Group 1 is a little higher than the value of Table 3.16, the two values are compatible in view of their uncertainties ($1.1336 \cdot 10^{-2} \mu m^2$, $1.1326 \cdot 10^{-2}$ μm^2, ($12 \cdot 10^{-6}$ μm^2)). In the case of n_∞, the value of λ_{uv} is higher, but the differences remain below $2.4 \cdot 10^{-5} \mu m^2$. These results support, what we have previously concluded, that the resonance wavelength, λ_{uv}, is independent on the number of carbons in the alkyl chain of the cation.

As it is visualized in Figure 3.23, the coefficients *A* and *B* for almost all of the ionic liquids of Group 1, Group 2 and Subgroup 3.1, keep between the limit values of *A* and *B* determined by the fit of the Sellmeier equation to n_0 and n_∞. The only liquid that deviates from this behavior is [C_2MIm] [$HySO_4$] since its corresponding *A* value is lower than the obtained for n_0. This may be other indicators that we should not consider this ionic liquid as a member of subgroup 3.1. The origin of this differentiated behavior can be attributed to the protic nature of this ionic liquid, reported by other authors [36]; protic ionic liquids have a hight hydrogen-bonding ability, in contrast to the other ILs of Subgroup 3.1 that is aprotic.

3.4 ABBE NUMBER

Abbe number is a parameter that provides qualitative information about the dispersive power of a material. It is usually defined for the *D* line of sodium (λ_D) as in (3.10):

$$v_D = (n_D - 1)/(n_F - n_C) \qquad (3.10)$$

where n_F, n_D, and n_C represent refractive indices at wavelengths of 486.1, 589.3, and 656.3 nm, respectively.

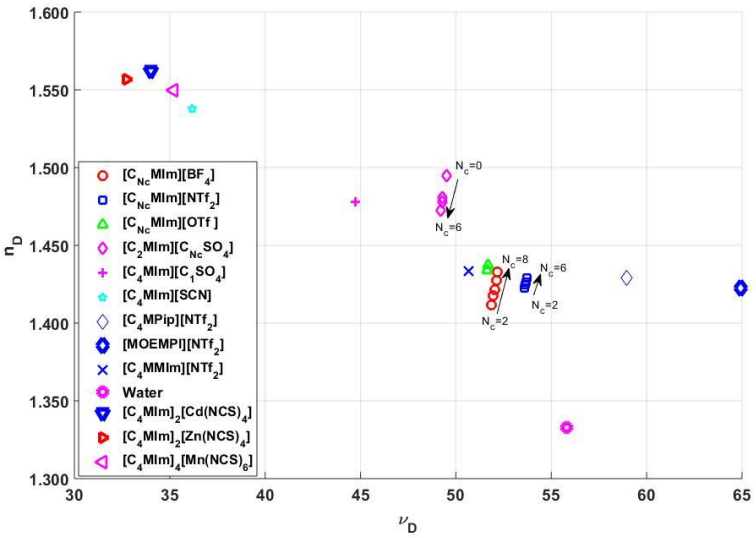

Figure 3.24. Representation of the ionic liquids and water in an Abbe diagram at 298.15 and 297.15 K, respectively. Arrows indicate the direction of growth of *Nc*.

It is usual to represent an optical material in terms of its Abbe number and refractive index, normally at λ_D. This representation is known as the Abbe diagram. In Figure 3.24, we plot the Abbe diagram of the ionic liquids under study together with that of water [37]. In this diagram, we identified several clusters formed by alkyl-methylimidazolium ionic liquids containing the same anion but varying the size of the alkyl tail. After a simple inspection of the graphic, we notice that:

- Ionic liquids sharing the anions [BF_4] or [OTf] present medium dispersion (their Abbe numbers are around 51-52) and refractive indices between 1.4100 and 1.4400, that correspond to the lowest values obtained in this work.

-Ionic liquids sharing the anion [NTf_2] present similar characteristics to the previous ones but with a slightly greater Abbe number (53-54).

- Ionic liquids with 1-alkyl-3-methylimidazolium cations and alkyl sulfate anions present higher refractive indices (around 1.4750) but similar Abbe number values. The exception in the ionic liquids [C_4MIm] [C_1SO_4] characterized by a slightly lower value equal to 45.

-The ionic liquid [C_2MIm][$HySO_4$] presents a higher refractive index than the former, about 1.4920, and an Abbe number close to 49.

- The ionic liquid [C_4MIm][SCN] presents the highest refractive index and also the highest dispersion. The addition of anions consisting of coordination compounds formed by transition metals (Cd, Zn and Mn) and NCS groups increases the refractive index (1.5623, 1.5567 and 1.5499, respectively) and the dispersion (Abbe numbers are 34, 32 and 35, respectively), with respect to the corresponding values obtained for the ionic liquid [C_4MIm][SCN] .

- The ionic liquids formed by [C_4MPip], [MOEMPl] and [C_4MMIm] cations and the [NTf_2] anion have Abbe numbers of 59, 65, 50 and refractive indices of 1.4290, 1.4230, 1.4330, respectively.

It must be noticed that water has a lower refractive index than the studied ionic liquids, but higher Abbe numbers than most of them. Ionic liquids formed by 1-alkyl-3 methylimidazolium cations are more dispersive than water since their Abbe number are lower than 55. The addition of a second methyl group in position 2 of the imidazolium ring seems to increase the dispersion without varying too much the refractive index. On the contrary, lower dispersion than water is encountered in ionic liquids formed by [C_4MPip] and [MOEMPl] cations and the [NTf_2] anion, although the refractive index barely varies with respect to the [C_{Nc}MIm][NTf_2] ionic liquids.

3.4.1 Effect of temperature:

In Figure 3.25 it is represented the pair (ν_D, n_D) at different temperatures from 298.15 K to 323 K for three representative liquids of Groups 1, 2 and Subgroup 3.1. In the three plots, it is observed a linear

behavior. The linear fit $n_D(T)=a\cdot v_D(T)+b$ returns the values a and b listed in Table 3.19 where we also include the regression coefficient:

Table 3.19. Coefficients a, b and R^2 resulting from the linear fit of the function $n_D(T)=a\cdot v_D(T)+b$ to the experimental data.

Ionic liquid	*a*	*b*	R^2
$[C_2MIm]$ $[BF_4]$	0.065021	-1.96410	0.999999
$[C_3MIm]$ $[BF_4]$	0.065332	-1.98025	0.999999
$[C_4MIm]$ $[BF_4]$	0.065542	-1.99116	0.999999
$[C_6MIm]$ $[BF_4]$	0.065877	-2.00859	0.999999
$[C_8MIm]$ $[BF_4]$	0.066159	-2.02329	0.999999
$[C_2MIm][OTf]$	0.066975	-2.02640	0.999999
$[C_4MIm][OTf]$	0.067152	-2.03558	0.999999
$[C_2MIm]$ $[NTf_2]$	0.063693	-1.99423	0.999999
$[C_3MIm]$ $[NTf_2]$	0.063801	-2.00004	0.999999
$[C_4MIm]$ $[NTf_2]$	0.063896	-2.00513	0.999999
$[C_6MIm]$ $[NTf_2]$	0.064034	-2.01254	0.999999
$[C_2MIm]$ $[HySO_4]$	0.074681	-2.20526	0.999999
$[C_2MIm]$ $[C_1SO_4]$	0.073803	-2.16187	0.999999
$[C_2MIm]$ $[C_2SO_4]$	0.073621	-2.15294	0.999999
$[C_2MIm]$ $[C_6SO_4]$	0.073300	-2.13711	0.999999

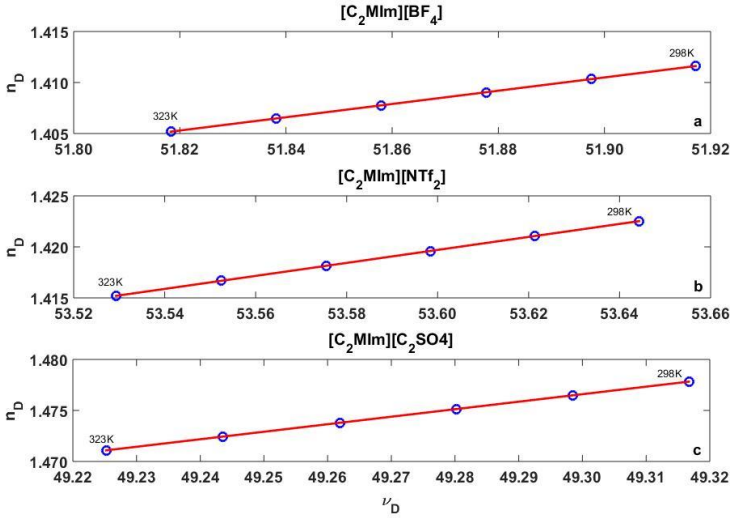

Figure 3.25. Refractive index at 589.3 nm versus Abbe number at different temperatures from 298.15 K to 323 K of three representative liquids of Group 1, Group 2, and Subgroup 3.1.

3.4.2 Effect of number of carbons in the alkyl chain (N_c)

A similar trend it is observed if we plot (ν_D, n_D) as function of *Nc* at a fixed temperature, $n_D(Nc)=c\cdot\nu_D(Nc)+d$. In Figure 3.26 we plot that pair of coordinates for the liquids of Group 1 (Figure 3.26.a), Group 2 (Figure 3.26.b) and Subgroup 3.1 (Figure 3.26.c). The values of the fitting parameters, c and d, as well as the regression coefficient are listed in Table 3.20. Notice that are very similar to the coefficients a and b of Table 3.19.

Table 3.20. Coefficients *c*, *d* and R^2 resulting from the linear fit between coefficients c and d and regrassion coefficient resulting from the linear fit of the function $n_D(Nc)=c\cdot\nu_D(Nc)+d$ to the experimental data. Data were taken at six temperatures between 298 and 323.

Group	Temperature	*c*	*d*	R^2
$[C_{Nc}MIm][BF_4]$	298 K	0.065776	-2.003338	0.999993
	303 K	0.065703	-1.999527	0.999993
	308 K	0.065630	-1.995715	0.999993
	313 K	0.065556	-1.991904	0.999993
	318 K	0.065483	-1.988093	0.999993
	323 K	0.065410	-1.984282	0.999993
$[C_{Nc}MIm][NTf_2]$	298 K	0.064067	-2.014331	0.999999
	303 K	0.063986	-2.010000	0.999999
	308 K	0.063906	-2.005669	0.999999
	313 K	0.063825	-2.001338	0.999999
	318 K	0.063744	-1.997007	0.999999
	323 K	0.063663	-1.992675	0.999999
$[C_2MIm][C_{Nc}SO_4]$	298 K	0.074232	-2.183054	0.999994
	303 K	0.074153	-2.179147	0.999993
	308 K	0.074074	-2.175239	0.999993
	313 K	0.073994	-2.171330	0.999993
	318 K	0.073915	-2.167421	0.999993
	323 K	0.073836	-2.163510	0.999993

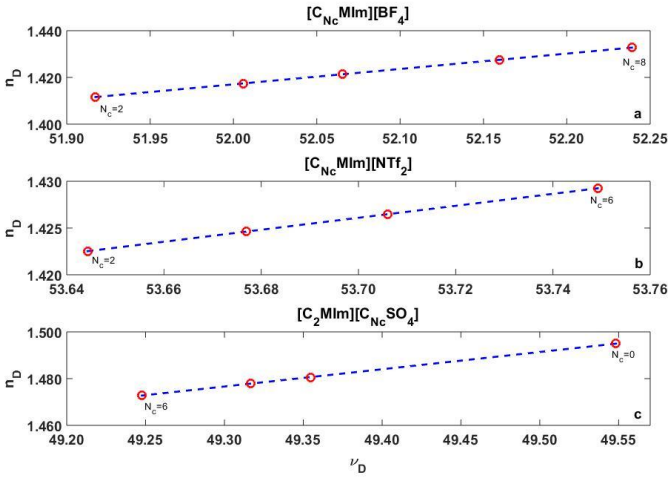

Figure 3.26. Refractive index at 589.3 nm versus Abbe number as a function of *Nc* at 298.15 K of three representative liquids of Group 1, 2 and Subgroup 3.1.

Assuming the linear trend of the molar refraction and the molar volume with *Nc*, by using the Lorentz-Lorenz equation it is possible to identify the Limit values of the Abbe number defined when *Nc* tends to zero and infinity (Table 3.21):

Table 3.21 Upper and lower limits of n_D, n_F, n_C and V_D at 298.15 K.

GROUP	$n_{D\infty}$	$n_{F\infty}$	$n_{C\infty}$	$v_{D\infty}$
GROUP 1	1.4649	1.4712	1.4624	52.59
GROUP 2	1.4551	1.4611	1.4527	54.08
SUBGROUP 3.1	1.4470	1.4535	1.4443	48.81
GROUP	n_{D0}	n_{F0}	n_{C0}	v_{D0}
GROUP 1	1.3974	1.4029	1.3952	51.64
GROUP 2	1.4178	1.4233	1.4155	53.56
SUBGROUP 3.1	1.4888	1.4958	1.4859	49.46

As it happens with the refractive index, this linear behavior allows predicting the Abbe number of ionic liquids of Groups 1, 2 and Subgroup 3.1 with no more requirements than knowing the refractive index at the three wavelengths that define the Abbe number. Table 3.22 show the quality of the prediction, which is visualized in Figure 3.27

for the ionic liquid [C_{Nc}MIm][BF_4], where ν_D is the Abbe number obtained directly from the experimental data and ν_{De} the estimated values calculated by using the refractive index data of [C_2MIm][BF_4] and [C_4MIm][BF_4] for ionic liquids of Group 1, [C_2MIm][NTf_2] and [C_6MIm][NTf_2] for ionic liquids of Group 2 and [C_2MIm][C_6SO_4] and [C_2MIm][$HySO_4$] for ionic liquids of Subgroup 3.1.

Table 3.22. The value of Abbe number obtained directly from the experimental data (ν_D) and the estimated values (ν_{De})

GROUP1: [BF_4]	ν_D	ν_{De}	GROUP 2: [NTf_2]	ν_D	ν_{De}	SUBGROUP 3.1: [C_2MIm]	ν_D	ν_{De}
[C_2MIm]	51.92	____	[C_2MIm]	53.64	____	[$HySO_4$]	49.55	49.39
[C_3MIm]	52.00	52.00	[C_3MIm]	53.68	53.68	[C_1SO_4]	49.36	____
[C_4MIm]	52.07	____	[C_4MIm]	53.71	53.70	[C_2SO_4]	49.32	49.33
[C_6MIm]	52.16	52.16	[C_6MIm]	53.75	____	[C_6SO_4]	49.25	____
[C_8MIm]	52.24	52.23						

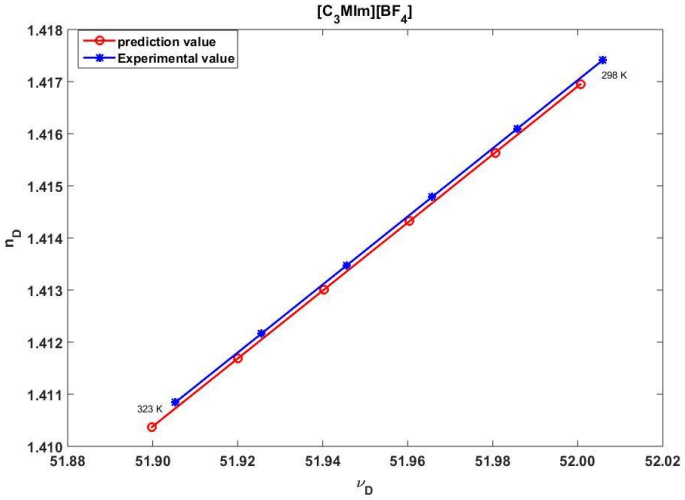

Figure 3.27: Abbe number of the ionic liquid [C_3MIm][BF_4] for temperatures varying between 298 K and 323 K. Blue stars: Calculated values from the refractive index data of the ionic liquid. Red circles: estimated values from the refractive index data of [C_2MIm] [BF_4] and [C_4MIm] [BF_4]. The lines are the result of the linear fit.

3.5 DISPERSION OF THE THERMOOPTIC COEFFICIENT

The thermo-optic coefficient (TOC) is defined as the changing rate of the refractive index concerning temperature variation. The simultaneous measurements of temperature and refractive index are considered as being somewhat meaningful to investigate the optical properties of ILs because the refractive index of liquids depends strongly on temperature. The thermo-optical coefficient, *dn/dT*, could be obtained directly from the derivative of eq. (3.9) and get the expression as we can see in equation (3.11) :

$$\frac{dn}{dT} = \frac{B}{2n}\left(\frac{\lambda^2}{\lambda^2 - \lambda_{uv}^2}\right) \qquad (3.11)$$

In Table **3.23**. we list the coefficients *B* and λ_{uv} resulting from the fit of the Sellmeier equation (3.9) to the TOC data at 400, 700 and 1000 nm at 298.15 K.

Since *B* and λ_{uv} are independent of temperature, the only contribution of the temperature to the refractive index change comes from the factor *1/n*. The introduced differences are rather small, resulting in values around 10^{-4} K^{-1}, but very wavelength sensitive. The dispersion of TOC is higher for short wavelengths as happen with refractive index in normal dispersion regime. The addition of CH_2 groups in the cation or in the anion increases slightly the TOC absolute value being more intense in the case of ionic liquids of subgroup 3.1 as can be seen in Table 3.23. A particular behavior is observed for $[C_1SO_4]^-$ anion, since the TOC absolute value of the $[C_4MIm][C_1SO_4]$ is higher than the ones of $[C_4MIm][BF_4]$ and $[C_4MIm][OTf]$ whereas in the case of $[C_2MIm]$ $[C_1SO_4]$ is just the contrary (see Figure 3.28 c and d).

Table 3.23. Termooptic coefficient at 400, 700 and 1000 nm calculated starting from the parameters *B* and λ_{uv} of equation (3.9). The temperature was 298.15 K.

Ionic liquid	$B_{(10^{-4}\ k^{-1})}$	$(\lambda_{uv})^2_{(10^{-2}\ \mu m^2)}$	$\frac{dn_{400nm}}{dT}$ $(10^{-3}\ k^{-1})$	$\frac{dn_{700nm}}{dT}$ $(10^{-3}\ k^{-1})$	$\frac{dn_{1000nm}}{dT}$ $(10^{-3}\ k^{-1})$
$[C_2MIm]\ [BF_4]$	-7.010(11)	1.1326 (12)	-0.2645	-0.2548	-0.2526
$[C_3MIm]\ [BF_4]$	-7.179(14)		-0.2697	-0.2599	-0.2576
$[C_4MIm]\ [BF_4]$	-7.355(13)		-0.2756	-0.2655	-0.2632
$[C_6MIm]\ [BF_4]$	-7.483(16)		-0.2791	-0.2689	-0.2666
$[C_8MIm]\ [BF_4]$	-7.763(13)		-0.2885	-0.2780	-0.2756
$[C_2MIm][OTf]$	-7.701(14)	1.1450 (10)	-0.2862	-0.2757	-0.2732
$[C_4MIm][OTf]$	-7.589(18)		-0.2813	-0.2710	-0.2687
$[C_2MIm]\ [NTf_2]$	-8.049(27)	1.1010 (10)	-0.3007	-0.2901	-0.2878
$[C_3MIm]\ [NTf_2]$	-8.156(13)		-0.3043	-0.2935	-0.2911
$[C_4MIm]\ [NTf_2]$	-8.309(18)		-0.3097	-0.2986	-0.2961
$[C_6MIm]\ [NTf_2]$	-8.701(13)		-0.3236	-0.3121	-0.3095
$[C_2MIm]\ [HySO_4]$	-6.769(18)	1.2114 (14)	-0.2419	-0.2328	-0.2307
$[C_2MIm]\ [C_1SO_4]$	-7.181(13)		-0.2593	-0.2493	-0.2470
$[C_2MIm]\ [C_2SO_4]$	-7.668(16)		-0.2774	-0.2667	-0.2643
$[C_2MIm]\ [C_6SO_4]$	-8.312(22)		-0.3019	-0.2901	-0.2875

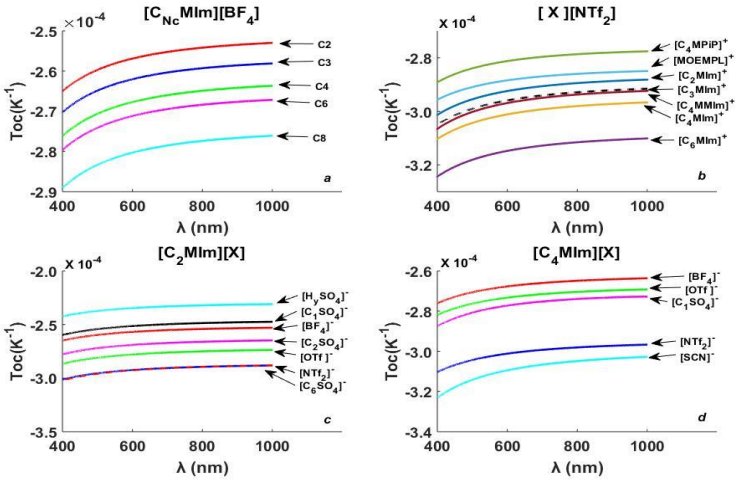

Figure 3.28. Dispersion curves of the thermooptic coefficient of the ionic liquids under study: (a) 1-alkyl-3-methylimidazolium cations paired with the anion $[BF_4]^-$ (b) ionic liquids containing the $[NTf_2]^-$ anion combined with different cations. (c) and (d) show the effects of the anion in the thermooptic coefficient dispersion of ionic liquids formed by 1-ethyl-3-methylimidazolium and butyl-3-methylimidazolium cations, respectively. Data were taken at T=308.15 K.

In Figure 3.28b, concerning ionic liquids sharing the $[NTf_2]^-$ anion, we see that the addition of a new methyl functional group at the position two in the imidazolium ring $[C_4MMIm]^+$ leads to a decrease of the TOC absolute value. On the other hand, the replacement of cation $[C_4MIm]^+$ by cation $[MOEMPl]^+$ causes a higher decrease in the magnitude of the TOC absolute value. Finally, the replacement of cation $[C_4MIm]^+$ by $[C_4MPip]^+$ gives the lower absolute value of TOC for all the ionic liquids sharing the $[NTf_2]^-$ anion.

By considering, once again, the linear variation of R_m and V_m with N_c, we have estimated the limit values of the thermooptic coefficient for ionic liquids of Groups 1, 2 and Subgroup 3.1. The values are shown in Table 3.24. In Figure 3.29 we plot the thermooptic coefficient of the ionic liquids of the selected groups together with the limit values. The calculated thermooptic coefficient curves are arranged between the limit curves, including the case of $[C_2MIm]$ $[HySO_4]$ that practically is superimposed to that of $\frac{dn_0}{dT}$.

Table 3.24. Limit values of the thermooptic coefficient at T=298.15 K.

	$B_{(10^{-4}\ K^{-1})}$	$(\lambda_{uv})^2_{(10^{-2}\ \mu m^2)}$	$\frac{dn_\infty(400nm)}{dT}$ $(10^{-3}\ K^{-1})$	$\frac{dn_\infty(700nm)}{dT}$ $(10^{-3}\ K^{-1})$	$\frac{dn_\infty(1000nm)}{dT}$ $(10^{-3}\ K^{-1})$
GROUP 1	-8.959	1.1350	-0.3256	-0.3139	-0.3111
GROUP 2	-11.378	1.1021	-0.4156	-0.4010	-0.3975
SUBGROUP 3.1	-10.162	1.2134	-0.3757	-0.3611	-0.3576
	$B_{(10^{-4}\ K^{-1})}$	$(\lambda_{uv})^2_{(10^{-2}\ \mu m^2)}$	$\frac{dn_0(400nm)}{dT}$ $(10^{-3}\ K^{-1})$	$\frac{dn_0(700nm)}{dT}$ $(10^{-3}\ K^{-1})$	$\frac{dn_0(1000nm)}{dT}$ $(10^{-3}\ K^{-1})$
GROUP 1	-6.529	1.1336	-0.2490	-0.2397	-0.2376
GROUP 2	-7.504	1.1010	-0.2814	-0.2714	-0.2690
SUBGROUP 3.1	-6.848	1.2114	-0.2459	-0.2365	-0.2343

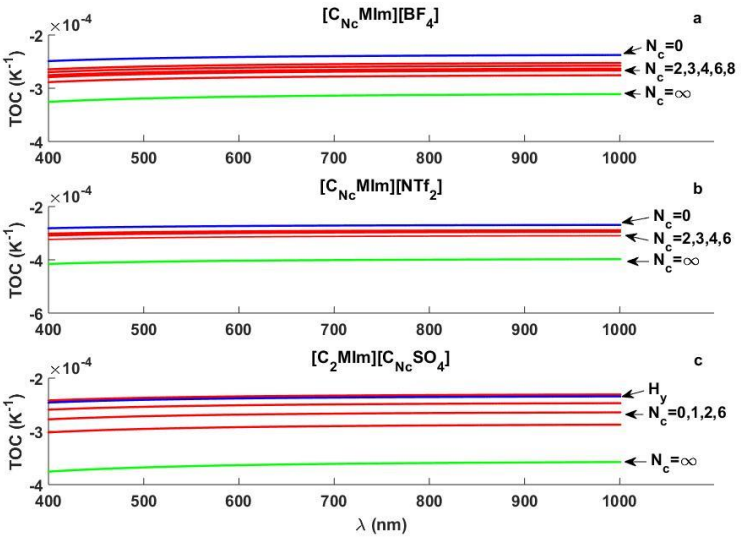

Figure 3.29. Thermooptic coefficient of the ionic liquids of Group 1, Group 2 and Subgroup 3.1 together with the limit values.

3.6 GROUP INDEX AND GROUP VELOCITY DISPERSION

Refractive index dispersion causes the different spectral components of a polychromatic beam travel at different velocities in dispersive media. Group velocity, v_g, refers to the velocity of the global wave packet and the ratio c/v_g is the group index, n_g, that can be calculated using the expression given by eq.(1.2).

In particular, for 1-alkyl-3-imidazolium-based ionic liquids in the spectral interval from 400 to 1000 nm and for the range of achieved temperatures, n_g can be calculated by using this expression:

$$n_g = n + \left[\frac{(A + B\Delta T)\lambda^2 \lambda_{uv}^2}{(\lambda^2 - \lambda_{uv}^2)^2}\frac{1}{n}\right] \qquad (3.12)$$

From (1.2) it is inferred that, due to the negative variation of the refractive index with wavelength, n_g in a medium with normal dispersion takes higher values than the refractive index. The frequency dependence of v_g and n_g is quantified by means of the group velocity dispersion, usually denoted by GVD or β_2, given by eq (1.3). whose units in the international system are s^2/m.

Related to GVD is the dispersion parameter D defined in eq (1.4), whose units are ps/nm.km. Combining eq.(1.2) and eq.(1.4) D becomes:

$$D = -\frac{1}{c}\left[\frac{(A + B\Delta T)\lambda\lambda_u^2}{n^3(\lambda^2 - \lambda_u^2)^3}(3\lambda^2 n^2 + \lambda_u^2)\right] \qquad (3.13)$$

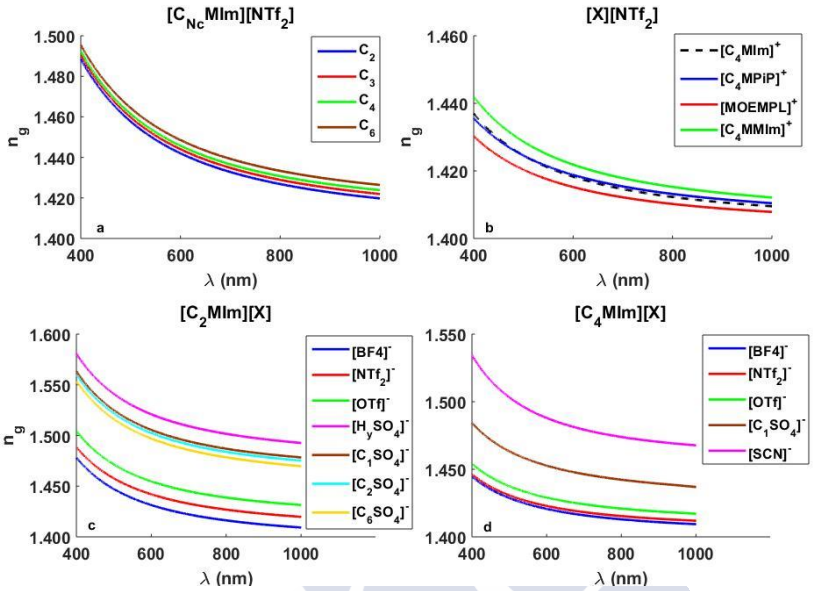

Figure 3.30. Wavelength dependence of the group index, n_g, at T=308.15 K. (a) 1-alkyl-3-methylimidazolium-cations combined with the [NTf_2] anion; (b) ionic liquids containing the [NTf_2] anion combined with different cations. (c) and (d) shows the effects of the anion in the group index dispersion of ionic liquids formed by 1-ethyl-3-methylimidazolium and 1-butyl-3-methylimidazolium cations, respectively.

Figure 3.30 shows the group index dispersion for the 20 ILs at 308.15 K. The group index curves follow the typical behavior of the refractive index in the normal dispersion region. But in some cases, as happens with [C_4MIm][NTf_2] and [C_4MPip][NTf_2], the n_g curves approach each other and even intersect (Figure 3.30.b) at 504.5nm; this effect has not been observed in the refractive index curves.

In Figure 3.31 it is observed the expected linear dependence of n_g with T but the slope is one order of magnitude less than the obtained for n, about $3 \cdot 10^{-5}$.

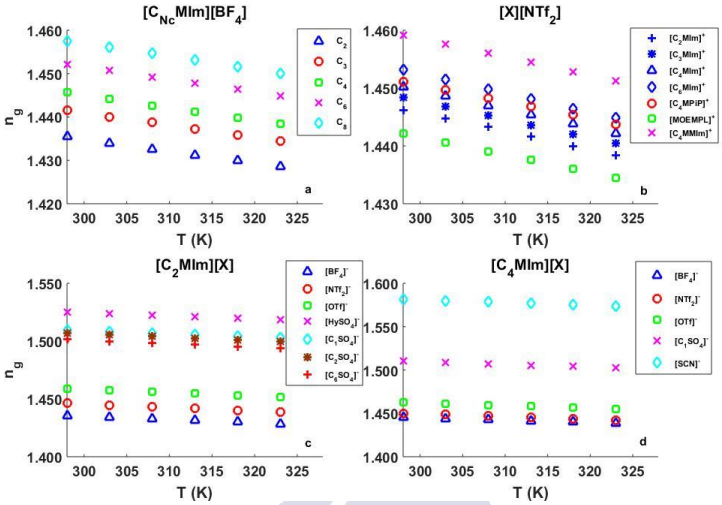

Figure 3.31. Group index versus temperature at 589.3 nm: (a) $[C_{Nc}MIm][BF_4]$ (*Nc*= 2, 3, 4, 6, 8); (b) ionic liquids sharing the $[NTf_2]$ anion combined with different cations; (c) and (d) shows the group index of ionic liquids composed, respectively, by 1-ethyl-3-methylimidazolium and 1-butyl-3-methylimidazolium cations, combined with different anions.

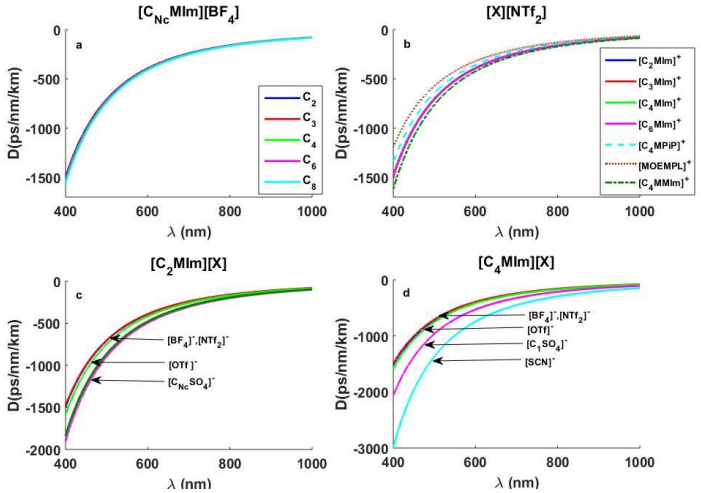

Figure 3.32. Wavelength dependence of *D* for the ionic liquids of Groups 1-4 at T=298.15 K. (a) 1-alkyl-3-methylimidazolium ionic liquids sharing the $[BF_4]^-$ (b) ionic liquids sharing the $[NTf_2]^-$ anion combined with different cations. (c) and (d) ionic liquids composed by 1-ethyl-3-methylimidazolium and 1-butyl-3-methylimidazolium cations, respectively.

Figure 3.32 plots the values of *D* versus wavelength for ILs of groups 1-4. Typically *D* varies between -3000 and -80 ps/nm/Km in the spectral interval 400-1000 nm. Note that the negative value of *D* corresponds to the normal dispersion regime. Figure 3.32a and b show that *D* practically remains unchanged when the alkyl chain length increases but exhibits a slight increase when replacing the $[C_4MIm]^+$cation by $[C_4MPip]^+$ or $[MOEMPl]^+$, and a slight decrease when adding a functional methyl group to the $[C_4MIm]^+$ cation. The dispersion parameter, *D*, of $[C_4MMIm]$ $[NTf_2]$ is shifted to -1620 ps/nm/km at 400 nm compared to the respective value calculated for $[C_4MIm]$ $[NTf_2]$. $[C_4MPiP][$ $NTF_2]$ has as *D*= -1350 ps/nm/km, and the lowest value was obtained for the ionic liquid $[MOEMPl][$ $NTF_2]$.

The anionic influence on the *D* parameter can be seen in Figure 3.32c and in Figure 3.32d. Figure 3.32d shows that the *D* parameter in the alkyl sulfate-based ionic liquids is not dependent on the anionic alkyl chain, and the stronger variation on the values of *D* is associated to anions containing sulphur atoms such as $[C_{Nc}SO_4]^-$ or $[SCN]^-$ anions. In fact, $[C_4MIM][SCN]$ has the highest absolute values.

The influence of the addition of anions constituted by coordination compounds formed by transition metals and isothiocyanate groups on the *D* parameter can be seen Figure 3.33. The dispersion parameter, *D*, of $[C_4MIm]_2$ $[Zn(NCS)_4]$ is shifted to -3479 ps/nm/km at 400nm. $[C_4MIm]_2$ $[Cd(NCS)_4]$ has as *D*= -3350 ps/nm/km, and the $[C_4MIm]_4$ $[Zn(NCS)_6]$ has *D*=-3142 ps/nm/km. In general case, we must be prudent at the time of considering these results because these ionic liquids are not free of impurities resulting from the synthesis process, factor that we are still trying to control.

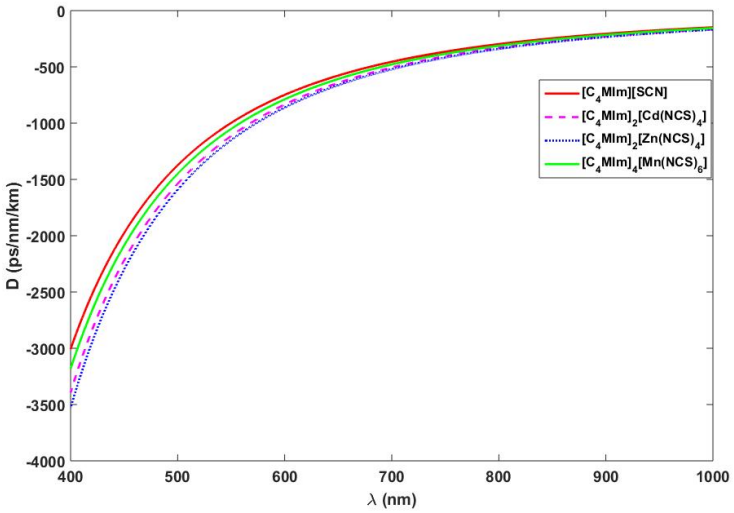

Figure 3.33.Wavelength dependence of *D* for the ionic liquid [C_4MIm][SCN] and for ionic liquids containing coordination complexes formed by transition metals (Cd, Zn, Mn) and NCS Groups as anions at T=298.15 K.

In Figure 3.34 we compare the value of *D* corresponding to the ionic liquid [C_2MIm] [BF_4] and the one of water where we can see that the dispersion achieves higher values and that the zero-dispersion wavelength is red-shifted with respect to that of water. This result suggests than the zero-dispersion wavelength can be useful to determine the quantity of water absorbed by the ionic liquid.

Figure 3.35 shows the variation of *D* with temperature for ionic liquids of groups 1-4 at six different temperatures between 298.15 and 323.15K at λ_D=589.3nm.

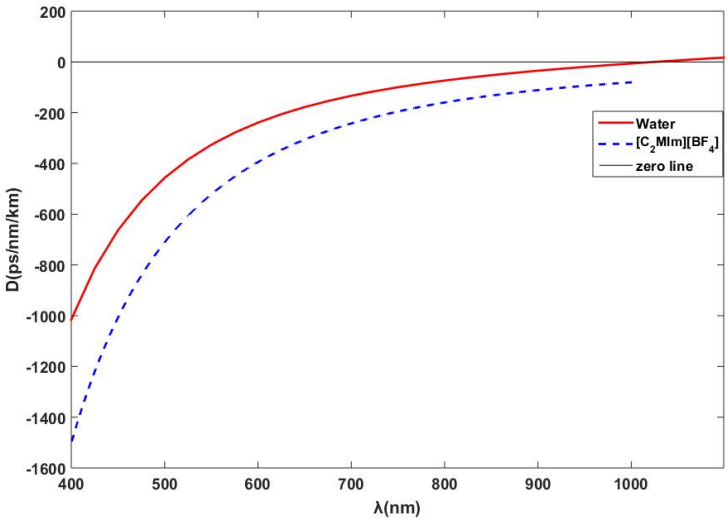

Figure 3.34. *D* of water and $[C_2MIM][BF_4]$ at T= 298.15K.

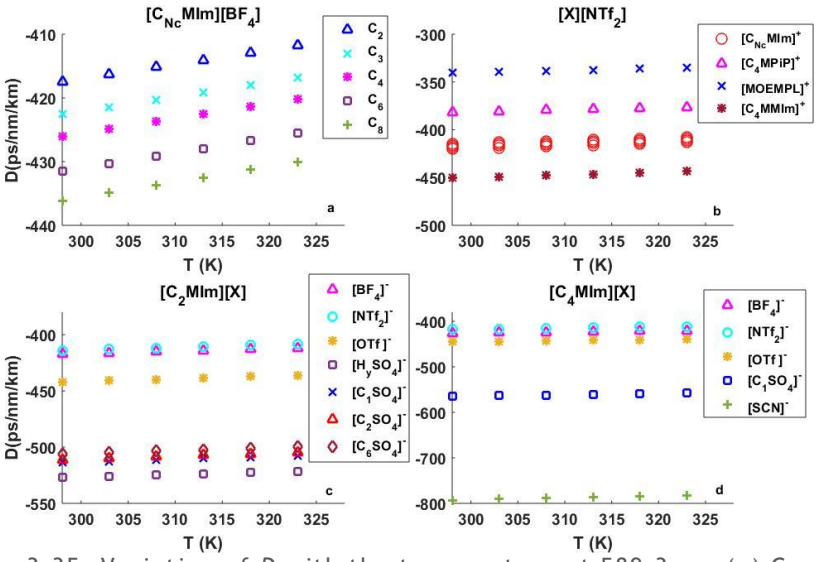

Figure 3.35. Variation of *D* with the temperature at 589.3 nm.(a) Group 1, (b) Group 2 and Group 5, (c) Group 3 and (d) Group 4.

The evolution of *D* with temperature and with *Nc* is represented in Figure 3.35 a and b; the absolute value of *D* decreases linearly with the temperature for all samples examined in this study, and it increases slightly with *Nc*; the slope value has been evaluated between 23-39·10^{-2} ps/(nm·km·K) as shown in Table 3.25. As it was previously mentioned, the substitution of the Imidazolium ring by a Piperidinium lowers the absolute value of *D*, as well as the replacement of $[C_4MIm]^+$ cation by $[MOEMPl]^+$ does. Nevertheless, the addition of a second CH_3 group makes the contrary effect. None of these substitutions seems to modify significantly the dependence of *D* with temperature as there is no appreciable change in the slope of the curves. With respect to the anionic influence, the results of the fit of the linear function $D=D_0+\Delta DT$ to the evolution of *D* with Temperature at 589 nm are shown in Table 3.25:

Table 3.25. Coefficients D_0, ΔD and R^2 resulting from the linear fit of the function $D_0+\Delta D \cdot T$ to the calculated data.

Ionic liquid	D_0	ΔD	R^2
$[C_2MIm]$ $[BF_4]$	-486.090	0.227736	0.99996
$[C_3MIm]$ $[BF_4]$	-492.453	0.231852	0.99998
$[C_4MIm]$ $[BF_4]$	-497.201	0.236087	0.99994
$[C_6MIm]$ $[BF_4]$	-503.382	0.238528	0.99998
$[C_8MIm]$ $[BF_4]$	-510.401	0.246426	0.99996
$[C_2MIm][OTf]$	-516.578	0.246464	0.99997
$[C_4MIm][OTf]$	-517.984	0.241883	0.99992
$[C_2MIm]$ $[NTf_2]$	-489.686	0.250368	0.99991
$[C_3MIm]$ $[NTf_2]$	-492.434	0.253468	0.99996
$[C_4MIm]$ $[NTf_2]$	-495.362	0.257853	0.99999
$[C_6MIm]$ $[NTf_2]$	-501.196	0.269495	0.99995
$[C_4MPiP]$ $[NTf_2]$	-447.729	0.219216	0.99993

[MOEMPL] [NTf_2]	-401.606	0.203396	0.99999
[C_4MMIm] [NTf_2]	-531.725	0.270012	0.99999
[C_2MIm] [$HySO_4$]	-592.084	0.215394	0.99994
[C_2MIm] [C_1SO_4]	-584.349	0.234043	0.99988
[C_2MIm] [C_2SO_4]	-585.972	0.248301	0.99993
[C_2MIm] [C_6SO_4]	-588.691	0.273299	0.99990
[C_4MIm] [C_1SO_4]	-650.062	0.282897	0.99996
[C_4MIm] [SCN]	-911.889	0.394576	0.99998

GVD is an important parameter that allows calculating the dispersion characteristic length of material, L_D, that gives an idea of how long can be a medium for the dispersive effects on a pulse traveling across be negligible. L_D is obtained by the expression in eq.(3.14):

$$L_D = \frac{t_0^2}{\beta_2} \qquad (3.14)$$

Being t_0 the pulse duration at half medium intensity and β_2 the group velocity dispersion. In Table 3.26, we show how L_D varies as function of the wavelength and pulse duration for some of the ionic liquids studied. Notice the change in the order of magnitude.

Table 3.26. L_D of the ionic liquids for different pulse durations. The corresponding D and β_2 are also listed. T=298.15 K.

T=298 .15K				Pulse duration		
Ionic Liquid	λ (nm)	D (ps/nm/km)	β_2*10^{-26} S^2/m	t_0= 100 fs	t_0= 10 ps	t_0= 1ns
				L_D (m)		
$[C_2MIm][BF_4]$	400	-1502.345	12.753	0.0784147741	784.147741	7841477.41
	1000	-80.174	4.259	0.2348115635	2348.115635	23481156.35
$[C_8MIm][BF_4]$	400	-1569.165	13.319	0.0750755774	750.755774	7507557.74
	1000	-83.790	4.450	0.2246767319	2246.767319	22467673.19
$[C_2MIm][NTF_2]$	400	-1485.463	12.609	0.0793059040	793.059040	7930590.40
	1000	-79.763	4.236	0.2360172869	2360.172869	23601728.69
$[C_6MIm][NTF_2]$	400	-1506.229	12.785	0.0782125436	782.125436	7821254.36
	1000	-80.837	4.293	0.2328841272	2328.841272	23288412.72
$[C_2MIm][H_ySO_4]$	400	-1908.907	16.203	0.0617138636	617.138636	6171386.36
	1000	-100.847	5.356	0.1866750656	1866.750656	18667506.56
$[C_2MIm][C_1SO_4]$	400	-1861.626	15.802	0.0632812365	632.812365	6328123.65
	1000	-98.274	5.220	0.1915620453	1915.620453	19156204.53
$[C_2MIm][C_6SO_4]$	400	-1836.645	15.590	0.0641419750	641.419750	6414197.50
	1000	-96.862	5.145	0.1943539128	1943.539128	19435391.28

3.7 THIRD ORDER DISPERSION

Starting from the calculated (GVD), we can determine the third-order dispersion (TOD) by using eq (1.5):

$$TOD = \beta_3 = -\frac{\lambda^4}{4\pi^2 c^3}\left(3\left(\frac{\partial^2 n}{\partial \lambda^2}\right) + \lambda\left(\frac{\partial^3 n}{\partial \lambda^3}\right)\right) \qquad (3.15)$$

whose units in the international system are s^3/m. Related to TOD, it is defined the dispersion parameter *S* as:

$$S = \frac{4\pi c}{\lambda^3}\beta_{2+}\left(\frac{2\pi c}{\lambda^2}\right)^2 \beta_3 \qquad (3.16)$$

$$S = -\frac{1}{c}\left(\frac{\partial^2 n}{\partial \lambda^2}\right) - \frac{\lambda}{c}\left(\frac{\partial^3 n}{\partial \lambda^3}\right) \qquad (3.17)$$

whose units are $ps/nm^2/km$, being *c* the speed of light.

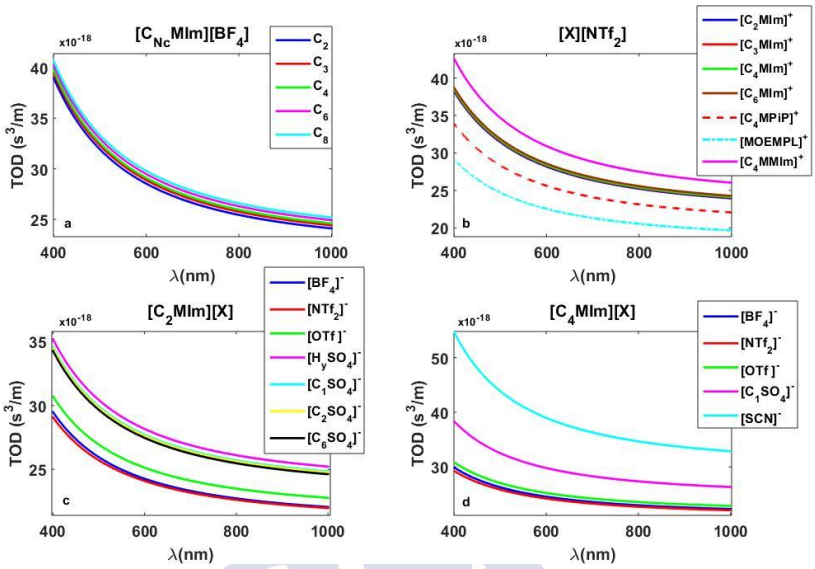

Figure 3.36. Wavelength dependence of TOD for the ionic liquids of groups 1-4 at T=298.15 K: (a) ionic liquids formed by 1-alkyl-3-methylimidazolium cations combined by [BF_4] anions; (b) ionic liquids sharing the [NTf_2] anion; (c) and (d) ionic liquids formed by 1-ethyl-3-methylimidazolium and 1-butyl-3-methylimidazolium cations paired with different anions, respectively.

Figure 3.36 plots the values of TOD versus wavelength for ILs of groups 1-4. Figure 3.36a and b show that TOD hardly varies when the alkyl chain length increases but exhibits a decrease when replacing the $[C_{Nc}MIm]^+$ cation by $[C_4MPip]^+$ or $[MOEMPl]^+$, and it experiences growth when adding a functional methyl group to the $[C_4MIm]^+$ cation. The lowest value was obtained for the ionic liquid [MOEMPl][NTf_2].

The anionic influence on the TOD can be seen in Figure 3.36c and d. Figure 3.36d shows that the TOD in the alkyl sulfate-based ionic liquids is not dependent on the anionic alkyl chain, and the stronger variation on the values of TOD are associated to anions containing sulfur atoms such as $[C_{Nc}SO_4]^-$or $[SCN]^-$ anions. In fact, $[C_4MIm][SCN]$ has the highest TOD parameter.

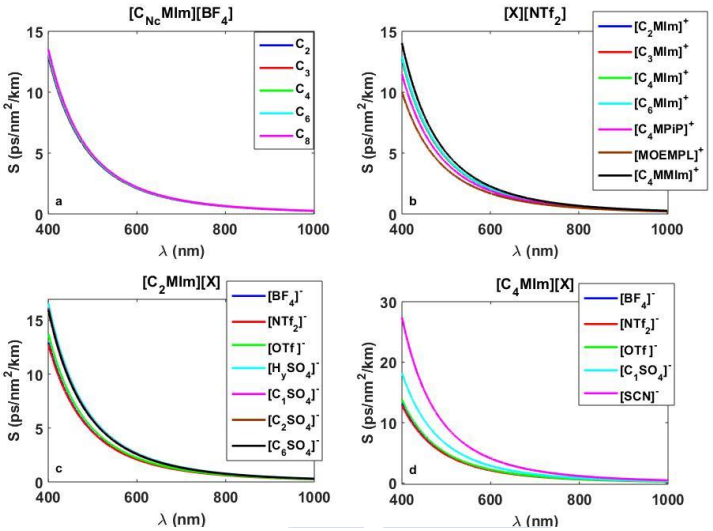

Figure 3.37. Wavelength dependence of *S* for the ionic liquids of groups 1-4 at T=298.15 K. (a) 1-alkyl-3-methylimidazolium cations paired with [BF_4] anions; (b) ionic liquids sharing the [NTf_2] anion combined with different cations; (c) and (d) 1-ethyl-3-methylimidazolium and 1-butyl-3-methylimidazolium cations, respectively, combined with different anions.

Figure 3.37 plots the values of *S* versus wavelength for ILs of groups 1-4. Figure 3.37a and b show that *S* practically remains unchanged when the alkyl chain length increases but exhibits a slight decrease when replacing the $[C_{Nc}MIm]^+$ cation by $[C_4MPip]^+$ or $[MOEMPl]^+$, and a slight increase when adding a functional methyl group at the position 2 to the $[C_4MIm]^+$ cation. The dispersion parameter, *S*, of [C_4MMIm] [NTf_2] lowers to 14.03 ps/nm^2·km at 400nm whereas [C_4MPiP][NTF_2] has as S value of 11.48 ps/nm^2·km; the lowest value of ionic liquids sharing the $[NTf_2]^-$ anion was obtained for the ionic liquid [MOEMPl][NTF_2] (*S*= 10.03 ps/nm^2·km at 400 nm).

The anionic influence on the *S* parameter can be seen in Figure 3.37c and d. Figure 3.37d shows that the *S* parameter in the alkyl sulfate-based ionic liquids is not dependent on the anionic alkyl chain, and the stronger variation on the values of *S* are associated to anions

containing sulfur atoms such as $[C_{Nc}SO_4]^-$or $[SCN]^-$ anions. In fact, $[C_4MIm][SCN]$ has the highest values for the *S* parameter.

For all of the ILs of groups 1-4, the *S* curves approach each other by the wavelength increase and approach to zero at 1000nm.

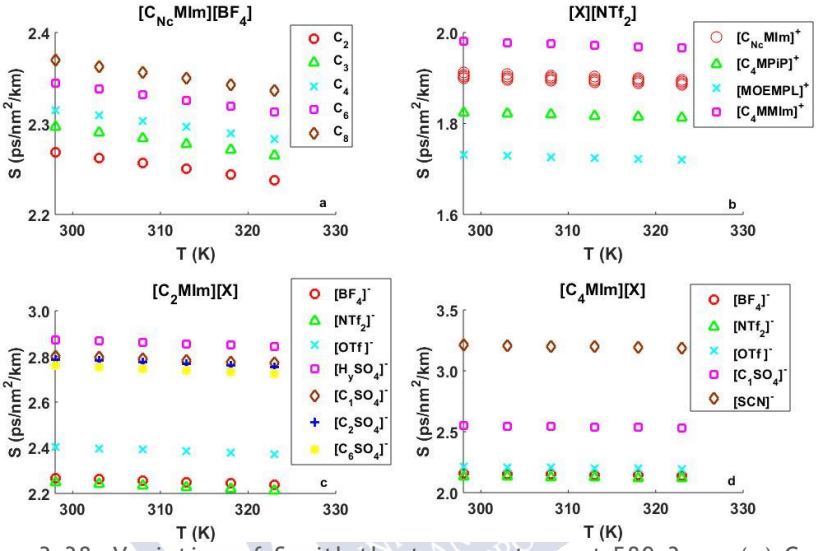

Figure 3.38. Variation of *S* with the temperature at 589.3 nm:(a) Group 1, (b)Group 2 and Group 5, (c) Group 3, and (d) Group 4.

The evolution of *S* with temperature is represented in Figure 3.38; the value of *S* decreases linearly with the temperature for all samples examined in this study and it increases slightly with *Nc*; the slope value has been evaluated between 12.3-14.6 $\cdot 10^{-2}$ ps/nm^2 km /K. The substitution of the Imidazolium ring by a Piperidinium lowers the value of *S*, as well as the replacement of $[C_4MIm]^+$ cation by $[MOEMPl]^+$ does. Nevertheless, the addition of a second CH_3 group makes the contrary effect. None of these substitutions seems to modify significantly the dependence of *S* with temperature as there is no appreciable change of the slope of the curves. With respect to the anionic influence, the main conclusions derived from the analysis of the cationic effect are extracted, as can be seen in Figure 3.38 c and d .

The results of the fit of the linear function $S=S_0+\Delta ST$ to the calculated data of the evolution of S with Temperature at 589.3 nm are shown in Table 3.27:

Table 3.27. Coefficients S_0, ΔS and R^2 resulting from the linear fit of the function $S=S_0+\Delta ST$ to the calculated data at 589.3 nm.

Ionic liquid	S_0	ΔS	R^2
$[C_2MIm]$ $[BF_4]$	2.635	$-1.228\cdot10^{-03}$	0.99997
$[C_3MIm]$ $[BF_4]$	2.669	$-1.250\cdot10^{-03}$	0.99998
$[C_4MIm]$ $[BF_4]$	2.694	$-1.273\cdot10^{-03}$	0.99994
$[C_6MIm]$ $[BF_4]$	2.728	$-1.286\cdot10^{-03}$	0.99998
$[C_8MIm]$ $[BF_4]$	2.766	$-1.329\cdot10^{-03}$	0.99996
$[C_2MIm][OTf]$	2.801	$-1.330\cdot10^{-03}$	0.99997
$[C_4MIm][OTf]$	2.808	$-1.305\cdot10^{-03}$	0.99992
$[C_2MIm]$ $[NTf_2]$	2.649	$-1.348\cdot10^{-03}$	0.99991
$[C_3MIm]$ $[NTf_2]$	2.664	$-1.365\cdot10^{-03}$	0.99996
$[C_4MIm]$ $[NTf_2]$	2.679	$-1.388\cdot10^{-03}$	0.99999
$[C_6MIm]$ $[NTf_2]$	2.711	$-1.451\cdot10^{-03}$	0.99995
$[C_4MPiP]$ $[NTf_2]$	2.409	$-1.174\cdot10^{-03}$	0.99993
[MOEMPL] $[NTf_2]$	2.150	$-1.085\cdot10^{-03}$	1.00000
$[C_4MMIm]$ $[NTf_2]$	2.886	$-1.458\cdot10^{-03}$	0.99999
$[C_2MIm]$ $[HySO_4]$	3.220	$-1.165\cdot10^{-03}$	0.99994
$[C_2MIm]$ $[C_1SO_4]$	3.179	$-1.266\cdot10^{-03}$	0.99989
$[C_2MIm]$ $[C_2SO_4]$	3.187	$-1.343\cdot10^{-03}$	0.99994
$[C_2MIm]$ $[C_6SO_4]$	3.202	$-1.479\cdot10^{-03}$	0.99990
$[C_4MIm]$ [SCN]	5.076	$-2.180\cdot10^{-03}$	0.99999

3.8 REFERENCES

[1] O. Ciocirlan, O. Croitoru, and O. Iulian, "Density and refractive index of binary mixtures of two 1-alkyl-3-methylimidazolium ionic liquids with 1, 4-dioxane and ethylene glycol," *Journal of Chemical & Engineering Data*, vol. 59, no. 4, pp. 1165-1174, 2014.

[2] X. He, Q. Shao, W. Kong, L. Yu, X. Zhang, and Y. Deng, "A simple method for estimating mutual diffusion coefficients of ionic liquids-water based on an optofluidic chip," *Fluid Phase Equilibria*, vol. 366, pp. 9-15, 2014.

[3] K.-S. Kim, B.-K. Shin, and H. Lee, "Physical and electrochemical properties of 1-butyl-3-methylimidazolium bromide, 1-butyl-3-methylimidazolium iodide, and 1-butyl-3-methylimidazolium tetrafluoroborate," *Korean Journal of Chemical Engineering*, vol. 21, no. 5, pp. 1010-1014, 2004.

[4] A. Kumar, "Estimates of internal pressure and molar refraction of imidazolium based ionic liquids as a function of temperature," *Journal of Solution Chemistry*, vol. 37, no. 2, pp. 203-214, 2008.

[5] M. Montalban, C. Bolivar, F. G. Díaz Baños, and G. Villora, "Effect of temperature, anion, and alkyl chain length on the density and refractive index of 1-alkyl-3-methylimidazolium-based ionic liquids," *Journal of Chemical & Engineering Data*, vol. 60, no. 7, pp. 1986-1996, 2015.

[6] P. Navarro, M. Larriba, S. García, J. n. García, and F. Rodríguez, "Physical properties of binary and ternary mixtures of 2-propanol, water, and 1-butyl-3-methylimidazolium tetrafluoroborate ionic liquid," *Journal of Chemical & Engineering Data*, vol. 57, no. 4, pp. 1165-1173, 2012.

[7] C. M. Neves, K. A. Kurnia, J. o. A. Coutinho, I. M. Marrucho, J. N. C. Lopes, M. G. Freire, and L. P. N. Rebelo, "Systematic study of the thermophysical properties of imidazolium-based ionic liquids with cyano-functionalized anions," *The Journal of Physical Chemistry B*, vol. 117, no. 35, pp. 10271-10283, 2013.

[8] S. G. Rao, T. M. Mohan, T. V. Krishna, K. Narendra, and B. S. Rao, "Thermophysical properties of 1-butyl-3-methylimidazolium tetrafluoroborate and N-methyl-2-pyrrolidinone as a function of temperature," *Journal of Molecular Liquids*, vol. 211, pp. 1009-1017, 2015.

[9] A. N. Soriano, B. T. Doma, and M.-H. Li, "Measurements of the density and refractive index for 1-n-butyl-3-methylimidazolium-based ionic liquids," *The Journal of Chemical Thermodynamics*, vol. 41, no. 3, pp. 301-307, 2009.

[10] G. R. Sunkara, M. M. Tadavarthi, V. K. Tadekoru, S. K. Tadikonda, and S. R. Bezawada, "Density, refractive index, and speed of sound of the binary mixture of 1-butyl-3-methylimidazolium tetrafluoroborate+ N-vinyl-2-pyrrolidinone from T=(298.15 to 323.15) K at atmospheric pressure," *Journal of Chemical & Engineering Data*, vol. 60, no. 3, pp. 886-894, 2015.

[11] M. M. Taib and T. Murugesan, "Density, refractive index, and excess properties of 1-butyl-3-methylimidazolium tetrafluoroborate with water and monoethanolamine," *Journal of Chemical & Engineering Data*, vol. 57, no. 1, pp. 120-126, 2011.

[12] M. Tariq, P. Forte, M. C. Gomes, J. C. Lopes, and L. Rebelo, "Densities and refractive indices of imidazolium-and phosphonium-based ionic liquids: Effect of temperature, alkyl chain length, and anion," *The Journal of Chemical Thermodynamics*, vol. 41, no. 6, pp. 790-798, 2009.

[13] G. Vakili-Nezhaad, M. Vatani, M. Asghari, and I. Ashour, "Effect of temperature on the physical properties of 1-butyl-3-methylimidazolium based ionic liquids with thiocyanate and tetrafluoroborate anions, and 1-hexyl-3-methylimidazolium with tetrafluoroborate and hexafluorophosphate anions," *The Journal of Chemical Thermodynamics*, vol. 54, pp. 148-154, 2012.

[14] E. Vercher, F. J. Llopis, V. González-Alfaro, P. J. Miguel, V. Orchillés, and A. Martínez-Andreu, "Volumetric properties, viscosities and refractive indices of binary liquid mixtures of

tetrafluoroborate-based ionic liquids with methanol at several temperatures," *The Journal of Chemical Thermodynamics,* vol. 90, pp. 174-184, 2015.

[15] W.-G. Xu, L. Li, X.-X. Ma, J. Wei, W.-B. Duan, W. Guan, and J.-Z. Yang, "Density, surface tension, and refractive index of ionic liquids homologue of 1-alkyl-3-methylimidazolium tetrafluoroborate [C n mim][BF4](n= 2, 3, 4, 5, 6)," *Journal of Chemical & Engineering Data,* vol. 57, no. 8, pp. 2177-2184, 2012.

[16] Q. Zhang, Z. Li, J. Zhang, S. Zhang, L. Zhu, J. Yang, X. Zhang, and Y. Deng, "Physicochemical properties of nitrile-functionalized ionic liquids," *The Journal of Physical Chemistry B,* vol. 111, no. 11, pp. 2864-2872, 2007.

[17] V. S. Rao, M. S. Reddy, S. M. Nayeem, K. T. S. Raju, K. B. M. Krishna, and B. H. Babu, "Investigation of solute-solvent interactions in {1-butyl-3-methyl imidazoliumBis (trifluoromethylsulfonyl) imide+ dimethylcarbonate} mixture using physicochemical properties," *The Journal of Chemical Thermodynamics,* vol. 115, pp. 133-147, 2017.

[18] R. G. Seoane, E. J. González, and B. González, "1-Alkyl-3-methylimidazolium bis (trifluoromethylsulfonyl) imide ionic liquids as solvents in the separation of azeotropic mixtures," *The Journal of Chemical Thermodynamics,* vol. 53, pp. 152-157, 2012.

[19] A. E. Andreatta, M. Francisco, E. Rodil, A. Soto, and A. Arce, "Isobaric vapour–liquid equilibria and physical properties for isopropyl acetate+ isopropanol+ 1-butyl-3-methyl-imidazolium bis (trifluoromethylsulfonyl) imide mixtures," *Fluid Phase Equilibria,* vol. 300, no. 1, pp. 162-171, 2011.

[20] A. Cháfer, J. de la Torre, A. Font, and E. Lladosa, "Liquid–liquid equilibria of water+ ethanol+ 1-butyl-3-methylimidazolium bis (trifluoromethanesulfonyl) imide ternary system: measurements and correlation at different temperatures," *Journal of Chemical & Engineering Data,* vol. 60, no. 8, pp. 2426-2433, 2015.

[21] S. Corderí, E. J. González, N. Calvar, and Á. Domínguez, "Application of [HMim][NTf2],[HMim][TfO] and [BMim][TfO] ionic liquids on the extraction of toluene from alkanes: Effect of the anion and the alkyl chain length of the cation on the LLE," *The Journal of Chemical Thermodynamics,* vol. 53, pp. 60-66, 2012.

[22] E. Vercher, F. J. Llopis, V. González-Alfaro, P. J. Miguel, and A. Martínez-Andreu, "Refractive indices and deviations in refractive indices of trifluoromethanesulfonate-based ionic liquids in water," *Journal of Chemical & Engineering Data,* vol. 56, no. 12, pp. 4499-4504, 2011.

[23] M. S. Reddy, I. Khan, K. T. S. Raju, P. Suresh, and B. H. Babu, "The study of molecular interactions in 1-ethyl-3-methylimidazolium trifluoromethanesulfonate+ 1-pentanol from density, speed of sound and refractive index measurements," *The Journal of Chemical Thermodynamics,* vol. 98, pp. 298-308, 2016.

[24] M. G. Freire, A. R. R. Teles, M. A. Rocha, B. Schröder, C. M. Neves, P. J. Carvalho, D. V. Evtuguin, L. M. Santos, and J. A. Coutinho, "Thermophysical characterization of ionic liquids able to dissolve biomass," *Journal of Chemical & Engineering Data,* vol. 56, no. 12, pp. 4813-4822, 2011.

[25] E. J. González, Á. Domínguez, and E. A. Macedo, "Physical and excess properties of eight binary mixtures containing water and ionic liquids," *Journal of Chemical & Engineering Data,* vol. 57, no. 8, pp. 2165-2176, 2012.

[26] F. Yebra, K. Zemánková, and J. Troncoso, "Speed of sound in ionic liquids with a common ion as a function of pressure and temperature," *The Journal of Chemical Thermodynamics,* vol. 116, pp. 235-240, 2018.

[27] K. Bica, M. Deetlefs, C. Schröder, and K. R. Seddon, "Polarisabilities of alkylimidazolium ionic liquids," *Physical Chemistry Chemical Physics,* vol. 15, no. 8, pp. 2703-2711, 2013.

[28] O. Borodin, "Polarizable force field development and molecular dynamics simulations of ionic liquids," *The Journal of Physical Chemistry B*, vol. 113, no. 33, pp. 11463-11478, 2009.

[29] C. Millot, A. Chaumont, E. Engler, and G. Wipff, "Distributed Polarizability Models for Imidazolium-Based Ionic Liquids," *The Journal of Physical Chemistry A*, vol. 118, no. 38, pp. 8842-8851, 2014.

[30] J. D. Holbrey and K. R. Seddon, "The phase behaviour of 1-alkyl-3-methylimidazolium tetrafluoroborates; ionic liquids and ionic liquid crystals," *Journal of the Chemical Society, Dalton Transactions*, no. 13, pp. 2133-2140, 1999.

[31] C. M. Gordon, J. D. Holbrey, A. R. Kennedy, and K. R. Seddon, "Ionic liquid crystals: hexafluorophosphate salts," *Journal of Materials Chemistry*, vol. 8, no. 12, pp. 2627-2636, 1998.

[32] O. Cabeza, J. Vila, E. Rilo, M. Domínguez-Pérez, L. Otero-Cernadas, E. López-Lago, T. Méndez-Morales, and L. Varela, "Physical properties of aqueous mixtures of the ionic 1-ethl-3-methyl imidazolium octyl sulfate: A new ionic rigid gel," *The Journal of Chemical Thermodynamics*, vol. 75, pp. 52-57, 2014.

[33] R. G. Seoane, S. Corderí, E. Gómez, N. Calvar, E. J. González, E. A. Macedo, and Á. Domínguez, "Temperature dependence and structural influence on the thermophysical properties of eleven commercial ionic liquids," *Industrial & Engineering Chemistry Research*, vol. 51, no. 5, pp. 2492-2504, 2012.

[34] S. Corderí, B. González, N. Calvar, and E. Gómez, "Ionic liquids as solvents to separate the azeotropic mixture hexane/ethanol," *Fluid Phase Equilibria*, vol. 337, pp. 11-17, 2013.

[35] Y. Arosa, B. S. AlGnamat, C. D. Rodríguez Fernández, E. Lopez Lago, L. M. Varela, and R. de la Fuente, "Modeling the Temperature Dependent Material Dispersion of Imidazolium Based Ionic Liquids in the Vis-NIR," *The Journal of Physical Chemistry C*, 2018.

[36] S. García-Garabal, J. Vila, E. Rilo, M. Domínguez-Pérez, L. Segade, E. Tojo, P. Verdía, L. Varela, and O. Cabeza, "Transport properties for 1-ethyl-3-methylimidazolium n-alkyl

sulfates: possible evidence of Grotthuss mechanism," *Electrochimica Acta,* vol. 231, pp. 94-102, 2017.

[37] M. Daimon and A. Masumura, "Measurement of the refractive index of distilled water from the near-infrared region to the ultraviolet region," *Applied optics,* vol. 46, no. 18, pp. 3811-3820, 2007.

4 Conclusions

The refractive index of 20 ionic liquids has been measured and studied over the spectral range from 400 nm to 1000 nm, by using the RISBI technique assisted with Abbe refractometry. That technique allows measuring with high accuracy the refractive index as a quasi-continuous function of the wavelength over a broad spectral band with a resolution better than 1 nm and an uncertainty in the refractive index around $2 \cdot 10^{-4}$. Comparison of our data with measures of other authors taken at the sodium *D* line confirms the high accuracy and precision of our method.

The density of the ionic liquids was also measured at the same temperatures as the refractive index. The overall precision in experimental density measurements for all samples was found to be better than $\pm 2 \cdot 10^{-6}$ g·cm^{-3}.

It was found that the refractive index curve for versus wavelength shows the characteristics of the normal dispersion regime, with larger refractive indices and refractive index variations at smaller wavelengths. Furthermore, dispersion is similar for all the ILs analyzed.

We investigate systematically the effect on optical properties of the increasing alkyl chain length of the 1-alkyl-3-methylimidazolium cations, temperature, and the nature of the anion or the cation. The refractive index of 1-alkyl-3-methylimidazolium- based ionic liquids increases with the increase of the alkyl chain length, for ILs in Group 1 and Group 2, while the Subgroup 3.1 shows the opposite trend. Refractive indices also increase according to the following list of anions, $[BF_4]^- < [NTf_2]^- < [OTf]^- < [C_1SO_4]^- < [SCN]^-$, when combined

with $[C_4MIm]^+$ cation, and $[BF_4]^- < [NTf_2]^- < [OTf]^- < [C_{Nc}SO_4]^-$, when combined with $[C_2MIm]^+$ cation. Note that the refractive index of the sulfate family decreases when the number of carbons increases.

The refractive index is also highly cation dependent. In this case we have found that the refractive index is related to the inverse of the free molar volume

With respect to the relation between refractive index and temperature, it is almost linear with a negative slope and a value that increases in absolute terms with the alkyl chain length and decreases with the wavelength.

By using the Lorentz Lorenz equation and complementary density measurements, molar refraction, R_m, and molar volume, V_m, were calculated. As the change of R_m and V_m with the number of carbons in the alkyl chain was found to be linear, we insert this dependence in the Lorentz-Lorenz equation to predict the value of refractive index of a family of ionic liquids resulting from the addition of CH_2 groups to one of the alkyl chains present in the anion or in the cation; the prediction requires the knowledge of the refractive index and density values of at least two ionic liquids of the same family. Comparison of our data with other measures confirms the high accuracy($\Delta n<10^{-3}$).

On the other hand, we found that the behavior of n with Nc depends on the relation between $\Delta R/\Delta V$ and R_0/V_0 . If $\Delta R/\Delta V > R_0/V_0$, then the refractive index increases with number of carbon (*Nc*), whereas if it verifies the opposite relation, the refractive index decreases with *Nc*.

The Abbe number was also calculated as a function of temperature and the number of carbons of the longest alkyl chain; the results have been represented in an Abbe diagram that reveals that the pair of coordinates (n_D, V_D) follows a linear behavior, both by varying the temperature or by varying the number of carbons.

Most of the ionic liquids have a refractive index about 1.45 and a Abbe number between 45 and 65, except the ones containing the $[SCN]^-$

anion or coordination complexes formed by $[NCS]^-$ groups and transition metals. The refractive index of these ionic liquids is around 1.55 and the Abbe number is between 30 and 36, being the most dispersive ILs.

It must be noticed that water has a lower refractive index than the studied ionic liquids, but higher Abbe numbers than most of them. Note that the addition of a second methyl group in position 2 of the imidazolium ring seems to increase the dispersion without varying too much the refractive index. On the contrary, lower dispersion than water is encountered in ionic liquids formed by $[C_4MPip]^+$ and $[MOEMPl]^+$ cations and the $[NTf_2]^-$ anion.

A single resonance Sellmier function was employed to model the refractive index and to calculate the thermooptic coefficient, group index, second-order dispersión through the dispersion parameter *D* and third-order dispersion through the dispersion parameter *S*. It has been found that these properties are barely dependent of temperature and they are dependent on the carbon number in the alkyl chain, cation, and anion. Their behavior is similar to the refractive index except *D* and *S* that remain practically unchanged when the alkyl chain length increases.

The characteristics of dispersion of TOC are like the ones of refractive index, higher for smaller wavelengths. Besides, the absolute value of TOC increases with the addition of CH_2 groups in the cation (as in Group 1 and 2) or in the anion (as in Subgroup 3.1). With respect to compounds sharing the same cation, the order the anions do not follow the observed order in the refractive index order in the refractive index. This could be attributed to a change in the thermal dilatation.

We have calculated the *D* parameter for all the ionic liquids. Zero dispersion wavelength is out of the achievable spectral range of this setup. We estimated that it is located around 1300 nm by comparing the ionic liquids dispersion curves with that of water.

S exhibits a slight decrease when replacing the $[C_{Nc}MIm]^+$ cation by $[C_4MPip]^+$, and a slight increase when adding a functional methyl group at the position 2 to the $[C_4MIm]^+$ cation, while *D* behaves the opposite.

The stronger variation on the values of *S* are associated to anions containing sulfur atoms such as $[C_{Nc}SO_4]^-$ or $[SCN]^-$ anions. In fact, $[C_4MIm][SCN]$ has the highest value.

Related works

- E. López Lago, Julio A. Seijas, I. de Pedro, J. Rodríguez Fernández, M. P. Vázquez-Tato, J. A. Gonzalez, E. Rilo, L.M. Segade, O. Cabeza, C. D. Rodríguez Fernández, Y. Arosa, **B. AlGnamat**, L. M. Varela, J. Troncoso, R. de la Fuente. *Structural and physical properties of a new reversible and continuous thermochromic ionic liquid in a wide temperature interval:[BMIM]$_4$ [Ni(NCS)$_6$]*, New Journal of Chemistry **42** (2018) 15561-15571.
- Y. Arosa, **B. S. AlGnamat**, C. D. Rodríguez Fernández, E. López Lago, L. M. Varela, R. de la Fuente, *Modeling the Temperature Dependent Material Dispersion of Imidazolium Based Ionic Liquids in the Vis-NIR*. The Journal of Physical Chemistry C **122** (2018) 29470-29478.
- **B. S. AlGnamat**, Y. Arosa, E. López Lago, R. de la Fuente. *A first inspection of the dispersive properties of Imidazolium-based ionic liquids in the Vis-NIR* (Submitted).
- E. López Lago, J. A. Nóvoa, **B. AlGnamat**, R. de la Fuente, J.A. Seijas, M.P. Vázquez-Tato, J. Troncoso y H. Michinel, *Multiphoton absorption in ionic liquids at 810nm*, XI Reunión Nacional de Óptica, Salamanca, España, 1-4 septiembre 2015.
- **B. AlGnamat**, R. de la Fuente, E. López Lago, *Refractive index behaviour in different families of ionic liquids* XI Reunión Nacional de Óptica, Salamanca, España, 1-4 septiembre 2015.
- Y. Arosa, C. D. Rodríguez Fernández, **B. S. Algnamat**, E. López-Lago, R. de la Fuente, *White light spectral interferometer for measuring dispersion in the visible-near*

infrared, 3rd International Conference on Applications of Optics and Photonics, Faro, Portugal, 8-12 mayo 2017.

- E. López-Lago, R. de la Fuente, J. A. Seijas, M.P. Vázquez-Tato, J. Troncoso, Y.Arosa, **B. AlGnamat**, J.M. Otero Mato, L.M. Varela, O. Cabeza, *Thermochromic behavior in* $BMIM_4Ni(SCN)_6$, 26 EUCHEM Conference on Molten Salts and Ionic liquids, Viena, Austria, 3-8 julio 2016.
- D. Rodríguez, Y. Arosa, **B. S. Algnamat**, E. López-Lago, R. de la Fuente, *White light spectral interferometry for measuring dispersion of the thermo-optic coefficient of liquids*, 36 Reunión Bienal de la Real Sociedad Española de Física, Santiago de Compostela, España, 17-21 de julio de 2017.
- C. D. R. Fernández, Y. Arosa, **B. S. Algnamat**, E.-L. Lago, L. M. Varela, and R. de la Fuente, "*Predicting refractive index dispersion of ionic liquids*," in Frontiers in Optics, 2019, p. JTu4A. 33: Optical Society of America.

List of figures

USC
UNIVERSIDADE
DE SANTIAGO
DE COMPOSTELA

List of tables

USC
UNIVERSIDADE
DE SANTIAGO
DE COMPOSTELA

Appendix

Table A1. Refractive index of studied ILs at different temperatures and wavelengths

IL	T(K)	λ(nm)						
		A (759.37)	B (686.72)	C (656.28)	D (589.60)	E (527.04)	F (486.13)	G (430.80)
$[C_2MIm][BF_4]$	298.15	1.4070	1.4085	1.4093	1.4116	1.4146	1.4173	1.4222
	303.15	1.4057	1.4072	1.4081	1.4103	1.4133	1.4160	1.4209
	308.15	1.4044	1.4060	1.4068	1.4090	1.4120	1.4147	1.4196
	313.15	1.4031	1.4047	1.4055	1.4078	1.4107	1.4134	1.4183
	318.15	1.4019	1.4034	1.4042	1.4065	1.4094	1.4121	1.4170
	323.15	1.4006	1.4021	1.4029	1.4052	1.4081	1.4107	1.4156
$[C_3MIm][BF_4]$	298.15	1.4127	1.4143	1.4151	1.4174	1.4204	1.4231	1.4281
	303.15	1.4114	1.4130	1.4138	1.4161	1.4191	1.4218	1.4268
	308.15	1.4101	1.4117	1.4125	1.4148	1.4178	1.4205	1.4255
	313.15	1.4088	1.4104	1.4112	1.4135	1.4165	1.4191	1.4241
	318.15	1.4075	1.4091	1.4099	1.4122	1.4152	1.4178	1.4228
	323.15	1.4062	1.4077	1.4086	1.4108	1.4138	1.4165	1.4214

[C_4MIm][BF_4]	298.15	1.4166	1.4182	1.4190	1.4213	1.4244	1.4271	1.4321
	303.15	1.4152	1.4168	1.4177	1.4200	1.4230	1.4257	1.4308
	308.15	1.4139	1.4155	1.4163	1.4187	1.4217	1.4244	1.4294
	313.15	1.4126	1.4142	1.4150	1.4173	1.4203	1.4230	1.4280
	318.15	1.4113	1.4128	1.4137	1.4160	1.4190	1.4217	1.4267
	323.15	1.4099	1.4115	1.4123	1.4146	1.4176	1.4203	1.4253
[C_6MIm][BF_4]	298.15	1.4227	1.4243	1.4252	1.4275	1.4306	1.4333	1.4385
	303.15	1.4214	1.4230	1.4238	1.4262	1.4292	1.4320	1.4371
	308.15	1.4200	1.4216	1.4225	1.4248	1.4279	1.4306	1.4357
	313.15	1.4187	1.4203	1.4211	1.4234	1.4265	1.4292	1.4343
	318.15	1.4173	1.4189	1.4198	1.4221	1.4251	1.4278	1.4329
	323.15	1.4160	1.4176	1.4184	1.4207	1.4238	1.4265	1.4315
[C_8MIm][BF_4]	298.15	1.4279	1.4295	1.4304	1.4328	1.4359	1.4387	1.4439
	303.15	1.4265	1.4282	1.4290	1.4314	1.4345	1.4373	1.4424
	308.15	1.4251	1.4268	1.4276	1.4300	1.4331	1.4358	1.4410
	313.15	1.4237	1.4254	1.4262	1.4286	1.4317	1.4344	1.4396
	318.15	1.4224	1.4240	1.4248	1.4272	1.4303	1.4330	1.4381
	323.15	1.4210	1.4226	1.4234	1.4258	1.4288	1.4316	1.4367
[C_2MIm][NTf_2]	298.15	1.4179	1.4194	1.4203	1.4225	1.4255	1.4281	1.4330
	303.15	1.4164	1.4180	1.4188	1.4211	1.4240	1.4266	1.4316
	308.15	1.4150	1.4165	1.4173	1.4196	1.4226	1.4252	1.4301
	313.15	1.4135	1.4151	1.4159	1.4181	1.4211	1.4237	1.4286
	318.15	1.4121	1.4136	1.4144	1.4167	1.4196	1.4222	1.4271
	323.15	1.4106	1.4122	1.4130	1.4152	1.4181	1.4207	1.4256

[C_3Mim][NTf_2]	298.15	1.4200	1.4215	1.4223	1.4246	1.4276	1.4302	1.4352
	303.15	1.4185	1.4201	1.4209	1.4231	1.4261	1.4287	1.4337
	308.15	1.4170	1.4186	1.4194	1.4217	1.4246	1.4272	1.4322
	313.15	1.4156	1.4171	1.4179	1.4202	1.4231	1.4258	1.4306
	318.15	1.4141	1.4156	1.4164	1.4187	1.4216	1.4242	1.4291
	323.15	1.4126	1.4142	1.4150	1.4172	1.4201	1.4227	1.4276
[C_4Mim][NTf_2]	298.15	1.4218	1.4234	1.4242	1.4265	1.4295	1.4321	1.4371
	303.15	1.4203	1.4219	1.4227	1.4250	1.4280	1.4306	1.4355
	308.15	1.4188	1.4204	1.4212	1.4235	1.4264	1.4291	1.4340
	313.15	1.4173	1.4189	1.4197	1.4220	1.4249	1.4275	1.4325
	318.15	1.4158	1.4174	1.4182	1.4204	1.4234	1.4260	1.4309
	323.15	1.4143	1.4159	1.4167	1.4189	1.4219	1.4245	1.4294
[C_6Mim][NTf_2]	298.15	1.4245	1.4261	1.4269	1.4292	1.4323	1.4349	1.4399
	303.15	1.4230	1.4246	1.4254	1.4277	1.4307	1.4333	1.4383
	308.15	1.4214	1.4230	1.4238	1.4261	1.4291	1.4317	1.4367
	313.15	1.4199	1.4214	1.4222	1.4245	1.4275	1.4301	1.4351
	318.15	1.4183	1.4199	1.4207	1.4229	1.4259	1.4286	1.4335
	323.15	1.4167	1.4183	1.4191	1.4214	1.4243	1.4270	1.4319
[C_2Mim][OTf]	298.15	1.4290	1.4306	1.4315	1.4339	1.4371	1.4399	1.4451
	303.15	1.4276	1.4293	1.4301	1.4325	1.4357	1.4385	1.4437
	308.15	1.4262	1.4279	1.4287	1.4311	1.4343	1.4371	1.4423
	313.15	1.4249	1.4265	1.4274	1.4298	1.4329	1.4357	1.4409
	318.15	1.4235	1.4251	1.4260	1.4284	1.4315	1.4343	1.4395
	323.15	1.4221	1.4237	1.4246	1.4270	1.4301	1.4329	1.4380

[C_4MIm][OTf]	298.15	1.4321	1.4338	1.4346	1.4371	1.4403	1.4431	1.4484
	303.15	1.4308	1.4324	1.4333	1.4357	1.4389	1.4417	1.4470
	308.15	1.4294	1.4310	1.4319	1.4343	1.4375	1.4403	1.4456
	313.15	1.4280	1.4297	1.4306	1.4330	1.4361	1.4389	1.4442
	318.15	1.4267	1.4283	1.4292	1.4316	1.4348	1.4375	1.4428
	323.15	1.4253	1.4270	1.4278	1.4302	1.4334	1.4362	1.4414
[C_2MIm][$H_y SO_4$]	298.15	1.4892	1.4911	1.4922	1.4950	1.4988	1.5022	1.5084
	303.15	1.4880	1.4900	1.4910	1.4939	1.4976	1.5010	1.5072
	308.15	1.4869	1.4888	1.4898	1.4927	1.4964	1.4998	1.5060
	313.15	1.4857	1.4876	1.4887	1.4915	1.4953	1.4986	1.5048
	318.15	1.4845	1.4865	1.4875	1.4903	1.4941	1.4974	1.5036
	323.15	1.4834	1.4853	1.4863	1.4892	1.4929	1.4962	1.5024
[C_2MIm][C_1SO_4]	298.15	1.4749	1.4768	1.4778	1.4806	1.4843	1.4876	1.4937
	303.15	1.4737	1.4756	1.4766	1.4794	1.4830	1.4863	1.4924
	308.15	1.4724	1.4743	1.4753	1.4781	1.4818	1.4850	1.4911
	313.15	1.4712	1.4731	1.4741	1.4769	1.4805	1.4837	1.4898
	318.15	1.4699	1.4718	1.4728	1.4756	1.4792	1.4825	1.4885
	323.15	1.4687	1.4706	1.4716	1.4743	1.4780	1.4812	1.4872
[C_2MIm][C_2SO_4]	298.15	1.4721	1.4740	1.4750	1.4778	1.4815	1.4847	1.4908
	303.15	1.4708	1.4727	1.4737	1.4765	1.4801	1.4834	1.4894
	308.15	1.4695	1.4714	1.4724	1.4751	1.4788	1.4820	1.4880
	313.15	1.4681	1.4700	1.4710	1.4738	1.4774	1.4806	1.4867
	318.15	1.4668	1.4687	1.4697	1.4724	1.4761	1.4793	1.4853
	323.15	1.4655	1.4673	1.4683	1.4711	1.4747	1.4779	1.4839

[C_2Mim][C_6SO_4]	298.15	1.4671	1.4690	1.4700	1.4727	1.4764	1.4796	1.4856
	303.15	1.4657	1.4675	1.4685	1.4713	1.4749	1.4781	1.4841
	308.15	1.4642	1.4661	1.4671	1.4698	1.4734	1.4766	1.4826
	313.15	1.4628	1.4646	1.4656	1.4683	1.4719	1.4751	1.4811
	318.15	1.4613	1.4632	1.4641	1.4669	1.4705	1.4736	1.4796
	323.15	1.4599	1.4617	1.4627	1.4654	1.4690	1.4722	1.4781
[C_4Mim][C_1SO_4]	298.15	1.4716	1.4737	1.4748	1.4779	1.4819	1.4855	1.4922
	303.15	1.4702	1.4723	1.4734	1.4765	1.4805	1.4841	1.4908
	308.15	1.4689	1.4709	1.4720	1.4751	1.4791	1.4827	1.4893
	313.15	1.4675	1.4696	1.4707	1.4737	1.4777	1.4812	1.4879
	318.15	1.4661	1.4682	1.4693	1.4723	1.4763	1.4798	1.4865
	323.15	1.4647	1.4668	1.4679	1.4709	1.4749	1.4784	1.4851
[C_4Mim][SCN]	298.15	1.5291	1.5320	1.5336	1.5378	1.5434	1.5484	1.5578
	303.15	1.5276	1.5305	1.5320	1.5363	1.5418	1.5468	1.5562
	308.15	1.5261	1.5290	1.5305	1.5347	1.5403	1.5453	1.5546
	313.15	1.5246	1.5274	1.5289	1.5332	1.5387	1.5437	1.5530
	318.15	1.5230	1.5259	1.5274	1.5316	1.5372	1.5421	1.5514
	323.15	1.5215	1.5244	1.5259	1.5301	1.5356	1.5405	1.5498
[C_4MPip][NTf_2]	298.15	1.4249	1.4263	1.4271	1.4292	1.4319	1.4344	1.4389
	303.15	1.4235	1.4249	1.4257	1.4278	1.4305	1.4329	1.4375
	308.15	1.4221	1.4235	1.4243	1.4264	1.4291	1.4315	1.4360
	313.15	1.4207	1.4221	1.4229	1.4250	1.4277	1.4301	1.4346
	318.15	1.4193	1.4207	1.4215	1.4236	1.4263	1.4287	1.4331
	323.15	1.4179	1.4193	1.4201	1.4221	1.4248	1.4272	1.4317

[MOEMPL][NTf_2]	298.15	1.4187	1.4200	1.4207	1.4226	1.4250	1.4272	1.4312
	303.15	1.4173	1.4186	1.4192	1.4211	1.4236	1.4257	1.4297
	308.15	1.4159	1.4171	1.4178	1.4197	1.4221	1.4243	1.4283
	313.15	1.4144	1.4157	1.4164	1.4182	1.4207	1.4228	1.4268
	318.15	1.4130	1.4143	1.4149	1.4168	1.4192	1.4213	1.4253
	323.15	1.4116	1.4128	1.4135	1.4153	1.4177	1.4199	1.4239
[C_4MMIm][NTf_2]	298.15	1.4284	1.4301	1.4310	1.4334	1.4367	1.4395	1.4449
	303.15	1.4269	1.4286	1.4295	1.4319	1.4352	1.4380	1.4433
	308.15	1.4255	1.4271	1.4280	1.4305	1.4337	1.4365	1.4418
	313.15	1.4240	1.4257	1.4265	1.4290	1.4322	1.4350	1.4403
	318.15	1.4225	1.4242	1.4251	1.4275	1.4307	1.4335	1.4388
	323.15	1.4210	1.4227	1.4236	1.4260	1.4292	1.4320	1.4373

Table A2. Density (g/cm^3) as a function of temperature

IL	T(K)					
	298.15	303.15	308.15	313.15	318.15	323.15
$[C_2MIm][BF_4]$	1.284912	1.281171	1.277384	1.273614	1.269854	1.266119
$[C_3MIm][BF_4]$	1.237089	1.233412	1.229747	1.226094	1.222455	1.218832
$[C_4MIm][BF_4]$	1.201029	1.197482	1.193946	1.190413	1.186887	1.183384
$[C_6MIm][BF_4]$	1.145176	1.141773	1.138366	1.134947	1.131540	1.128139
$[C_8MIm][BF_4]$	1.104262	1.100835	1.097424	1.094107	1.090781	1.087464
$[C_2MIm][NTf_2]$	1.518490	1.513442	1.508417	1.503401	1.498412	1.493448
$[C_3MIm][NTf_2]$	1.474690	1.469760	1.464848	1.459957	1.455077	1.450228
$[C_4MIm][NTf_2]$	1.436639	1.431862	1.427094	1.422349	1.417620	1.412910
$[C_6MIm][NTf_2]$	1.372197	1.367620	1.363050	1.358490	1.353936	1.349405
$[C_4MPip][NTf_2]$	1.382353	1.378103	1.373846	1.369582	1.365324	1.361075
$[MOEMPL][NTf_2]$	1.453158	1.448435	1.443751	1.439074	1.434411	1.429778
$[C_4MMIm][NTf_2]$	1.418644	1.414066	1.409462	1.404867	1.400274	1.395693
$[C_2MIm][OTf]$	1.382060	1.377875	1.373702	1.369539	1.365386	1.361260
$[C_4MIm][OTf]$	1.297670	1.293744	1.289810	1.285879	1.281955	1.278053
$[C_2MIm][H_ySO_4]$	1.370980	1.367881	1.364784	1.361700	1.358625	1.355554
$[C_2MIm][C_1SO_4]$	1.288246	1.284873	1.281502	1.278144	1.274798	1.271462
$[C_2MIm][C_2SO_4]$	1.237665	1.234291	1.230921	1.227548	1.224189	1.220844
$[C_2MIm][C_6SO_4]$	1.130178	1.126833	1.123518	1.120283	1.117061	1.113832
$[C_4MIm][C_1SO_4]$	1.212159	1.208853	1.205537	1.202218	1.198900	1.195593
$[C_2MIm][SCN]$	1.069328	1.066393	1.063443	1.060504	1.057581	1.054670

Table A3. Coefficients of the linear fit of densities as a function of temperature

. $\rho = \rho_0 + \rho_1 T$	ρ_0 (g/cm^3)	ρ_1 (g/cm^3K)	R^2
$[C_2MIm][BF_4]$	1.5091576	-7.52491 10^4	0.999996
$[C_3MIm][BF_4]$	1.4547078	-7.30337 104	0.999992
$[C_4MIm][BF_4]$	1.4113907	-7.05960 104	0.999996
$[C_6MIm][BF_4]$	1.3483344	-6.81731 104	0.999999
$[C_8MIm][BF_4]$	1.3042357	-6.71251 104	0.999994
$[C_2MIm][NTf_2]$	1.8169957	-1.001810 104	0.999991
$[C_3MIm][NTf_2]$	1.7662731	-9.78571 104	0.999991
$[C_4MIm][NTf_2]$	1.7194829	-9.49234 104	0.999992
$[C_6MIm][NTf_2]$	1.6439093	-9.11840 104	0.999997
$[C_4MPip][NTf_2]$	1.6360664	-8.51377 104	0.9999997
$[MOEMPL][NTf_2]$	1.7317946	-9.35137 104	0.999991
$[C_4MMIm][NTf_2]$	1.6923415	-9.18434 104	0.9999994
$[C_2MIm][OTf]$	1.6300262	-8.32171 104	0.999994
$[C_4MIm][OTf]$	1.5316085	-7.85046 104	0.999998
$[C_2MIm][H_ySO_4]$	1.5548449	-6.17040 104	0.999996
$[C_2MIm][C_1SO_4]$	1.4883214	-6.71446 104	0.999995
$[C_2MIm][C_2SO_4]$	1.4382255	-6.73051 104	0.999997
$[C_2MIm][C_6SO_4]$	1.3247180	-6.53034 104	0.99993
$[C_4MIm][C_1SO_4]$	1.4097080	-6.62903 104	0.9999996
$[C_2MIm][SCN]$	1.2441435	-5.86657 104	0.999994

USC
UNIVERSIDADE
DE SANTIAGO
DE COMPOSTELA